# ANTIFREEZE PROTEINS FROM THE SEA ICE DIATOM *FRAGILARIOPSIS CYLINDRUS*

DISSERTATION

Vorgelegt von
Maddalena Bayer aus Triest (Italien)

zur Erlangung des Doktorgrades
Dr. rer. nat.

Fachbereich Biologie und Chemie
Universität Bremen

Universität Bremen

AWI Alfred-Wegener-Institut für Polar- und Meeresforschung in der Helmholtz-Gemeinschaft

Cover image:

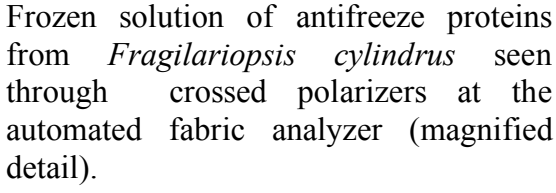

Frozen solution of antifreeze proteins from *Fragilariopsis cylindrus* seen through crossed polarizers at the automated fabric analyzer (magnified detail).

| Gutachter | Prüfer |
| --- | --- |
| Prof. Dr. Ulrich Bathmann | Prof. Dr. Kai Bischof |
| Prof. Dr. Allan Cembella | Dr. Ilka Weikusat |

Bremen, September 2011

# ANTIFREEZE PROTEINS FROM THE SEA ICE DIATOM *FRAGILARIOPSIS CYLINDRUS*

## ABSTRACT

A molecular and crystallographic characterization of antifreeze proteins from the sea ice diatom *Fragilariopsis cylindrus* (fcAFPs) is presented here. The molecular study relies on sequence analyses, phylogenetic studies, gene and protein expression analyses. These AFPs constitute a multigene family of isoforms with a conserved antifreeze domain. The exposure of *F. cylindrus* to subzero conditions typical for sea ice brine caused differential regulation of the isoforms, as revealed by gene expression analysis. Some fcAFP genes were downregulated to nearly zero, whereas selected isoforms were strongly upregulated (up to 200-fold). Differential gene regulation was reflected in protein expression pattern. The widespread occurrence of fcAFPs and fcAFP-like proteins in polar or cold-tolerant organisms further underlines their importance as elements of adaptation to subzero conditions. Several events of horizontal gene transfer seem to have contributed to the distribution of the fcAFP genes. These results suggest a strong relevance of these proteins for *F. cylindrus*, probably contributing to its dominat position within sea ice assemblages.
Studies with a recombinant isoform of fcAFP, chosen based on the molecular results, confirmed its antifreeze activity. The protein caused moderate freezing point depression and strong recrystallization inhibition. These effects were enhanced in concentrated saline solutions.
In order to shed light on the physical antifreeze mechanism of this protein, its interaction with ice is presented in more detail here. Several crystal planes are suggested for preferential protein-ice interaction. Habit modification in the presence of fcAFPs, with inhibited ice growth on the lateral (prismatic) planes, indicates binding on the primary and secondary prismatic faces. Pitting observed on the basal plane of a pure crystal submerged in an fcAFP solution suggests further protein binding on non-lateral planes of the ice crystal.
The most prominent feature shown here is the influence of fcAFPs on ice microstructure. The proteins clearly affected ice texture, causing a marked pattern of oriented striations, interpreted as ice fibers with inclusions and not observed without fcAFPs.
Analysis of c-axis orientation revealed a strong influence on axis distribution within individual crystals and further indicates an inhibiting effect of fcAFPs on ice nucleation.
Considered in the frame of the natural environment of *F. cylindrus*, results on antifreeze activity of fcAFPs and crystallographic analyses suggest that the effect on ice texture is

the most relevant biological role of fcAFPs. Modifications of the microstructure of brine inclusions change physical properties of sea ice, which determine its habitability.

# ZUSAMMENFASSUNG

In dieser Arbeit wird eine molekulare und kristallographische Charakterisierung von Gefrierschutzproteinen aus der Meereisdiatomee *Fragilariopsis cylindrus* vorgestellt. Die molekularen Untersuchungen basieren auf Sequenzanalysen, Untersuchungen der Phylogenie, sowie der Gen- und Proteinexpression. Es wird gezeigt, dass die Gefrierschutzproteine eine Multigenfamilie mit konservierter Gefrierschutzdomäne bilden. Bei Temperaturen unter Null wurden die verschiedenen Isoformen differentiell exprimiert, wie eine Genexpressionsanalyse gezeigt hat. Während einige Gefrierschutzgene bis annährend Null runterreguliert wurden, wurden andere Isoformen stark hochreguliert (bis zu 200-fach). Die differentielle Genregulierung widerspiegelte sich in dem Muster der Proteinexpression. Die Verbreitung von Gefrierschutz- oder ähnlichen Proteinen in polaren oder kältetoleranten Organismen unterstreicht ihre Bedeutung als Anpassungsmechanismus an niedrige Temperaturen. Mehrere Ereignisse von horizontalem Gentranfer scheinen zur Verbreitung der Proteine beigetragen zu haben. Diese Ergebnisse weisen auf eine große Bedeutung dieser Proteine für *F. cylindrus* hin, und auf einen Beitrag der Proteine zum Erfolg dieser Diatomee unter den Meereisarten.

Untersuchungen mit einer rekombinanten Isoform des Gefrierschutz-proteins, ausgesucht basierend auf Ergebnissen der molekularen Analysen, bestätigte seine Gefrierschutzaktivität. Das Protein verursachte eine moderate Gefrierpunkts-erniedrigung und eine starke Hemmung der Rekristallisation. Diese Effekte wurden in konzentrierter Salzlösung verstärkt.

Um den physikalischen Gefrierschutzmechanismus des Proteins besser verstehen zu können, wird hier die Wechselwirkung mit Eis im Detail vorgestellt. Mehrere Ebenen der Eiskristalle scheinen für bevorzugte Protein-Eis-Interaktion zu dienen. Die Veränderung der Kristallform in Anwesenheit von Gefrierschutzproteinen, mit gehemmtem Wachstum auf den seitlichen (prismatischen) Kristallebenen, deutet auf Bindungen des Proteins an der primären und sekundären prismatischen Ebene hin. Weiterhin wurden Vertiefungen auf der basalen Ebene eines Kristalls in einer Lösung mit Gefrierschutzproteinen von Bindungen an nicht-lateralen Ebenen des Kristalls verursacht.

Das markanteste Ergebnis ist der Einfluss des Gefrierschutzproteins auf die Mikrostruktur von Eis. Die Proteine zeigten eine deutliche Wirkung und verursachten ein Muster mit orientierter Streifung, welches als Eisfaser mit Einschlüssen interpretiert wurde und ohne Gefrierschutzproteine nicht beobachtet werden konnte.

Die Analyse der c-Achsen-Orientierung zeigte einen starken Einfluss auf die Verteilung der Achsen innerhalb einzelner Kristalle sowie einen hemmenden Effekt der Proteine auf die Nukleation von Eis.

Im Rahmen der natürlichen Umgebung von *F. cylindrus* suggerieren die Ergebnisse der Analysen zur Gefrierschutzaktivität und der kristallographischen Untersuchungen dass der Effekt auf die Mikrostruktur von Eis die bedeutendste biologische Funktion der Proteine ist. Veränderungen der Mikrostruktur von Soleeinschlüssen beeinflussen die physikalischen Eigenschaften von Meereis, welche seine Besiedelung durch Organismen bestimmen.

# INDEX OF CONTENTS

**ABSTRACT** ..... **I**

**ZUSAMMENFASSUNG** ..... **II**

**LIST OF ABBREVIATIONS** ..... **1**

**1. INTRODUCTION** ..... **3**

1.1. THE ENVIRONMENT ..... 3
*1.1.1. SEA ICE - ITS FORMATION AND STRUCTURE* ..... *3*
*1.1.2. THE BRINE NETWORK* ..... *4*
1.2. SEA ICE BIOLOGY ..... 6
*1.2.1. THE DIATOM FRAGILARIOPSIS CYLINDRUS* ..... *7*
1.3. ANTIFREEZE PROTEINS ..... 8
*1.3.1. GENERAL CONSIDERATIONS* ..... *8*
*1.3.2. THE BIOLOGICAL ROLE OF AFPs* ..... *8*
*1.3.3. MECHANISMS OF ACTION* ..... *9*
*1.3.4. PROTEIN-ICE ATTACHMENT* ..... *11*
*1.3.5. APPLICATIONS* ..... *12*
*1.3.6. THE IAFP FAMILY* ..... *12*
1.4. OBJECTIVES ..... 13

**2. METHODS** ..... **14**

2.1. DETERMINATION OF FCAFP ISOFORMS ..... 14
2.2. PHYLOGENETIC ANALYSES ..... 14
2.3. FCAFP GENE EXPRESSION ..... 15
2.4. EXPRESSION OF RECOMBINANT FCAFP IN E. COLI ..... 15
2.5. BIOLISTIC TRANSFORMATION ..... 16
2.6. PROTEIN ANALYSIS ..... 17
2.7. ANTIFREEZE ACTIVITY - THERMAL HYSTERESIS, RECRYSTALLIZATION ... INHIBITION AND HABIT MODIFICATION ..... 18
2.8. ICE MICROSTRUCTURE ..... 19
2.9. ANALYSIS OF CRYSTAL ORIENTATION IN ICE ..... 19

**3. RESULTS AND DISCUSSION** ..... **22**

3.1. DIVERSITY AND EVOLUTION OF FCAFPS ..... 22
*3.1.1. SEQUENCE ANALYSES* ..... *22*
*3.1.2. PHYLOGENY AND EVOLUTION* ..... *23*
3.2. GENE AND PROTEIN ACTIVITY ..... 26
*3.2.1. GENE EXPRESSION* ..... *26*
*3.2.2. PROTEIN EXPRESSION* ..... *28*
*3.2.3. ONLY ONE FUNCTION OF fcAFPs?* ..... *29*
*3.2.4. THE ROLE OF E/G POINT MUTATION* ..... *29*
3.3. HETEROLOGOUS EXPRESSION OF AN FCAFP ..... 30
*3.3.1. EXPRESSION IN E. COLI* ..... *31*
*3.3.2. EXPRESSION IN P. TRICORNUTUM* ..... *31*
3.4. ANTIFREEZE ACTIVITY OF A RECOMBINANT FCAFP ..... 32
*3.4.1. THERMAL HYSTERESIS* ..... *33*
*3.4.2. RECRYSTALLIZATION INHIBITION* ..... *34*
*3.4.3. THE EFFECT OF SALTS* ..... *34*
*3.4.4. CRYSTAL HABIT* ..... *35*
*3.4.5. PROTEIN-ICE INTERACTION SITES* ..... *37*

3.5. THE EFFECT OF FCAFP ON ICE MICROSTRUCTURE AND FABRIC ANALYSES ..... 40
*3.5.1. THE MICROSTRUCTURE OF ICE ..... 40*
*3.5.2. THE FABRIC OF ICE ..... 43*
3.6. PUBLICATION 1 ..... 47
3.7. PUBLICATION 2 ..... 60

**4. SUMMARY AND CONCLUSIONS ..... 85**

4.1. SUMMARY ..... 85
4.2. WHAT COULD BE THE BIOLOGICAL ROLE OF FCAFPS? ..... 86
4.3. PROBLEMS AND LIMITATIONS ..... 86

**5. OUTLOOK ..... 88**

**BIBLIOGRAPHY ..... 91**

**A. APPENDIX ..... 101**

A.1. PUBLICATION 3 ..... 101
A.2. PUBLICATION 1 - SUPPLEMENTARY INFORMATION ..... 129
A.3. EXPRESSION OF RECOMBINANT FCAFP IN *E. COLI* - PROTOCOL ..... 132
A.4. BIOLISTIC BOMBARDMENT - PROTOCOL ..... 133
A.5. VECTOR MAPS ..... 134
A.6. CONFOCAL RAMAN MICROSCOPY ..... 136

**AKNOWLEDGEMENTS ..... 137**

# LIST OF ABBREVIATIONS

| | |
|---|---|
| AFGP | Antifreeze glycoprotein |
| AFP | Antifreeze protein |
| *afp* | AFP-coding gene |
| AVA | Achsenverteilungsanalyse (axis distribution analysis) |
| BSA | Bovine serum albumin |
| cDNA | Complementary DNA |
| E | Glutamic acid |
| EPS | Exopolymeric substances |
| EST | Expressed sequence tag |
| fcAFP | Antifreeze protein from *Fragilariopsis cylindrus* |
| *fcafp* | FcAFP-coding gene |
| G | Glycine |
| GFP | Green fluorescent protein |
| HGT | Horizontal gene transfer |
| His-tag | Histidine-tag |
| IAFP | Family of AFPs (including among others proteins from sea „ice“ organisms, e.g. fcAFPs) |
| *iafp* | IAFP-coding gene |
| IPTG | Isopropyl-β-D-thiogalactoside |
| Ni-NTA | Nickel-nitrilotriacetic acid |
| PBS | Phosphate buffered saline |
| PCR | Polymerase chain reaction |
| QLL | Quasi-liquid layer |
| qPCR | Quantitative real-time PCR |
| RI | Recrystallization inhibition |
| SUMO | Small ubiquitin-related modifier protein |
| TH | Thermal hysteresis |

# 1. INTRODUCTION

Sea ice represents a dominant feature on earth, covering, at its maximum extent, 16 x $10^6$ $km^2$ in the Arctic and 19 x $10^6$ $km^2$ in the Antarctic [Dieckmann and Hellmer, 2010], thus 10% of the oceans' surface area. Its structure is a mushy layer, with a solid matrix permeated by pores and channels filled with brine (brine inclusions), formed by sea salt segregated from the growing ice lattice. Brine inclusions offer a favorable environment for a certain microalgae, which live and thrive within the ice. These assemblages are a crucial element in the polar ecosystem. However, organisms within sea ice are exposed to extreme conditions, of which low temperatures down to -20°C and salinities of up to 200, on the Practical Salinity Scale, are an example.

The mechanisms evolved by sea ice organisms to cope with these conditions are various, but still an open question. The diatom *Fragilariopsis cylindrus*, a dominant species within the ice, produces proteins similar to antifreeze proteins (AFPs) known from cold-tolerant fungi. The proteins from *F. cylindrus* (fcAFPs) have been suggested as a main factor for survival of this organism in sea ice [Krell et al., 2008]. A deeper knowledge of these proteins, their distribution and activity, means a further contribution in unraveling the puzzle of sea ice biology, with implications in molecular and physiological aspects, in biogeochemistry and possibly brine inclusions formation. Furthermore, understanding the mechanism of action of fcAFPs could result in several industrial applications.

This study presents a characterization of fcAFPs, unifying molecular analyses of the proteins and their genes (*fcafp*s), and crystallographic observations of the effect of fcAFPs on ice.

## 1.1. THE ENVIRONMENT

### 1.1.1. SEA ICE
### ITS FORMATION AND STRUCTURE

The structure of sea ice is a signature of its formation dynamics. The generation of the first ice sheet is governed by mechanical effects. In supercooled seawater, at temperatures below -1.8°C, several ice nuclei are formed [Weeks and Ackley, 1982; Petrich and Eicken, 2010]. Initial discoid crystals develop into dendrites, but turbulent wave motion with its abrasive action quickly smoothes and cuts the grains, increasing the number of crystallization nuclei. This so called frazil ice agglomerates by wind

action, and by further consolidation it forms larger aggregates of grease ice, pancake ice and finally a closed cover of granular ice. This layer is characterized by fine crystals with random orientation due to their quick formation under turbulent sea conditions.

| Ice texture | Grain size | Grain shape | Layer thickness |
|---|---|---|---|
| Granular | < 1 cm | Isometric | < 1 m |
| Transition zone | 1-10 cm | Slightly elongated | 5-10 cm |
| Columnar | 1-10 cm and more | Elongated | < 1 m |
| Platelet | 1-10 cm | Platy grains | 0.5-4 m |

Table 1: Texture, grain size, grain shape and thickness of the characteristic layers that constitute sea ice [Dayton et al., 1969; Weeks and Ackley, 1982; Eicken and Lange, 1989; Petrich and Eicken, 2010].

After the formation of this first ice sheet, further ice growth within the so called transition zone [Perey and Pounder, 1958] is not mechanically driven, but merely dependent on thermal mechanisms related to the temperature gradient within the ice sheet and its conductivity (congelation growth). The transition zone represents a shift from the granular ice to the columnar ice zone, a structure with grains elongated into the melt and regular horizontal crystallographic orientation. The growing ice front is lamellar [Weeks and Ackley, 1982], and individual lamellae are separated by brine layers. Spacing between brine layers is typically 0.1-1 mm.
Beneath the columnar ice, a layer of lose platelet ice may accumulate and eventually consolidate. Platelets are mostly formed in landfast ice in deep, supercooled water under the influence of ice shelves [Dayton et al., 1969; Robin, 1979].

## 1.1.2. THE BRINE NETWORK

Sea ice is mainly a two-phase system, and its porous structure is largely determinant for biological activity within ice. During ice formation, solutes in the seawater are excluded from the ice matrix and segregate into interconnected brine droplets (granular ice) or laterally in brine layers between lamellae (columnar ice) [Weeks and Ackley, 1982]. The brine space, formed by channels and pockets, constitutes mainly a network,

connected, among others, through cracks that form due to pressure of fractional freezing of brine inclusions.

The negative temperature gradient in growing sea ice causes an initial profile of low porosity/high brine concentration close to the ice-atmosphere interface, and high porosity/low brine concentration in bottom ice layers close to the water. However, this density profile is hydrostatically unstable and leads to gravity drainage, which is the main mechanism of desalination in winter sea ice [Understeiner, 1967; Weeks and Ackley, 1982; Notz and Worster, 2009]. Other desalination processes such as diffusion, brine pocket migration, brine expulsion and flushing only play a minor role. Due to the density gradient, small perturbations in the network of brine inclusions can expand and instability may develop into advective brine flow downwards and out of the ice, alternated to inflow of seawater with lower salinity into the inclusions network [Lake and Lewis, 1970].

Desalination of sea ice and further cooling result in additional freezing, a decrease in ice porosity and in ice permeability (Figure 1). Porosity, defined as volume fraction of brine inclusions in total ice volume (air inclusions are assumed to be negligible [Cox and Weeks, 1983]), decreases with decreasing inclusion size. Permeability depends on porosity, as well as on microstructural characteristics of brine channels. Outflow of high salinity brine and inflow of seawater of lower salinity, as well as cooling, cause brine inclusions to narrow and eventually separate into individual pockets divided by ice bridges.

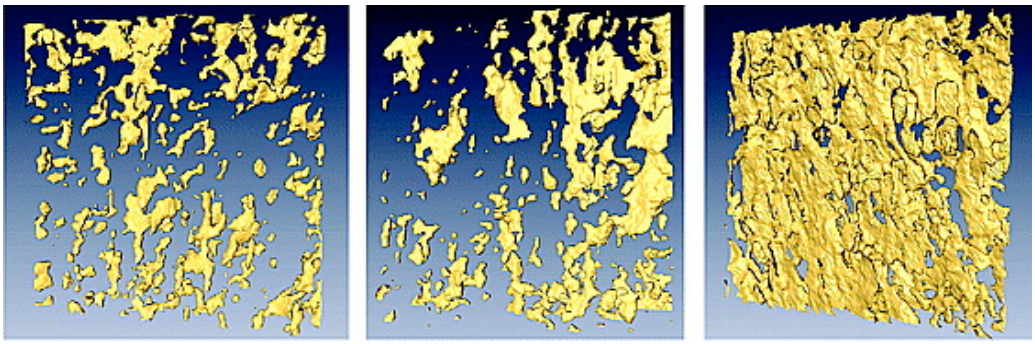


Figure 1: X-ray computed tomography images of brine layers (represented in gold) in an artificially grown sea ice single crystal. Porosity ($\Phi$) and connectivity increase with rising temperatures. Image from Golden et al. [2007], with permission.

Permeability and brine viscosity modulate brine flow, and periods of flux are alternated to phases of stabilization. A preferential drainage system develops with time, consisting of a drainage channel surrounded by a feeding brine network.

At temperatures between −2 to −6°C, channels of diameter <40 µm determine half of the porosity of sea ice. Estimations of brine channels surface area, available for organisms attachment, ranges from 0.3 to 4 $m^2$ $kg^{-1}$ ice [Krembs et al., 2000; Krembs et al., 2001].

## 1.2. SEA ICE BIOLOGY

Despite the harsh conditions that govern within sea ice, it offers a habitat for a variety of microalgae. High standing stocks of 10-1000 mg Chl $m^{-3}$ [Lizotte, 2001; Thomas and Dieckmann, 2002] have been measured within sea ice, whereas chlorophyll in the water under the ice is usually below 0.1 mg $m^{-3}$ [Lizotte, 2001]. The annual primary production estimated for Antarctic sea ice (63-70 Tg C $year^{-1}$ [Legendre et al., 1992]) represents only 5% of the Antarctic production in the sea ice-influenced area [Arrigo et al., 1998], but it plays a crucial role for the ecology of the Southern Ocean. Ice algae represent a concentrated food source in the low-productivity ice-covered sea, and in the months of melting they initiate blooms by seeding the water column [Lizotte, 2001].
Algae have been found distributed within brine channels and pockets (Figure 2) throughout the entire thickness of the ice column. They are incorporated into ice by scavenging by frazil and platelet crystals during sea ice formation, and also by the pumping action of waves [Ackley and Sullivan, 1994]. Highest cell abundances are in the bottom centimeters of columnar ice and in the platelet layer, due to the higher porosity and to the constant flushing with nutrient-rich seawater in these layers [Ackley and Sullivan, 1994; Werner et al., 2007]. However, in bottom ice organisms are stressed by low light intensities, whereas in the upper layers of the ice sheet limiting factors for growth are given by low temperatures, higher brine salinities, low nutrient availability and dissolved gas concentration [Eicken, 1992; Thomas and Dieckmann, 2002; Arrigo and Thomas, 2004].

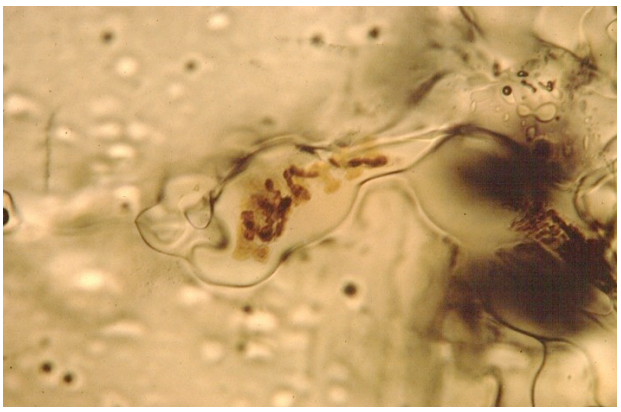

Figure 2: In the center of the picture, diatoms (brown cells) in a brine pocket within sea ice. Image: AWI.

Species composition changes with the aging of ice and the stabilization of brine channel system [Krembs et al., 2001], resulting in a dominance of pennate diatom species [Arrigo and Thomas, 2004; Werner et al., 2007]. The selection of raphid, "sticky" species is favored since, attached to the surface of brine channels, they are more easily retained within the ice. Attachment and gliding of sea ice organisms on ice surfaces has been frequently suggested [Riebesell et al., 1991; Ikävalko and Gradinger, 1997; Krembs et al., 2000]. Several studies focused on exopolymeric substances (EPS) as responsible for attachment of cells to ice surfaces [Riedel et al., 2007; Ewert and Deming, 2011]. EPS consists of a matrix made of different carbohydrates, but also uronic acids, sulfates and proteins [Decho, 1990]. The polymers may be tightly bound to the cell and coat it (particulate EPS, pEPS, >0.4 μm) or be loosely attached to it forming a mucus (dissolved EPS, dEPS, <0.4 μm). The role and formation dynamics of EPS is not clear yet, but in sea ice it seems to be involved not only in attachment mechanisms but also in protecting cells, buffering them in an unfavorable environment [Krembs et al., 2002; Collins et al., 2008], and in shaping ice microstructure [Krembs et al., 2011].

## 1.2.1. THE DIATOM *FRAGILARIOPSIS CYLINDRUS*

*Fragilariopsis cylindrus* (Grunow) Krieger is a pennate diatom often described as a dominant or co-dominat species within sea ice assemblages in Arctic and Antarctic [Garrison and Buck, 1985; Bartsch, 1989; Poulin, 1990; Riebesell et al., 1991; Garrison and Close, 1993; Lizotte, 2001] and in the water column near the ice edge [Kang and Fryxell, 1992]. This diatom is a raphid species, in our observations 10-20 μm in length (Figure 3). *F. cylindrus* is widely distributed within the whole sea ice column, from the slush-like surface [Garrison and Buck, 1989] to the under-ice platelet layer [Mangoni et al., 2009] and shows no specific seasonality.

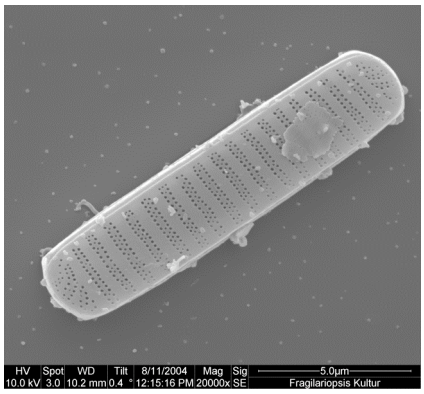


Figure 3: *F. cylindrus* cell in valve view photographed under scanning electron microscopy. Image: Courtesy of Henrik Lange and Friedel Hinz, AWI.

The organisms used in this study were isolated from sea ice samples of the Weddell Sea, Antarctica. They were collected in 1999 during the Polarstern ANT XVI/3 expedition. Another strain, *F. cylindrus* CCMP 1102, has recently been sequenced at the DOE Joint Genome Institute (JGI, USA).

Its common occurrence in sea ice makes *F.*

*cylindrus* an ideal candidate for representative studies of mechanisms of response to polar conditions. Analyses of acclimation and adaptation of *F. cylindrus* to the extreme environment within ice include physiological [Bartsch, 1989; Fiala and Oriol, 1990; McMinn et al., 2005; Mock and Hoch, 2005; Pankowski and McMinn, 2009] and molecular studies [Mock and Valentin, 2004; Mock et al., 2006; Krell et al., 2007]. Recent publications [Janech et al., 2006; Krell et al., 2008] presented AFPs discovered in *F. cylindrus* and proposed them as possible adaptation to the sea ice environment.

## 1.3.ANTIFREEZE PROTEINS

### 1.3.1. GENERAL CONSIDERATIONS

Antifreeze proteins are structurally diverse proteins with the common characteristics of influencing ice crystal growth [for a review see Barrett, 2001; Venketesh and Dayananda, 2008].

One of the most prominent aspects of AFP activity on ice is thermal hysteresis (TH), i.e. the shift of the melting point away from the freezing point of a solution. This mechanism is non-colligative and differs from equilibrium freezing point depression, where freezing and melting temperatures still coincide. Thermal hysteresis is largely determined by the depression of the freezing point below the equilibrium melting temperature (freezing hysteresis). The degree of supercooling due to AFPs can range between 1°C (moderate AFPs) and 6°C (hyperactive AFPs) at millimolar protein concentration. Recent publications also showed examples of a rise of the melting temperature (melting hysteresis) due to AFPs, which however is approximately an order of magnitude weaker than the freezing hysteresis [Celik et al., 2010a; Celik et al., 2010b].

Another effect of AFPs is recrystallization inhibition (RI). Recrystallization defines ice grain boundary migration and leads to the growth of large crystals at the expenses of small grains.

### 1.3.2. THE BIOLOGICAL ROLE OF AFPs

Antifreeze proteins are present in a wide range of polar or cold-tolerant organisms, but each of the different types of AFPs has only a narrow taxonomic distribution. The different AFP types can act inside the cells and inhibit intracellular ice growth [Fletcher et al., 2001; Kawahara et al., 2007], but most AFPs are secreted and bind to ice in the extracellular space.

One of the main biological roles of AFPs may be to prevent ice formation (TH activity), as it is in freeze-avoiding insects and in fishes from icy waters, or to avoid the formation of large ice crystals by keeping the grains small (RI activity), as in several freeze-tolerant plants. The formation of ice crystals, apart from subtracting water to the cells, may decrease living space, as in the case of sea ice diatoms. Furthermore crystals, especially large grains, may mechanically damage cells.
Dependent on whether the TH or the RI effect is dominant, AFPs are also called thermal hysteresis, ice-binding or ice-structuring proteins.
However, parallel functions of AFPs cannot be excluded. Indeed, some AFPs seem to have developed by subfunctionalization and may retain their original acitivity. Antifreeze proteins from winter rye, for instance, are homologous to pathogenesis-related proteins and still provide protection against pathogens, in addition to their antifreeze properties [Griffith and Yaish, 2004].

### 1.3.3. MECHANISMS OF ACTION

Although studies indicate that the mechanism of action of AFPs must rely on ice surface attachment, the exact nature of this interaction is still not defined. The attachment seems to happen in a two-steps event [Kristiansen and Zachariassen, 2005; Zepeda et al., 2008]. It is suggested that proteins have a first, reversible association with ice in the quasi-liquid layer (QLL) that surrounds the ice crystal, a region that may reach several nm and represents a transition layer between phases, where water molecules become gradually ordered into an ice lattice. In a second step, AFPs tightly bind, in a permanent attachment, to defined planes of the growing ice crystal [Pertaya et al., 2007]. Both hydrophobic effects and hydrophilic interactions seem to be responsible for the protein attachment to ice, as shown in several studies with amino acid substitutions [DeLuca et al., 1996; Cheng and Merz, 1997; Harding et al., 1999; Bar et al., 2008]. The former lower the solubility of the AFPs, enhancing protein exclusion from the solvent and adsorption to ice, the latter act by binding AFPs to the ice by hydrogen bonds and van der Waals forces.

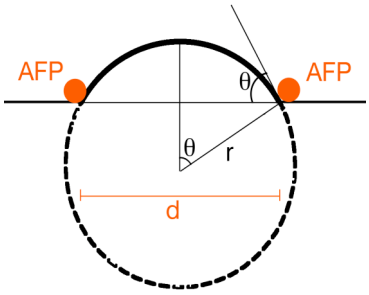


Figure 4: Ice “cap” (thick continuous line) between two adsorbed AFPs (red dots). The relationship between the radius r and the angle of curvature θ is shown. The spacing between the adsorbed proteins is indicated as d. Modified after Kristiansen and Zachariassen [2005].

The adsorption-inhibition model is the most accepted model for describing the mechanism of action of AFPs [Raymond and DeVries, 1977; Kristiansen and Zachariassen, 2005]. According to this model, AFPs bound to the ice surface force crystal growth to happen between the attached proteins, developing a curved ice surface defined by its radius r (Figure 4). The curvature causes a shift in pressure, an effect known as the Kelvin or Gibbs-Thomson effect, meaning that the water molecules at a convex ice surface have a tendency to leave the crystal, depressing the freezing temperature [Kang, 2005]. In the hysteresis gap between the melting and the freezing point, ice growth is stopped at a critical radius typical for each temperature, at which the molecules leaving the ice equal the molecules joining the ice lattice. At any temperature, the radius of each ice "cap" growing between the proteins, not observable macroscopically at light microscopy, will be the same, whereas the angle θ will depend on the spacing d between the AFPs (Figure 4).

The hysteresis freezing point will be reached when maximal convexity is reached, with $r = \frac{d}{2\sin\theta}$ (Figure 5). The hysteresis freezing point is described by $\Delta T = \frac{4\sigma T m \sin\theta}{\Delta H d}$ where ΔT is the degree of supercooling, σ the interfacial tension (32 ergs/cm$^2$), $T_m$ the melting temperature, ΔH the heat of fusion of water (3.3 x 10$^9$ ergs/cm$^3$). Any further temperature depression will result in crystal growth.

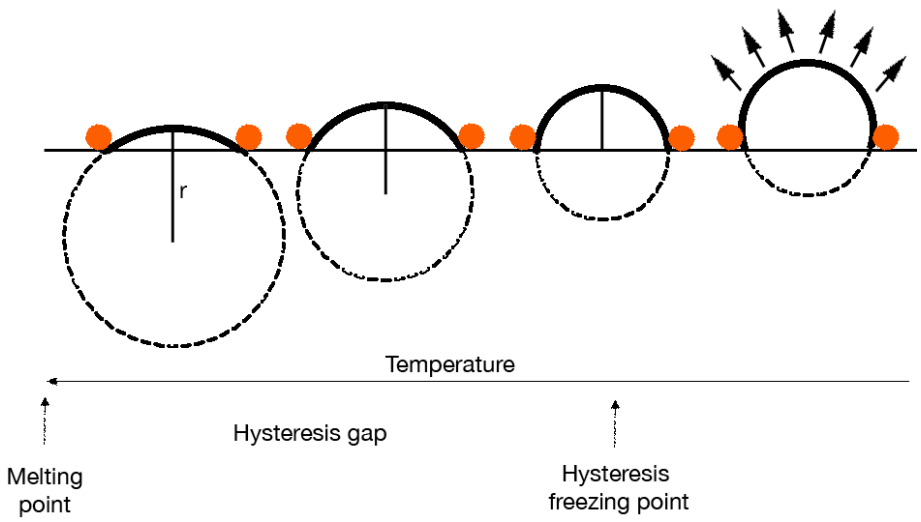


Figure 5: Model for inhibited ice growth within the hysteresis gap. The scheme shows one ice "cap", at different temperatures, between AFPs (red dots) adsorbed to the crystal suface. The temperature decreases from left to right. The radius r decreases with lowering temperature. When r = d/2 the solution reaches the hysteresis freezing point, further temperature depression results in explosive growth. Modified after Kristiansen and Zachariassen [2005].

The adsorption-inhibition model describes not only the TH effect of AFPs, but also their RI activity. Small ice grains have a larger surface convexity than large grains. Due to the Kelvin effect the shift in the pressure on the curved interface causes melting at the convex surface and, on the other side, freezing at the concave interface. This results in a net transfer of molecules from the small to the large crystal, eventually leading to a single large crystal.

Alternative models excluding the Kelvin effect [Wilson, 1994] and a rigid, irreversible match between AFPs and ice have been proposed [Zepeda et al., 2008; Ebbinghaus et al., 2010]. These studies focused on attachment as a dynamic process, reinforcing the role of solvation layers, increased around AFGPs, in long-distance water perturbation and as a disrupting factor in the quasi-ordered structure of the QLL.

## 1.3.4. PROTEIN-ICE ATTACHMENT

Several factors such as size, solubility, and protein-ice attachment site influence the effectiveness of AFPs in inhibiting ice growth. Most AFP types bind to characteristic planes of the ice crystal. Inhibited growth on these planes may result in specific crystal shapes (habit) with faceted morphologies within the hysteresis gap, and crystal expansion in selected directions below the freezing point. Therefore, observation of the shape and growth pattern of ice crystals allows for drawing conclusions about the sites of protein attachment.
The structure of an ice crystal is described by its 3 a-axes, which define the hexagonal basal plane, normal to the main crystallographic axis, called the c-axis (Figure 6).
Whereas the basal plane is smooth at a molecular level, the faces parallel to the c-axis, the prismatic planes, are rough. This results in an anisotropy in growth rates.

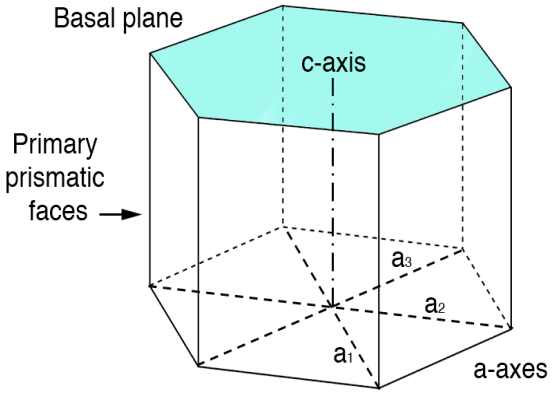


Figure 6:
Schematic representation of the crystal structure of ice. The basal plane (blue) and the 6 primary prismatic (lateral) planes are shown, together with the characteristic axes.

An ice crystal freely growing in a solution expands first its basal plane, along the a-axes, whereas growth of the prismatic faces along the c-axis in slower. This growth dynamics confers to the ice crystal developing in a melt a discoid shape [Hobbs, 2010a]. Due to AFPs, crystals grow preferentially as spicules along the c-axis. Only hyperactive AFPs are characterized by explosive ice growth along the a-axes of the crystal.

### 1.3.5. APPLICATIONS

AFPs have a variety of potential industrial applications, for which it is crucial to understand their physical antifreeze mechanism. In the medical sector AFPs may be applied for cryopreservation of blood and organs [Mugnano et al., 1995; Chao et al., 1996; Amir et al., 2004], in the food industry to control ice crystal size in order to avoid tissue injury of frozen goods and improve the taste of ice cream [Griffith and Ewart, 1995; Payne and Young, 1995; Gaukel and Spieß, 2004], and they may also be used as additives in paint and varnish to protect surfaces from ice damage [IFAM, 2006/2007]. Lately, AFPs have been proposed as hydrate inhibitors, to avoid the formation of plugs in oil and gas pipelines [Gordienko et al., 2010].

### 1.3.6. THE IAFP FAMILY

At the beginning of this work, very little was known about the AFP from *F. cylindrus* or related proteins. Hoshino et al. [2003a; 2003b] isolated AFPs from the growth media of the snow mold fungi *Typhula ishikariensis* and *Coprinus psychromorbidus*, determined TH activity, crystal habit modifications and published the sequences of various isoforms of *T. ishikariensis* AFPs. Janech et al. [2006] determined similar AFPs is the sea ice diatoms *F. cylindrus* and *Navicula glaciei*. This constituted the first molecular evidence of the presence of AFPs in sea ice diatoms, which had been presumed before [Raymond et al., 1994; Raymond and Knight, 2003]. Data for *F. cylindrus* AFP (fcAFP) were limited to sequence information of a few isoforms of the protein, obtained from a salt-stress induced cDNA library [Krell et al., 2008].
Within the last few years (2007-2010), several organisms were screened for the presence of AFPs and the family comprising the proteins from *T. ishikariensis, F. cylindrus*, and *N. glaciei* has enlarged significantly. Following Bayer-Giraldi et al. [2010] I am going to call this family IAFP, since it has been found in several sea ice organisms. A sea ice bacterium and crustacean [Raymond et al., 2007; Kiko, 2010], a polar diatom [Gwak et al., 2010], bacteria from the Vostok ice core [Raymond et al., 2008], an Arctic yeast [Lee et al., 2010] and cold-tolerant shiitake and enoki

mushrooms [Raymond and Janech, 2009] were found to have IAFPs. This wide taxonomic distribution has to my knowledge not been observed in other AFP families, and thus makes IAFPs particularly interesting from an evolutionary point of view. Moreover, the extreme conditions of the environment where these proteins appear, in sea ice organisms exposed to lower temperatures than polar fishes or most cold-tolerant crops or insects, lead to the assumption that this type of AFPs may be particularly effective. However, most studies have been limited to the identification of these proteins in the different organisms, and detailed genetic or activity analysis of this protein family, or its representatives, is scarce.

## 1.4. OBJECTIVES

This thesis tries to enhance the understanding of AFPs from the sea ice diatom *F. cylindrus*, aiming to offer a consistent analysis with first answers about the distribution and activity of fcAFPs and their effect on ice. Due to the very limited knowledge about fcAFPs, and IAFPs in general, it was first necessary to gain basic molecular information on fcAFP genes. This led to an analysis of the genes, setting them in relation to other IAFPs, and provided the background necessary for further work at protein level.

Contributions were made to:
(1) the sequence characterization of fcAFP and their genes, their diversity and phylogeny;
(2) the expression of fcAFPs and their genes;
(3) the heterologous expression of a selected isoform;
(4) the characterization of the antifreeze activity of the recombinant fcAFP;
(5) the analyses of the effect of the recombinant fcAFP on ice micro-structure and fabric.

# 2. METHODS

The methods used in this thesis can be divided into two sections, one including molecular tools and the second based on crystallographic analyses of ice. Methods reported briefly in Chapters 2.1-2.3 and part of Chapter 2.6 are explained in detail in Bayer-Giraldi et al. [2010] (Publication 1, Chapter 3.6) , the Chapters 2.6-2.9 in Bayer-Giraldi et al. [2011] (Publication 2, Chapter 3.7). Techniques not included in these publications are reported here in more detail. Methodologies applied for topics of minor relevance for this work are explained briefly when needed.

## 2.1. DETERMINATION OF fcAFP ISOFORMS

The search for new isoforms was done with polymerase chain reaction (PCR), based on IAFP genes (*iafp*) published in Janech et al. [2006] and in the genetic database GenBank provided by the National Center for Biotechnology Information (NCBI). Genes comprised 1 sequence from *N. glaciei* and 3 from *F. cylindrus*. Primers for PCR were designed manually based on conserved regions in the DNA alignment. Several PCR were run with different settings and primer combinations, products cloned into *Escherichia coli* and sequenced. After processing, fcAFP gene sequences (*fcafp*) were divided into clades based on their similarity. Each clade was defined by one representative isoform, which was used for further analyses. Similarity between the clades, inferred with the BLAST algorithm, was calculated for each isoform relative to isoform 11, chosen as reference because of its application in further molecular and crystallographic analyses.

## 2.2. PHYLOGENETIC ANALYSES

To set the fcAFPs in broader frame, putative IAFP homologues were determined by similarity search in the *F. cylindrus* CCMP 1102 genome portal (DOE Joint Genome Institute) and in the GenBank database. A phylogenetic tree of the antifreeze domains, inferred by alignment of the retrieved sequences and the fcAFPs, was set up. In a second step, selected sequences were further analyzed with different phylogenetic approaches. Moreover, IAFPs and IAFP-like sequences were screened for functional

groups, in order to better understand the evolution and possible further functions of these proteins.

## 2.3. FcAFP GENE EXPRESSION

Gene expression in *F. cylindrus* exposed to different treatments was analyzed in order to infer the trigger for *fcafp* activity. Cultures grown under optimal growth conditions (f/2 medium, 5°C, salinity 34) were divided in the middle of the logarithmic growth phase to the following treatments:

- C-treatment, control under optimal growth conditions;
- S-treatment, with increased salinity (70);
- ST-treatments, with increased salinity (70) and decreased temperature (–4°C).

Analysis of gene expression was performed with quantitative real-time PCR (qPCR). To maximize the specificity of isoform detection, problematic due to high sequence similarity, TaqMan probes were used, capable of detecting single nucleotide polymorphisms. Primers and probes were designed to detect groups of clades or, when possible, single isoforms. Physiological parameters to follow the conditions of the cultures were also measured. Analysis of cell numbers was carried out with a Multisizer 3 particle counter (Beckmann-Coulter, Germany). Maximum quantum yield at photosystem II, an indicator for general cell fitness, was detected using a Xenon-PAM-Fluorometer (Walz GmbH, Germany).

## 2.4. EXPRESSION OF RECOMBINANT fcAFP IN *E. COLI*

An expression system for an fcAFP (isoform 11) had to be established, to obtain purified proteins for downstream applications like antibody production and analyses of protein activity.

The fcAFP gene, including the predicted signal peptide, was ligated into a vector with a histidine-tag (His-tag) and cloned into *E. coli*. The expression of the recombinant protein was induced with isopropyl-β-D-thiogalactoside (IPTG), the protein extracted under native and denaturing conditions and protein purification was tried with affinity chromatography (Ni-NTA resin). For protocol details see Chapter A.3 and Figure A 2.

Finally, the heterologue expression of isoform 11 was performed at the European Molecular Biology Laboratories (EBML, Germany) following the detailed protocol at page 65. Briefly, isoform 11, without the signal peptide sequence, was expressed as a fusion protein composed of a His-tag and a SUMO3 sequence (small ubiquitin-related modifier 3) positioned N-terminal to the fcAFP (Figure A 3). The SUMO-fusions

increase expression and solubility of the recombinant protein in the host cells. Fusion proteins were purified by affinity chromatography, the N-terminal tags removed by digestion with a His-tagged SenP2 protease, the sample dialysed and the proteins isolated after a new chromatographic step.

## 2.5. BIOLISTIC TRANSFORMATION

The contribution of fcAFPs to the survival of *F. cylindrus* within sea ice may be determined by the introduction of one fcAFP gene from the polar species into a closely related, but temperate, organism. The genetic transformation of the temperate diatom *Phaeodactylum tricornutum* is often used for studies on cellular localization, when the protein of interest is fused to a green fluorescent protein (GFP) for visualization. In this study the transformation was intended to analyze the possible improvement in survival of *P. tricornutum* under subzero conditions after introduction of an fcAFP (isoform 11).

The genetic transformation of diatoms is hindered by the organisms' silica cell wall. The biolistic procedure is based on a partial damage of the cells by biolistic bombardment, which allows the introduction of genetic material [Apt et al., 1996; Zaslavskaia et al., 2000]. Diatoms are bombarded by tungsten or gold particles (microcarriers) that enter the cells and transport a vector with the gene of interest into the nucleus, where it is randomly but stably integrated into the DNA. A marker protein allows selection of tranformants.

The transformation was performed in a biolistic PDS-1000 He particle delivery system (Biorad, USA) (Figure 7). A central bombardment chamber contains the microcarrier launch assembly, consisting of the microcarriers bound to DNA and positioned on a plastic disc (macrocarrier), and a stopping screen. A Petri dish with cells is positioned at an optimal distance from the macrocarriers. Vacuum is applied to the chamber in order to reduce fractional drag on the particles during bombardment. The rupture disc separates the bombardment chamber from the gas acceleration tube, where helium gas is compressed as soon as a vacuum is reached in the bombardment chamber. After achieving a determined pressure the rupture disc bursts and a helium wave enters the chamber. The pressure fires the microcarriers into the cells, while the stopping screen retains the macrocarrier discs.

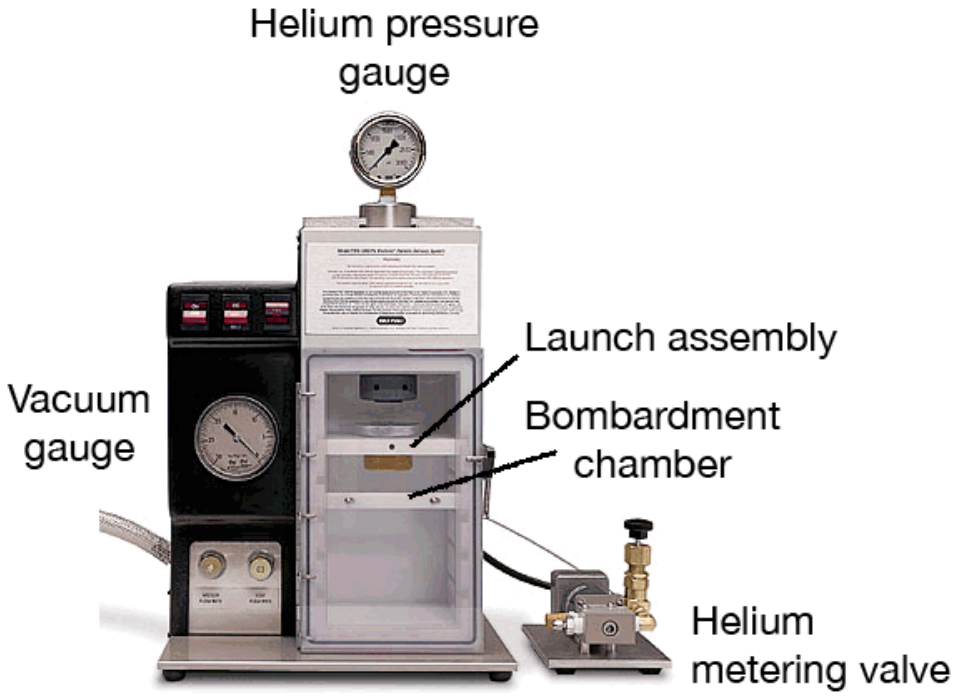


Figure 7: The biolistic PDS-1000 He transformation unit, with the bombardment chamber containing the launch assembly, vaccum and helium gauge and helium metering valve to control helium inflow. Image: www.bio-rad.com (modified).

The transformation is set up of the following steps [Kroth, 2007]: preparation of the material (cells, vector, transformation device), biolistic bombardment and selection of successful transformants. Details on the transformation protocol can be found in Chapter A.4 and Figure A 4.

## 2.6.PROTEIN ANALYSIS

The structure and expression of fcAFP was analyzed *in silica* and with immunoblotting. Signal peptide and glycosylation site predictions, amino acid composition, search for repetitive patterns was performed with different algorithms as described in Bayer-Giraldi et al. [2011].
Immunoblotting was optimized and applied for protein expression analysis using a polyclonal antibody against isoform 11 (BioGenes, Germany).

## 2.7.ANTIFREEZE ACTIVITY
## THERMAL HYSTERESIS, RECRYSTALLIZATION INHIBITION AND HABIT MODIFICATION

The determination of the antifreeze activity, defined as TH and RI effects, as well as observation of ice crystal habit modification, were carried out with a Clifton nanoliter osmometer (Clifton Technical Physics, USA). The osmometer consists of a cooling stage operated by a Peltier element, in contact wit a sample holder (Figure 8). The cooling stage is regulated by a controhller box, which permits temperature adjustment in the range of approximately 1mOs = 0.00186°C. Samples are viewed through a stereo microscope. The nanodrop osmometer allows determination of the freezing hysteresis by measuring the melting and the freezing points of 1-10 nl samples. The shock frozen samples are heated until one single crystal remains in the melt, which is then cooled until the freezing point is reached. By observing one individual crystal, the bias on the freezing point due to the supercooling effect is avoided. Sample drops are loaded into wells filled with oil to reduce sample evaporation. Furthermore, the RI effect can be estimated by shock freezing the sample at –40°C and subsequent annealing at temperatures close to the freezing point. Here, an annealing temperature of -4°C was applied for 7 hours. Crystal habit can be observed at different temperatures, within the hysteresis gap and below the freezing point.

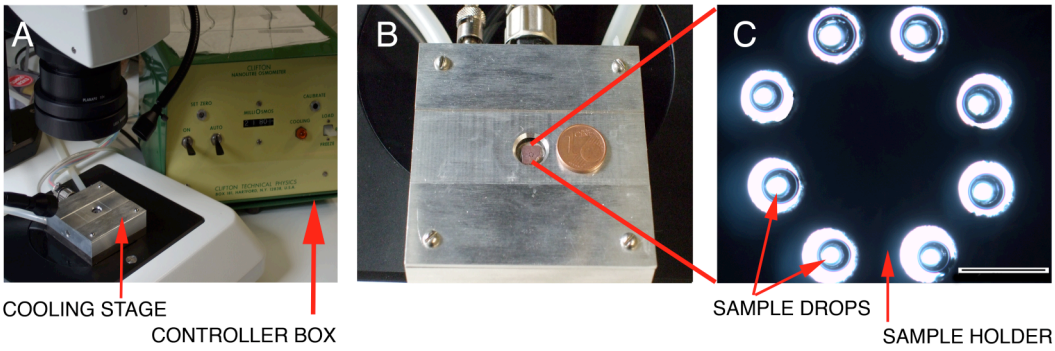


Figure 8: Clifton nanoliter osmometer and loaded samples.
A: Controller unit and cooling stage positioned on a stereo microscope;
B: Cooling stage with central sample holder, 1-cent coin for size comparison;
C: Sample holder viewed at stereo microscope, with samples within each of the 8 oil-loaded wells (the scale bar is 500 µm).

## 2.8.ICE MICROSTRUCTURE

The microstructure of ice, in the following also called ice texture, refers to the morphology, size, arrangement and substructure of single ice crystals. To analyze the microstructure of ice in the presence of fcAFPs, samples were frozen overnight and observed by reflected light microscopy in a temperature-controlled room at –20°C. Following Kipfstuhl et al. [2006], prior to observation samples were smoothed with a sled microtome to obtain polished, pristine surfaces.
Ice texture can also be observed from individual images obtained by polarization microscopy as described below.

## 2.9.ANALYSIS OF CRYSTAL ORIENTATION IN ICE

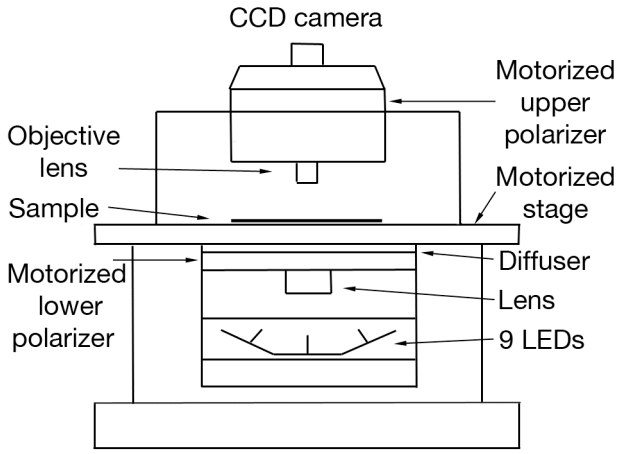


Figure 9: Schematic representation of a G50 Automated Fabric Analyzer (Russel-Head Instruments, Australia).

Analysis of the distribution of the c-axes in an assemblage of ice crystals (crystal fabric) was performed with a G50 Automated Fabric Analyzer (Figure 9), based on the polarization microscope principle [Wilen et al., 2003]. Optical methods for the determination of c-axis orientation in an ice crystal rely on the fact that ice is optically uniaxial, as light expands only along the c-axis. Hence, observing a crystal between crossed polarizers results in light extinction when held in a determined angle to the polarizers. Rotating the polarizers over a 90° range, the determination of the angle of extinction allows to find planes in which the c-axis of a crystal should lie. The combination of observations from different viewing points results in the determination of the exact direction of the c-axis within these planes. The automated optical ice fabric

analyzer used here [Wilson et al., 2007] consists of a computer-controlled microscope with motorized polarizers above and below the sample stage. The crossed polarizers are rotated between 0° and 90° in 18 small steps. The light source is given by 9 light emitting diodes (LED) positioned below the microscope stage and focusing the sample. For each of the 9 LED, a CCD camera captures 18 images at different angles of the polarizers, resulting in a total of 9 x 18 = 162 images. Individual images can also show ice texture (Figure 11). The combination of these images by the INVESTIGATOR software gives the c-axis orientation for each pixel within the sample, graphically represented in the axis-distribution diagram or AVA (Achsenverteilungsanalyse) map (Figure 12).

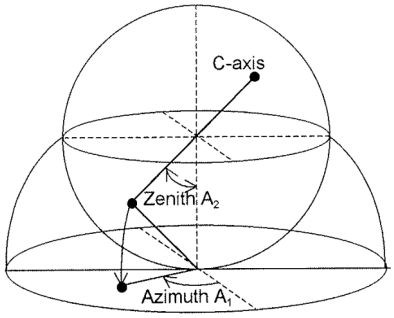


Figure 10: Representation of the c-axis direction.
Stereographic projection - C-axis direction, specified by polar (zenith) and azimuthal angles, is first represented as a point on a hemisphere, further projected on the observation plane. Image from Wang [1999].

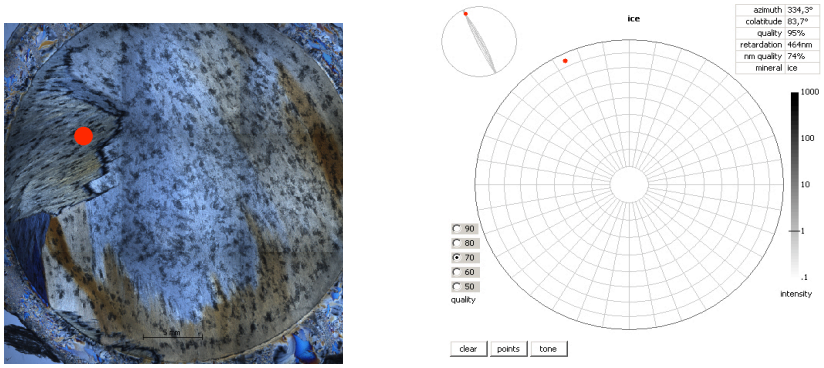


Figure 11:
Left: Single image of an ice sample viewed through crossed polarizers. The c-axis direction of the selected crystal (red dot) is shown on the right.
Right: The c-axis direction of the selected crystal is shown as stereographic projection parallel to the observed section plane. The c-axis represented here is shown to be nearly horizontal in N-NW direction.

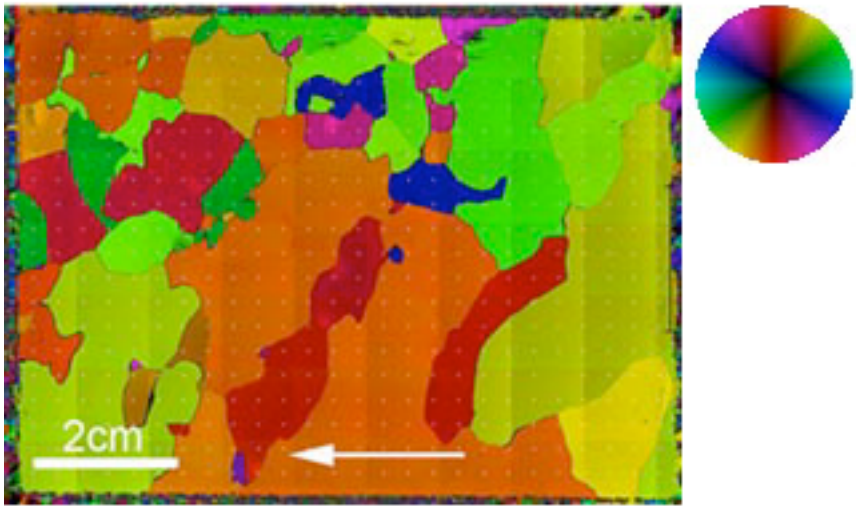


Figure 12: Example of a c-axis distribution diagram. The ice sample originates from the NEEM ice core (Greenland). The color direction wheel shows the color coding. Each color corresponds to a direction on the observation plane (azimuth) whereas the color intensity, from light on the margin to dark in the center, represents c-axis angle from horizontal, which increases from the periphery to the center.
Image: http://www.awi.de/de/forschung/fachbereiche/geowissenschaften/glaziologie/techniques/automated_fabric_analyzer/

# 3. RESULTS AND DISCUSSION

A first characterization of fcAFPs is presented here. Results of a molecular characterization of fcAFPs and their genes, a description of the antifreeze activity (TH and RI effects) of a selected fcAFP isoform and crystallographic analyses of its effect on ice structure are shown.
Data are presented and discussed in detail in Publication 1 (Chapter 3.6, [Bayer-Giraldi et al., 2010]) and in Publication 2 (Chapter 3.7, [Bayer-Giraldi et al., 2011]). Here, results discussed in these papers are briefly summarized and presented together with additional aspects not included there. Also, selected images from publications are presented here in a broader context than in the condensed text of the papers, with more information and additional pictures.

## 3.1. DIVERSITY AND EVOLUTION OF fcAFPs

Until now, research about IAFPs was mainly focused on interspecific diversity, and little was known about the diversity of fcAFP genes (*fcafp*s) within *F. cylindrus*. In the following, a genetic characterization of fcAFPs is presented. Starting from three fcAFP gene sequences published in Krell et al. [2008] the genome of *F. cylindrus* was searched by PCR for further *fcafp*s. The isoforms were characterized at a sequence level, set in a phylogenetic framework developed for the IAFP family and analyzed in terms of possible protein evolution.
This chapter contributes to objective 1 presented on page 13.

### 3.1.1. SEQUENCE ANALYSES

AFPs in *F. cylindrus* were shown to be a multigene family, composed of 10 different clades of isoforms [Bayer-Giraldi et al., 2010] (Table 2).

| Isoform | 1 | 2 | 3 | 5 | 6 | 7 | 8 | 9 | 10 | 11 |
|---|---|---|---|---|---|---|---|---|---|---|
| Acc. Nr. | GQ232744 | GQ232745 | GQ232746 | GQ232747 | GQ232748 | GQ232749 | GQ232750 | EL737280 | EL737258 | DR026070 |
| Identity | 94% | 92% | 95% | 87% | 80% | 84% | 80% | 57% | 83% | - |

Table 2: FcAFP isoforms, with corresponding GenBank Accession Numbers and protein identity to isoform 11, inferred with the BLAST algorithm.

Sequence analyses of the fcAFPs as conceptual translations of the genes revealed high similarity among the sequences, with 80-95% identity to isoform 11 (Table 2, [Bayer-Giraldi et al., 2011]). Amino acid contents of the different isoforms showed high amounts of alanine (10-13%), glycine (10-12%) and threonine (10-13%), and no cysteine. The distribution of the most common amino acids is consistent with results of other AFPs [DeVries, 1983; Hon et al., 1994; Graham et al., 2007], whereas the absence of the disulfide-bonds forming cysteine, relevant to protein folding, is striking. However, also the IAFP from *T. ishikariensis* showed no cysteine [Xiao et al., 2010].
Whereas most isoforms showed high sequence similarity, isoform 9 differed from the other sequences, with 57% identity to isoform 11 and one cysteine residue (Table 2).
Analyzed sequences were predicted to have a signal peptide, a N-terminal protein sequence which targets a protein for translocation across the cell membrane. After passing the membrane, the signal peptide may be cleaved, releasing the protein, or may remain integrated into the cell membrane and connect the extracellular protein to the cell. Low anchor probability suggests that after translocation the fcAFPs are released into the extracellular space. However, due to the morphology of diatoms, covered by a silica cell wall, proteins may be integrated into the wall, similarly to frustulins, silaffins or HEP200 which also have a signal peptide [Kröger et al., 1996; Kröger et al., 1997; Sumper and Kröger, 2004].

## 3.1.2. PHYLOGENY AND EVOLUTION

### *3.1.2.1. Phylogenetic analysis*

The fcAFP genes showed interspecific and intraspecific diversity when compared to the *fcafp*s of *F. cylindrus* CCMP 1102, recently sequenced at the JGI (USA), and to the polar diatom *Fragilariopsis curta*, respectively [Bayer-Giraldi et al., 2010]. Intraspecific differences may be due to the different strain types isolated both from the Weddell Sea, the strain used here originating from sea ice samples, strain CCMP 1102 from the water column of 20 years earlier.

The wide taxonomic distribution of IAFPs or IAFP-like proteins (Figure 13) detected by similarity search in Antarctic diatoms and bacteria, sea ice crustaceans, Arctic yeasts and cold-tolerant fungi, as well as in the genome of several other bacteria and archaea [Bayer-Giraldi et al., 2010] deserves a special mention here. All other AFP families are restricted to defined taxonomic groups, and different AFPs show a somehow random distribution in different, but related, groups. Closely related species like longhorn and shorthorn sculpins are protected from ice damage by different types of AFPs, both by type I and only the former by type IV, whereas fish gycosylated

AFPs (AFGPs) have undergone convergent evolution and developed in unrelated fishes like Antarctic notothenoids and Arctic cod [Cheng, 1998; Low et al., 2001]. The distribution of IAFPs across different kingdoms raises the question of the possible evolution of these genes.

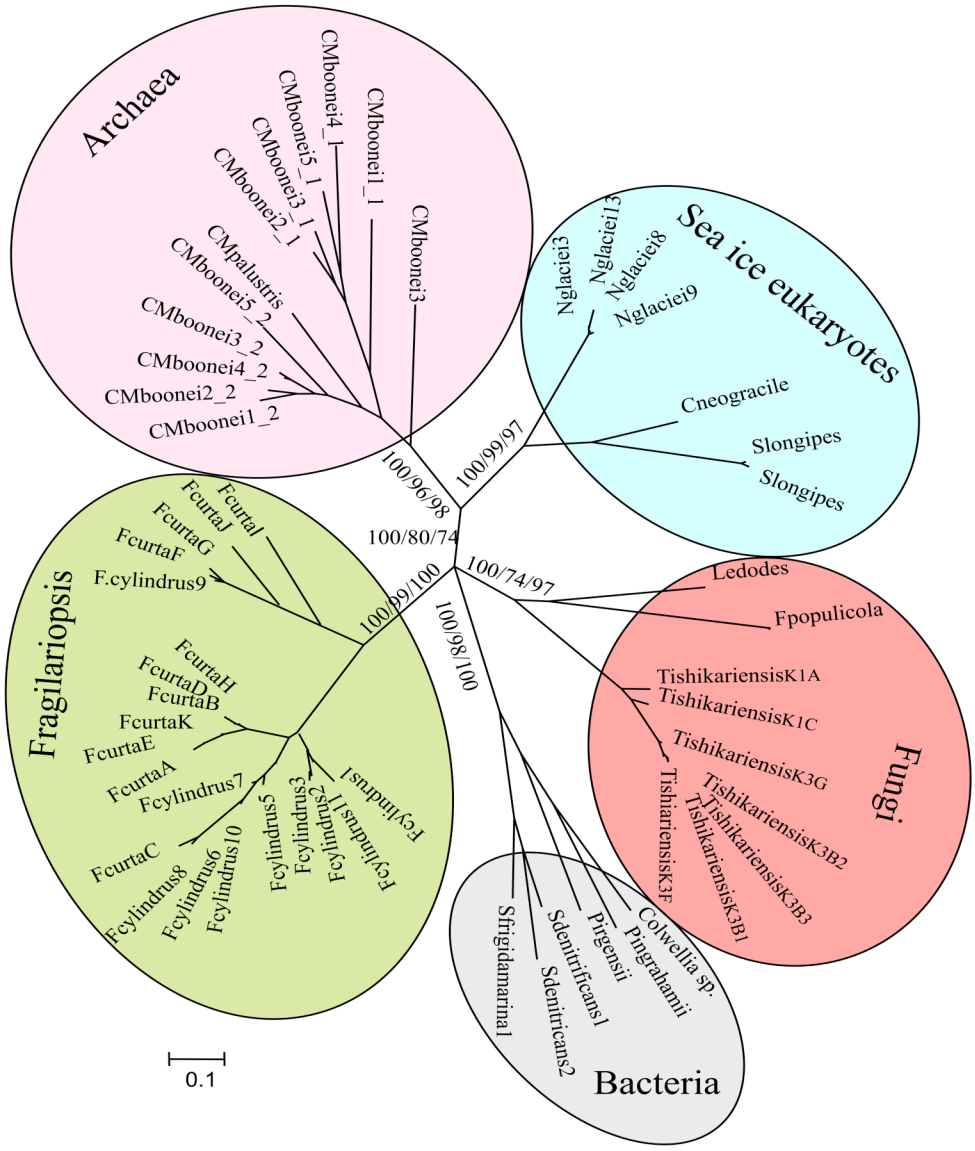


Figure 13: Molecular phylogeny of selected IAFPs based on Bayesian inference (unrooted tree). Bootstrap support at selected nodes is shown for Bayesian inference, Maximum Likelihood and Maximum Parsimony, which showed essentially the same topology. Algorithms and settings were as follows: MrBayes version 3.1.2 for Windows with posterior probabilities derived from 80,000 generations (four chains), random starting tree, sample frequency 100, WAG amino acid substitution model and discarding a burnin of 500; PAUP* 4.0b10 for Macintosh, simple weighting, 100 bootstraps; PhyML 2.4.4 with WAG amino acid substitution, initial tree BIONJ, gaps included, 100 bootstraps. Image from Bayer-Giraldi et al. [2010], with permissions.

### *3.1.2.2. Evolution in sea ice*

The patchy distribution of IAFP and IAFP-like proteins, revealed by the phylogenetic analysis, suggests that the genes are not orthologous, i.e. divided by speciation events [Bayer-Giraldi et al., 2010]. The phylogenetic tree indicates one or more events of horizontal gene transfer (HGT) or convergent evolution. Diatom IAFP are divided into different clades, one with the *Fragilariopsis* group and one containing *N. glaciei and Chaetoceros neogragile* (Figure 13). This distribution does not reflect organisms phylogenetic relationships, since *Fragilariopsis* and *Navicula* are raphid pennate diatoms [Lundholm et al., 2002] whereas *Chaetoceros* belongs to the order Centrales [Oh et al., 2010]. Instead, it indicates separated and repeated steps in the evolution of IAFPs within diatoms. The *Fragilariopsis* proteins are closely related to fungi and bacterial IAFPs. Both clades, the fungal (Basidiomycota) and the bacterial, contain organisms related to sea ice species. Basidiomycota have been reported to inhabit sea ice and the bacterium *Shewanella* is well known from sea ice studies [Janech et al., 2006]. It is therefore conceivable that the three clades acquired the IAFP genes from each other by HGT, as discussed in the following.

Gene duplication, followed by neo- or subfunctionalization, is one of the major driving forces of evolution. It has been reported in situations of cold stress, since multiple gene copies may compensate for reduced protein activity due to low temperatures, and furthermore new protein functions may be an advantage in a changed, colder environment [Zhang, 2003; Carginale et al., 2004]. When no putative common ancestor organism containing the original gene can be identified, genes have probably developed by convergent evolution or spread by horizontal gene transfer. Convergent evolution is easier to conceive having a sequence with a repetitive pattern, which may have arisen due to multiple duplications. Repeats are a common feature in AFPs due to the required regular matching between the protein and the ice lattice. However, convergent evolution is more puzzling with sequences like fcAFPs, showing no repeats. Horizontal gene transfer, the uptake of genetic material by an organism without reproduction, is known from Eukaryotes [Andersson, 2005], and it was shown that up to 14.5% of the bacterial and archaeal genes were acquired by HGT [Garcia-Vallvé et al., 2000]. Some studies showed that HGT frequency is dependent on donor concentration [Frischer et al., 1994; Dröge et al., 1998], and that it is higher at the solid-liquid interface than in the liquid phase [Lorenz et al., 1988]. Sea ice may represent a “hot spot” of HGT. The high concentration of extracellular DNA detected in sea ice brine (max. value 135 mg $L^{-1}$), enriched on average up to 13 times compared to under ice waters [Collins and Deming, 2011], the numbers of potential donor or receiving organisms, densely attached to the surface of the brine inclusions, and the

solid ice surface which may act as a stabilizing substrate for attached DNA, could offer more favorable conditions for HGT than seawaters.

Therefore, in the context of IAFP evolution, I suggest that HGT events should happen with a higher probability compared to convergent evolution, given the structure of the IAFP sequences, which lack any repetitive pattern, and the close proximity of different organisms within sea ice.

**CONTRIBUTION TO OBJECTIVE 1:**
This chapter contributes to objective 1 on page 13 about sequence characterization of fcAFP and their genes, their diversity and phylogeny. Results showed a high number of *fcafp* isoforms, a broad distribution in polar organisms and an apparent acquisition by HGT, indicating a great relevance of the IAFP genes for polar and cold-tolerant organisms. The remarkable taxonomic distribution of IAFP and IAFP-like genes, unknown from other types of AFPs in terrestrial or aquatic environments, could be explained by enhanced HGT, facilitated by the convenient conditions within sea ice.
The results are addressed in Publication 1 and Publication 2.

## 3.2.GENE AND PROTEIN ACTIVITY

This chapter focuses on objective 2 presented on page 13 concerning gene and protein expression, tries to characterize their regulation under environmentally relevant conditions and determine the trigger for *fcafp* expression. Cultures of *F. cylindrus* cultivated at optimal growth conditions (C-treatment) were exposed to stress treatments of high salinities alone (S-tretment) and combined with low temperature (ST-treatment) (for experimental set-up see page 15). Results presented here were obtained after qPCR analyses of gene expression and immunoblots for studies on protein expression in cells from control and stress treatments.

### 3.2.1. GENE EXPRESSION

Different genes showed different regulation patterns dependent on time and on treatments, as shown by qPCR (Figure 14) [Bayer-Giraldi et al., 2010]. The most prominent results were found in treatment ST. Whereas the expression of the group of isoforms 1+6 and of isoform 8 approached 0 already 2 days after the beginning of the treatments, groups 3+10, 5+11 and 2+5+11 were strongly upregulated. The expression of these groups of genes peaked on day 14 (groups 5+11 and 2+5+11) with up to 120-

fold upregulation and on day 20 (group 3+10) with 200-fold upregulation compared to the expression on the first day of the experiment.

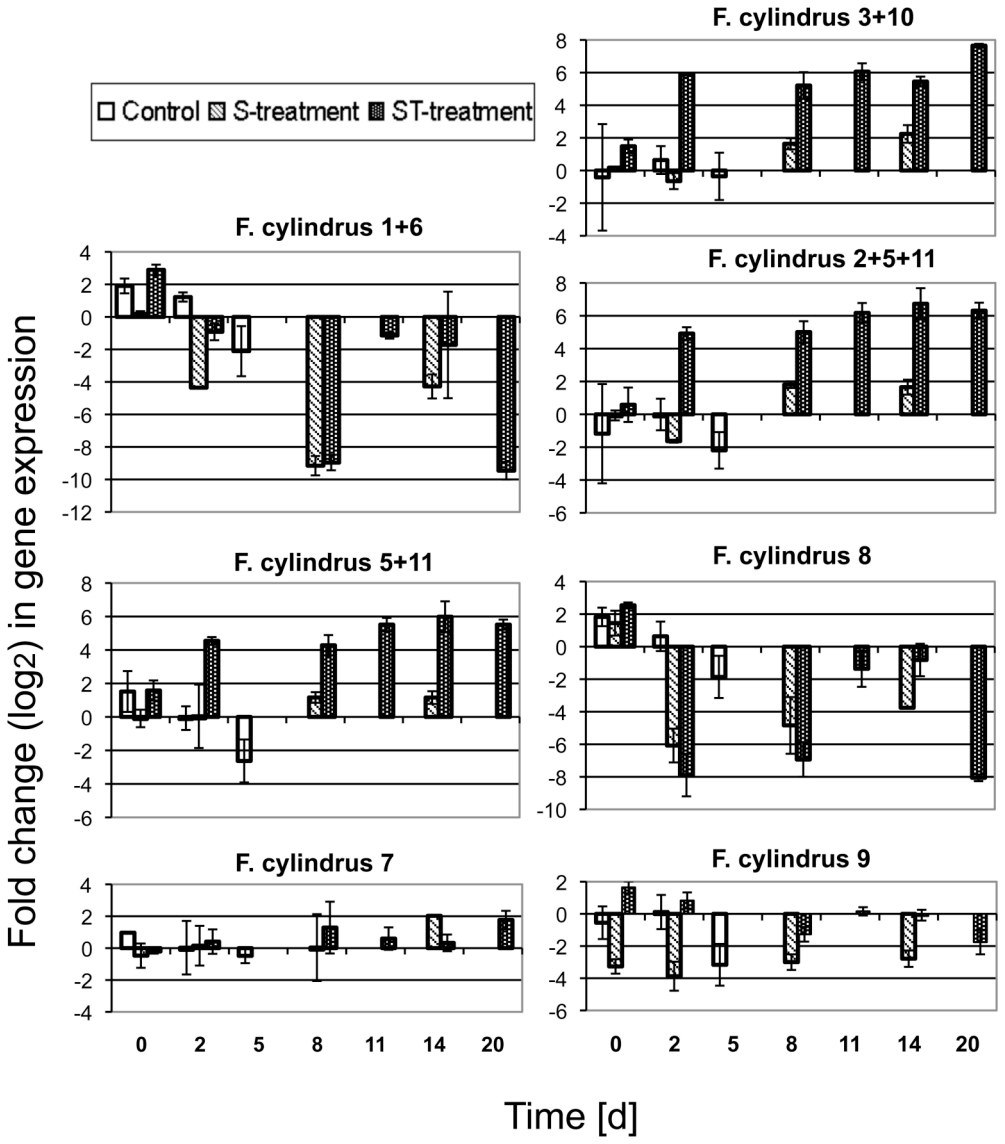


Figure 14: Quantitative real-time PCR analyses of *fcafp* expression. Change in expression of single isoforms or a set of isoforms are shown. Results are represented as log2 of fold change values. Image modified after Bayer-Giraldi et al. [2010], with permissions.

The strong gene upregulation in the ST-treatment was not observed in the C- or the S-treatments, suggesting that low temperatures, more than low cell fintness (C-treatment) or salt (S-treatment) are the major trigger for *fcafp* expression. Krell et al. [2008] first

observed *fcafp*s in a salt-stress induced cDNA library, and salt was suggested as the major trigger for fcAFP gene expression. However, experimental conditions applied (temperature 0°C, salinity increase from 33.6 to 60) did not resemble natural conditions in sea ice. Here experimental treatments better reflect environmentally relevant conditions.

## 3.2.2. PROTEIN EXPRESSION

Differential activation of *fcafp*s was mirrored in protein expression, as revealed by immunoblotting [Bayer-Giraldi et al., 2011]. The pattern of expressed proteins, revealed by the blotting, changed dependent on time and treatment (Figure 15). A quantitative estimate of fcAFPs on day 20 was in the range of 0.7 fg/cell.

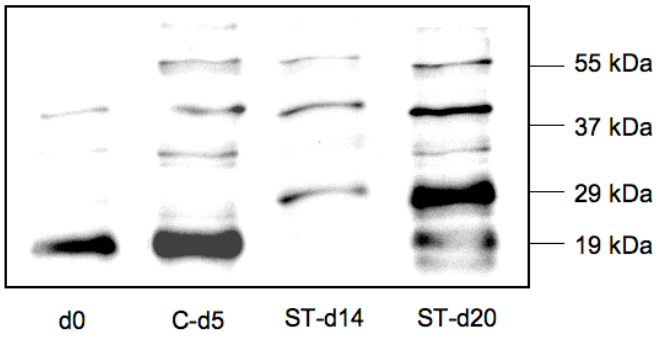


Figure 15: Immunoblotting of fcAFPs. d0: expression before separation of batches into C-and ST-treatments (day 0); C-d5: expression in the C-treatment at day 5, when cultures in control batches had reached stationary phase; ST-d14 and ST-d20: expression in the ST-treatment at days 14 and 20, respectively, when cells had reached the end of the logarithmic growth phase after recovery from the temperature and cold shock and fcAFP gene expression was highest. Image from Bayer-Giraldi et al. [2011], with permissions.

This value represents the lower range of fcAFP concentration in Uhlig et al. (in preparation, Chapter A.1 - Publication 3). However, these results are based on immunoblotting with polyclonal antibodies against isoform 11. Due to high sequence similarity between fcAFPs, the antibody should detect also other isoforms, but may not recognize all. Therefore, it underestimates the amount of total fcAFPs in the cell, which however I would expect to be in the same range. Results show fcAFPs related to the cells, which means within the cell or attached to them.

### 3.2.3. ONLY ONE FUNCTION OF fcAFPS?

The differential response of the *fcafps* could indicate a successive activation of the different isoforms, with some genes responsible for early response and other for long-term acclimation. Alternatively, fcAFPs could have another, still unknown function.
Several protein domains, situated N- and C-terminal of IAFP or IAFP-like domains, suggest a relation to adhesins, surface proteins that mediate cell-cell interactions in, for example, pathogenic proteobacteria (*E. coli, Bordatella pertussis, Yersinia*). Phylogenetic studies and analyses of IAFP and IAFP-like domains (see Bayer-Giraldi [2010] for details) led to the assumption that the proteobacterium *Shewanella frigidamarina* may have played a relevant role in the evolution of IAFPs, with events of duplication and subfunctionalization. It is conceivable that *S. frigidamarina* evolved its cell-binding sequence to an ice-binding domain.

### 3.2.4. THE ROLE OF E/G POINT MUTATION

Sequence analysis indicated a point mutation involving glutamic acid (E) and glycine (G) in position 18 of the alignment of *F. cylindrus* mature isoforms (Figure A 1) as possibly involved in protein activity [Bayer-Giraldi et al., 2010]. Whereas the polar glutamic acid is present in the genes upregulated under temperature and salt stress, it is replaced by the non-polar glycine in the down-regulated or not regulated sequences ( Figure 14). Several studies showed the important role single point mutations play in the activity of AFPs when the involved amino acids are in positions crucial for attachment to ice [Li and Hew, 1991; Cheng and Merz, 1997; Bar et al., 2008; Middleton et al., 2009]. Neofunctionalization related to the E/G replacement, resulting in higher TH or RI activity of the protein, may explain differential expression.
However, recent studies of the 3D structure of the *Typhula* IAFP (H. Kondo, AIST Sapporo, Japan, pers. comm.) shed light on possible binding sites of the protein to ice (Figure 16). A comparison of the fcAFP sequences with the similar *Typhula* protein (identity 45%, positives 60%, e-value 1e-47 as calculated with the BLAST algorithm) suggests that position 18 of the fcAFP should not be involved in ice binding.

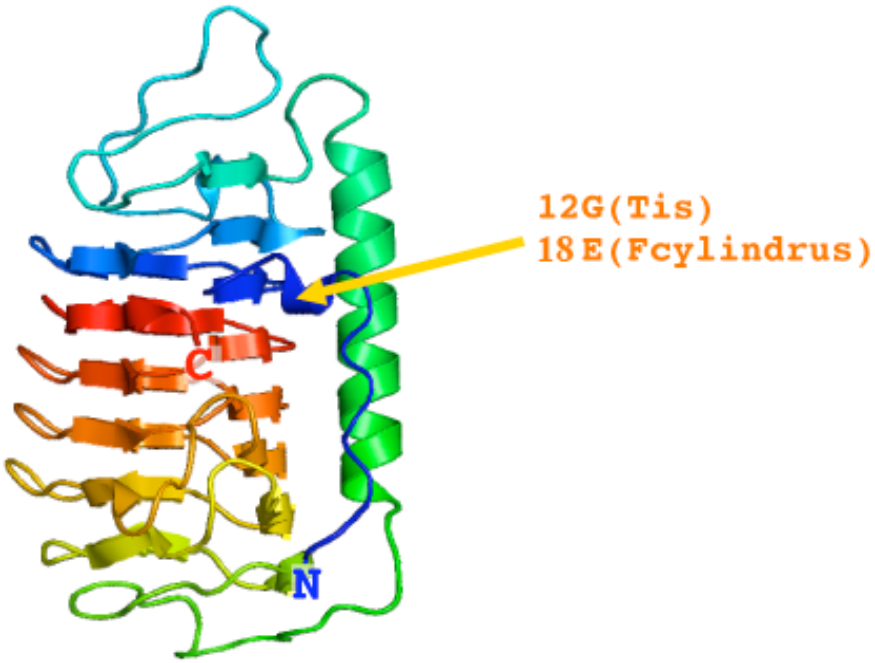


Figure 16: 3 D structure of the *T. ishikariensis* AFP with marked 12G position, corresponding to position 18 with the E/G point mutation in *F. cylindrus*. Image: Courtesy of H. Kondo, AIST Sapporo, Japan.

**CONTRIBUTION TO OBJECTIVE 2:**

This chapter is a contribution to objective 2 presented on page 13 and presents results on gene and protein expression under environmentally relevant conditions.

Gene and protein expression showed differences dependent on isoform type. Low temperature and high salinity triggered high upregulation of selected isoforms. A parallel, unknown function of fcAFPs is possible.

These topics are addressed in Publication 1 and Publication 2.

## 3.3. HETEROLOGOUS EXPRESSION OF AN fcAFP

In the following results of heterologous expression of a selected *fcafp* are shown (contribution to objective 3, page 13). The expression was tried in *E. coli* in order to obtain a recombinant, pure fcAFP isoform to use for downstream applications like protein activity characterization. Furthermore, heterologous expression was tried in the temperate diatom *P. tricornutum*, aiming to test whether the acquisition of an *fcafp* increases cold-tolerance of a recombinant, non-polar diatom.

## 3.3.1. EXPRESSION IN *E. COLI*

The expression of the recombinant protein (isoform 11) in *E. coli* resulted in a series of problems. In the subsamples taken 1, 2, 3 and 4 hours after induction with IPTG and observed with electrophoresis before treatment with the Ni-NTA resin, it was difficult to recognize the recombinant fcAFPs, due to the high density of *E. coli* proteins that may have masked the presence of the recombinant protein. However, results suggested a possible expression of the protein of interest 3 hours after induction. Visualization of the sample after treatment of the cell lysate with the Ni-NTA resin revealed no fcAFP in the eluate. Variations in the experimental conditions and extraction protocols did not lead to any improvement.

Further experiments at the EMBL led to comparable problems. However, purification was successful when the gene of interest was inserted into the vector without the predicted signal peptide sequence. It seems therefore that the signal peptide resulted in the formation of hydrophobic interactions between proteins that may have formed agglomerates, which clogged the Ni-NTA silica matrix.

## 3.3.2. EXPRESSION IN *P. TRICORNUTUM*

Repeated transformations of *P. tricornutum* did not lead to successful insertion of the fcAFP gene. The bombardment resulted in few transformants containing the selectable marker gene *sh ble* and thus resistant to Zeocin (Table 3).

| Microcarrier | Number of bombardments | Number of colonies | Efficiency |
|---|---|---|---|
| Tungsten | 13 | 4 | 0.3 / $10^8$ cells |
| Gold | 5 | 24 | 4.8 / $10^8$ cells |

Table 3: Recovery of resistant colonies after biolistic transformation with different microcarriers.

The largest number of transformed colonies was obtained when bombarding with gold particles. Gold microcarriers have the advantage of being of regular, spherical shape, which reduces the damage to the cells. However, PCR with primers for the *sh ble* and the *fcafp* confirmed the presence of the first, but could not detect the *fcafp* insert in any of the colonies. It seems that the DNA was not entirely integrated into the genome of *P. tricornutum*, but that the plasmid was being fragmented during the transformation procedure, as suggested by Armaleo et al. [1990]. The absence of the *fcafp* could be

due to an unknown toxic effect of the fcAFP, which would lead to a selection of the transformants missing the fcAFP gene. It could also be due to the low efficiency of the transformation which could be solved by further increasing the number of bombardments. However, it is unclear if after successful transformation of *P. tricornutum* with the *fcafp* this temperate diatom species would be tolerant to freezing conditions. Mock et al. [2005] analyzed the most frequently expressed genes in *F. cylindrus*, detected as expressed sequence tags (ESTs), and showed that cold adaptation in this organism is mostly related to genes specific for this diatom species. After exposure to subzero temperatures, six out of the ten most frequent ESTs were of unknown function, two (encoding Calmodulin-like and Sm-like proteins) were of not specific function. All ten ESTs were not related to genes from other temperate diatoms (*Thalassiosira pseudonana* or *Phaeodactylum tricornutum*). Therefore it seems unlikely that the fcAFP may adapt *P. tricornutum* to freezing conditions without the interplay with other proteins (not present in this temperate species).

**CONTRIBUTION TO OBJECTIVE 3:**
This chapter contributes to answers questions about heterologous expression of an fcAFP isoform (objective 3 on page 13).
The expression of the recombinant fcAFP (isoform 11) in *E. coli* and its isolation under native conditions with affinity chromatography over a Ni-NTA silica resin was not possible without removal of the signal peptide from the sequence of interest. The transformation in *P. tricornutum* was not successful probably due to a (still unknown) toxic effect of fcAFP in this temperate species or to generally low transformation efficiency.

## 3.4.ANTIFREEZE ACTIVITY OF A RECOMBINANT fcAFP

A characterization of the antifreeze activity of a recombinant fcAFP follows here the molecular characterization presented in the previous chapters. The activity was determined in terms of TH and RI at the nanoliter osmometer. Furthermore, results about modifications of ice crystal habit in the presence of fcAFPs are presented here, completed with speculations about possible crystallographic sites of protein-ice interaction.
This chapter is a contribution to objective 4 (page 13).

### 3.4.1. THERMAL HYSTERESIS

The recombinant fcAFP showed TH up to 0.9°C (Figure 17) [Bayer-Giraldi et al., 2011]. The hysteresis effect was detected at protein concentrations in the range from 1.2 µM to 345 µM (plateau reached at 230 µM). Higher concentrations were difficult to measure due to technical constraints (opacity of the sample). Therefore, the protein is classified as moderate, similar to fish AFPs. Thermal hysteresis values were already reached at a lower concentration than reported for fish AFPs, indicating, similar to *Typhula* IAFP [Xiao et al., 2010], a higher effectiveness of fcAFPs compared to other moderate AFPs.

Some publications report only low degree of TH caused by IAFPs [Raymond et al., 2007; Raymond and Janech, 2009]. However, these studies refer to proteins isolated from their natural environment, where IAFP concentrations might be low. Working with the recombinant protein enabled analyses at several concentrations.

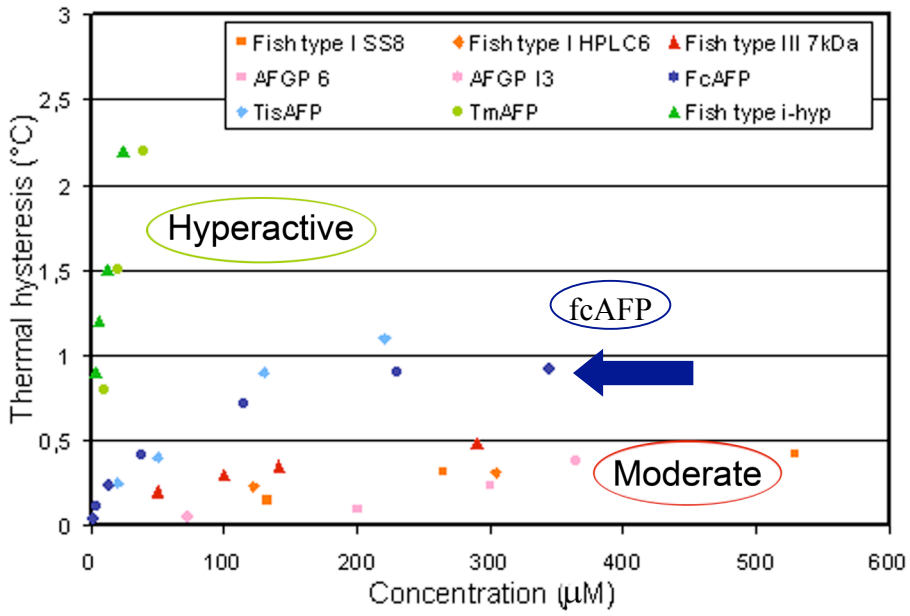


Figure 17: Thermal hysteresis activity of ● fcAFPs and selected hyperactive and moderate AFPs.
Hyperactive AFPs include ● *Tenebrio molitor* isoform 4-9 (TmAFP) [Marshall et al., 2004a] and ▲ fish type I-hyp [Marshall et al., 2004b]; moderate AFPs include fish type I, ■ isoforms SS8 [Baardsnes et al., 2001] and ◆ HPLC6 [Chao et al., 1997], ▲ fish type III (7kDa) [DeLuca et al., 1998], ■ AFGP 6 [Schrag et al., 1982], ● AFGP $I_3$ [Wu et al., 2001], ◆ *T. ishikariensis* wild type (TisAFP) [Xiao et al., 2010]. Images from Bayer-Giraldi et al. [2011], with permissions.

## 3.4.2. RECRYSTALLIZATION INHIBITION

The recrystaliization inhibition effect (annealing for 7 hours at –4°C) was strong at concentrations down to 1.2 µM and still weakly observed at 0.12 µM, which was defined as the endpoint concentration below which no RI could be detected (Figure 18) [Bayer-Giraldi et al., 2011]. Other AFP solutions showed RI endpoints between 0.2 µM and 1.3 µM [Knight and Duman, 1986; Smallwood et al., 1999; Sidebottom et al., 2000; Tomczak et al., 2003] are therefore mostly less effective than fcAFP in RI.

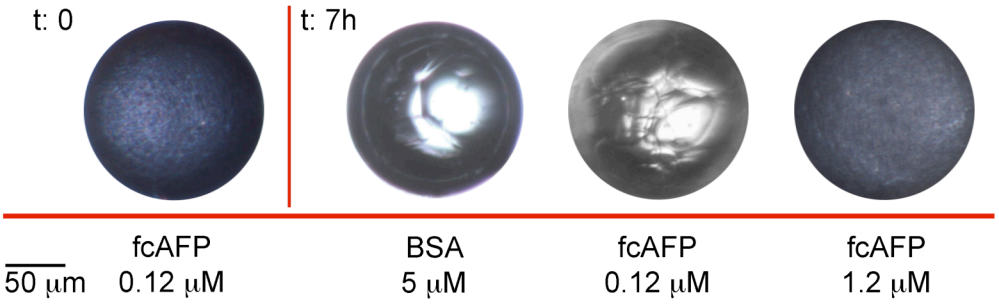


Figure 18: RI in negative control (BSA) and fcAFP solutions at different concentrations. At shock freezing at -40°C (t: 0) a polycrystalline structure formed, with single crystals too small to be distinguished at light microscopy. After 7 hours at –4°C, in the control sample single crystals of approx. 50 µm formed by recrystallization. The fcAFP samples showed little (0.12 µM) or no (1.2 µM) recrystallization. The recrytsallized sample appeared clear due to higher light transmission through the lower number of crystals, compared to the optic thick (dark) polycrystalline sample with fcAFPs. Images from Bayer-Giraldi et al. [2011].

## 3.4.3. THE EFFECT OF SALTS

The effect of salt on antifreeze activity was show to be enhancing [Bayer-Giraldi et al., 2011]. Thermal hysteresis of saline fcAFP solutions (salinity 60) were increased by 2-3 times compared to less saline conditions (phosphate buffered saline solution, PBS; salinity 10) and reached 2.5°C freezing point depression (325 µM) (Figure 19). Higher values may be possible, but could not be detected due to opacity of the sample at higher protein concentrations.

Endpoint concentration for RI shifted down one order of magnitude compared to the less saline solutions, and a moderate RI effect was still observable at 0.012 µM fcAFP.

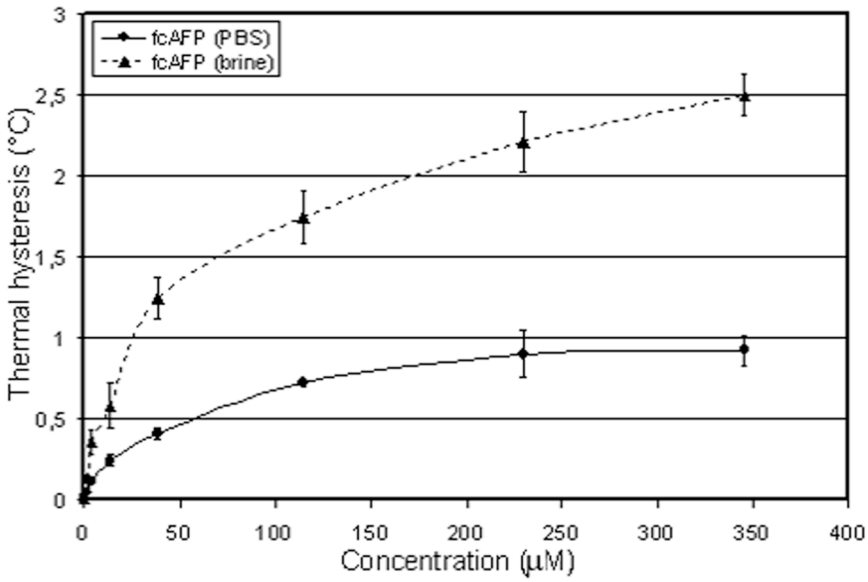


Figure 19: The hysteresis in phoshate buffered saline solution (PBS; salinity 10) and brine (salinity 60) is shown in relation to fcAFP concentration. Image from Bayer-Giraldi [2011] with permissions.

The enhancement of antifreeze activity by salt may be due to a salting-out effect, as suggested by Kristiansen et al. [2008]. The solubility of proteins in the liquid phase is influenced by salts. In the specific case of fcAFPs, it is assumed that in a saturated, liquid saline protein solution, more fcAFPs would precipitate on the ice surface region, increasing local protein concentration and thus antifreeze activity, compared to a less saline solution [Kristiansen et al., 2008].

### 3.4.4. CRYSTAL HABIT

Crystals growing in a solution of fcAFPs had a characteristic shape [Bayer-Giraldi et al., 2011], which was related to the proteins' attachment sites. Crystals slowly growing from a liquid phase without AFP develop a flat, discoid shape expanding perpendicular to the c-axis. This shape was observed here with a control protein (bovine serum albumine, BSA) known to have no antifreeze activity. Grains growing in the presence of fcAFPs had a hexagonal habit that gradually changed into a star-like shape with a six-fold symmetry (Figure 20, A). The basal plane of the crystal continued expansion and eventually the grain developed also in direction parallel to the c-axis, until the solution drop was completely frozen (Figure 20, B). The shape of the frozen fcAFP

solution droplet deserves special remark here. The solution was suspended in oil and able to expand and change its shape. Parallel striations sorrounding the round frozen droplet could be observed at 115 µM (Figure 20, C). At higher concentrations droplets developed ramified protrusions (Figure 20, D). These patterns were only observed after freezing at high protein concentration and were probably related to the high degree of supercooling (and therefore high growth velocities) at the hysteresis freezing point. In supercooled waters, the latent heat of fusion is transferred away from the crystal faster at dendritic tips than from a circular crystal, therefore dendrites develop more easily at larger supercoolings [Hobbs, 2010a]. The strong TH effect at 230 or 345 µM fcAFP resulted in a strong supercooling of the sample and a high growth rate after the freezing burst, which probably caused the development of protrusions. The same effect could not be obtained by cooling less concentrated fcAFP solutions, probably because the temperature adjustment in the nanoliter osmometer was too slow to reach effective supercooling below the hysteresis freezing point, and corresponding growth rates.

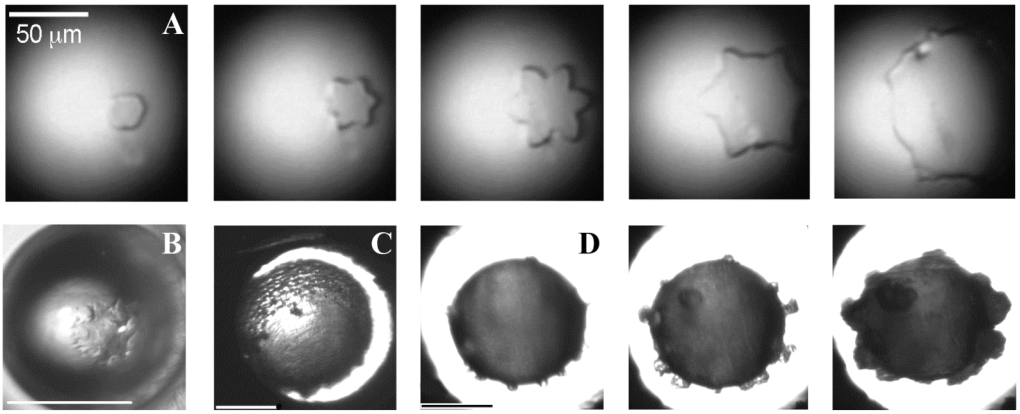


Figure 20:

A: Picture sequence showing the habit of a single ice crystal growing in a diluted fcAFP solution (0.012 µM). The pictures were taken in time intervals of approx. 10 seconds. Images from Bayer-Giraldi et al. [2011], with permissions.
B: Frozen droplet of fcAFP solution. The core of the crystal is visible in the center.
C: Frozen droplet (dark) floating in oil (white circle). The frozen fcAFP solution (115 µM) shows parallel striations on the droplet surface.
D: Picture sequence showing the evolution of protrusions formation in a frozen fcAFP solution (230 µM).

## 3.4.5. PROTEIN-ICE INTERACTION SITES

The observation of the ice crystal habit can shed light on the crystallographic sites of interaction between ice and the attached protein. The inhibition of crystal growth in the direction perpendicular to the c-axis, resulting in hexagonal and star-like shapes [Bayer-Giraldi et al., 2011], indicates protein attachment to the lateral planes of the crystal.

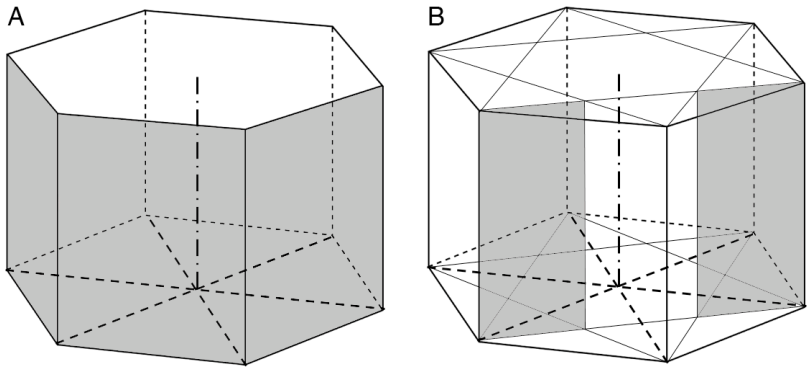


Figure 21: Schematic representation of the hexagonal crystal structure of ice, with c-axis, a-axes and marked primary (A) and secondary (B) prismatic faces.

A comparison between the habit in the presence of fcAFP and in the presence of poly(vinyl alcohol) (PVA), which also caused star-like morphologies [Budke and Koop, 2006], suggests that fcAFPs may bind to the same planes of the ice crystals as PVA, i.e. to the primary and secondary prismatic planes (Figure 21). However, fcAFPs probably also bind to other ice planes, as shown in pitting experiments [Bayer-Giraldi et al., 2011]. The experiments (measurements carried out by J. Raymond, University of Nevada Las Vegas, USA) were performed by submerging a pure crystal in an fcAFP solution slightly below its freezing point and observing its growth under the microscope. According to Raymond [1989], pits are defects in the crystal that form because of inhibition of ice growth in determined points of the grain, due for example to bound AFPs (Figure 22).

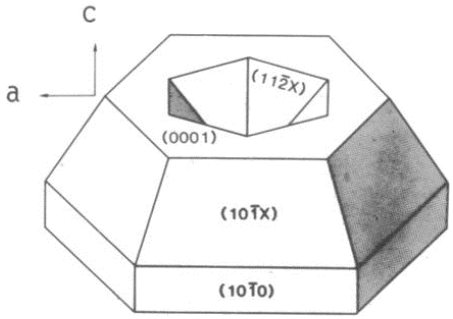


Figure 22: Schematic representation of the formation of pits on the basal plane of an ice crystal. Pits form due to punctual growth inhibition and they expand with growing ice. Image from Raymond et al. [1989], with permissions.

Pits observed on the basal plane of the crystals (Figure 23) indicate an attachment to the basal plane itself or any non-prismatic plane. Results suggest that fcAFPs bind to ice in a complex way at multiple planes.

**CONTRIBUTION TO OBJECTIVE 4:**

This chapter gives a contribution to objective 4 presented on page 13 concerning the antifreeze activity (TH and RI) of a recombinant fcAFP isoform. Results showed that the analyzed fcAFP had moderate TH and high RI activities. The effects were more pronounced in concentrated saline solutions. Furthermore, observation of the crystal habit indicative of inhibited growth perpendicular to the c-axis and pits formation on the basal plane suggest multiple crystallographic sites of interaction with the protein. Primary and secondary planes as well as other non-prismatic face are suggested as attachment sites.

These results are presented in Publication 2.

Figure 23 (next page): Ice pitting activity in solutions of recombinant fcAFP at concentrations of 0.38 µM (A-D), in spent medium (E) and crystal in control solution without fcAFP (F). Observation was along the c-axes and pictures show the basal plane of the crystals. A-B: The pure ice single crystal at the center of the picture is covered by pits in a regular arrangement on its basal plane. Around the original crystal, dendritic ice developed perpendicular to the c-axis. C-D: Details of the dendrites grown perpendicular to the c-axis. E: Pure ice crystal submerged in spent f/2 medium from a dense culture of *F. cylindrus* grown at 0°C. As with the recombinant protein, dense pitting on the basal plane and sharp dendritic growth at lateral planes can be observed. F: No pitting is visible on the basal plane of these crystals grown in a solution without fcAFPs. Dendrites eventually growing on the lateral planes are large and with round tips. Images: Courtesy of J. Raymond, Univ. Nevada Las Vegas, USA.

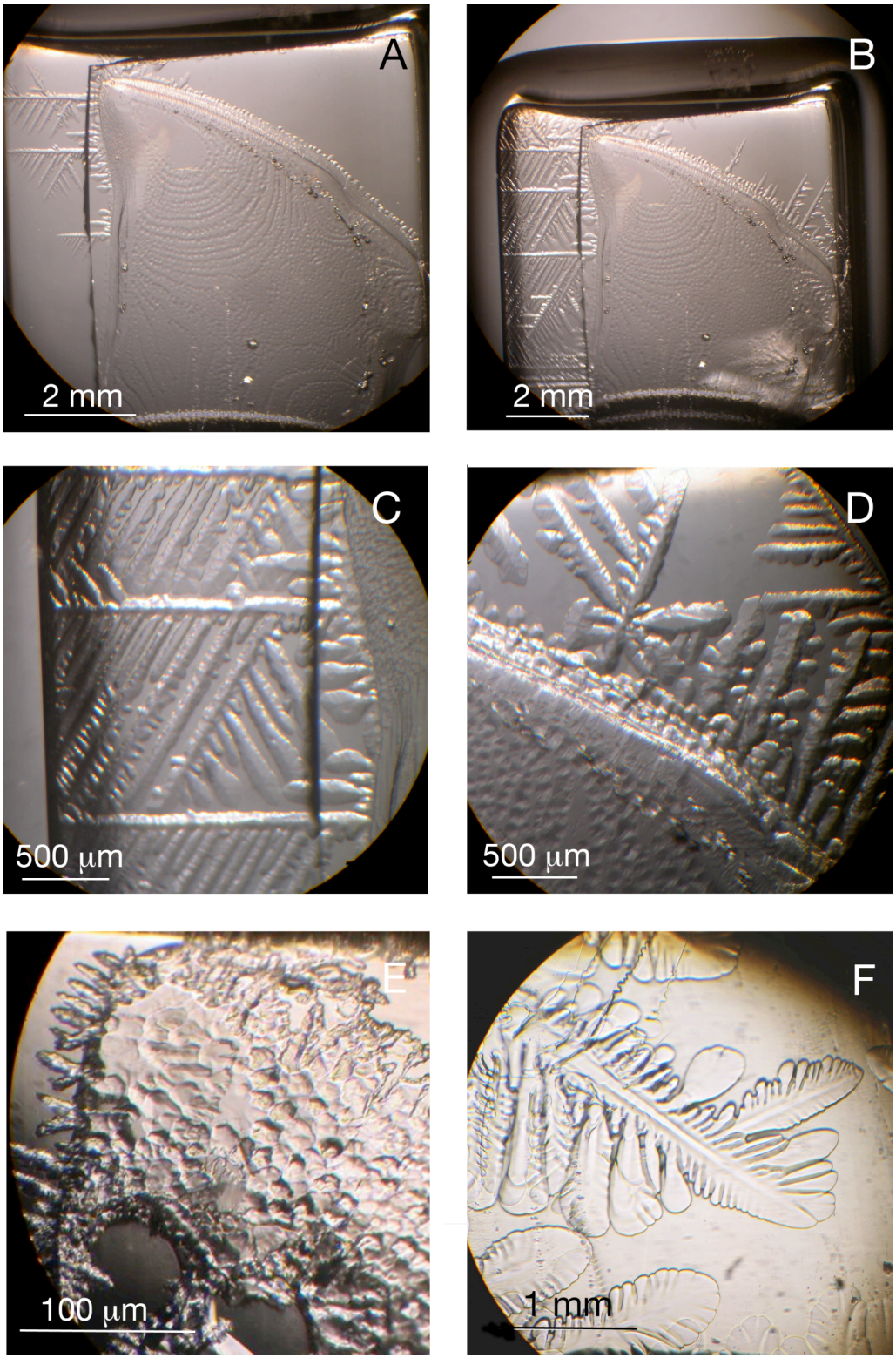
A
2 mm
B
2 mm
C
500 μm
D
500 μm
E
100 μm
F
1 mm

## 3.5.THE EFFECT OF fcAFP ON ICE MICROSTRUCTURE AND FABRIC ANALYSES

In the following results on the effect of fcAFPs on ice microstructure (texture) and c-axis distribution (fabric) are presented as contributions to objective 5 (page 13). Ice crystals were observed with optical methods like light microscopy and the automated fabric analyzer.

### 3.5.1. THE MICROSTRUCTURE OF ICE

Results of observations of the microtomed surface of frozen fcAFP solutions at light microscopy showed a marked microstructure of the crystals, primarily concerning a characteristic shape and substructure [Bayer-Giraldi et al., 2011]. Already at macroscopic observation samples appeared whitish in color and with a structured surface, compared to clear control samples with BSA, suggesting differences at microscopic level (Figure 24).

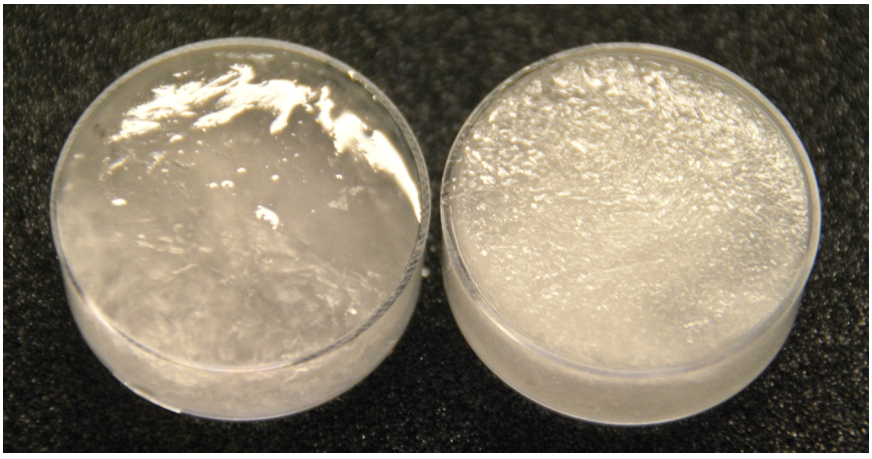

Figure 24: PBS solution of negative control protein (BSA 5 µM, left) and fcAFP (12 µM, right) frozen overnight at -4°C. The different texture can be seen macroscopically. FcAFP ice has a strongly structured appearance, observed at the surface of the sample and reflected by its color. Petri dishes are 3 cm in diameter.

Observations at light microscopy revealed a texture with oriented striations in the samples with fcAFPs (Figure 25 A-I) and clear grain boundaries with some ellipsoidal brine inclusions between individual crystals in the frozen control solution (Figure 25 J-K).

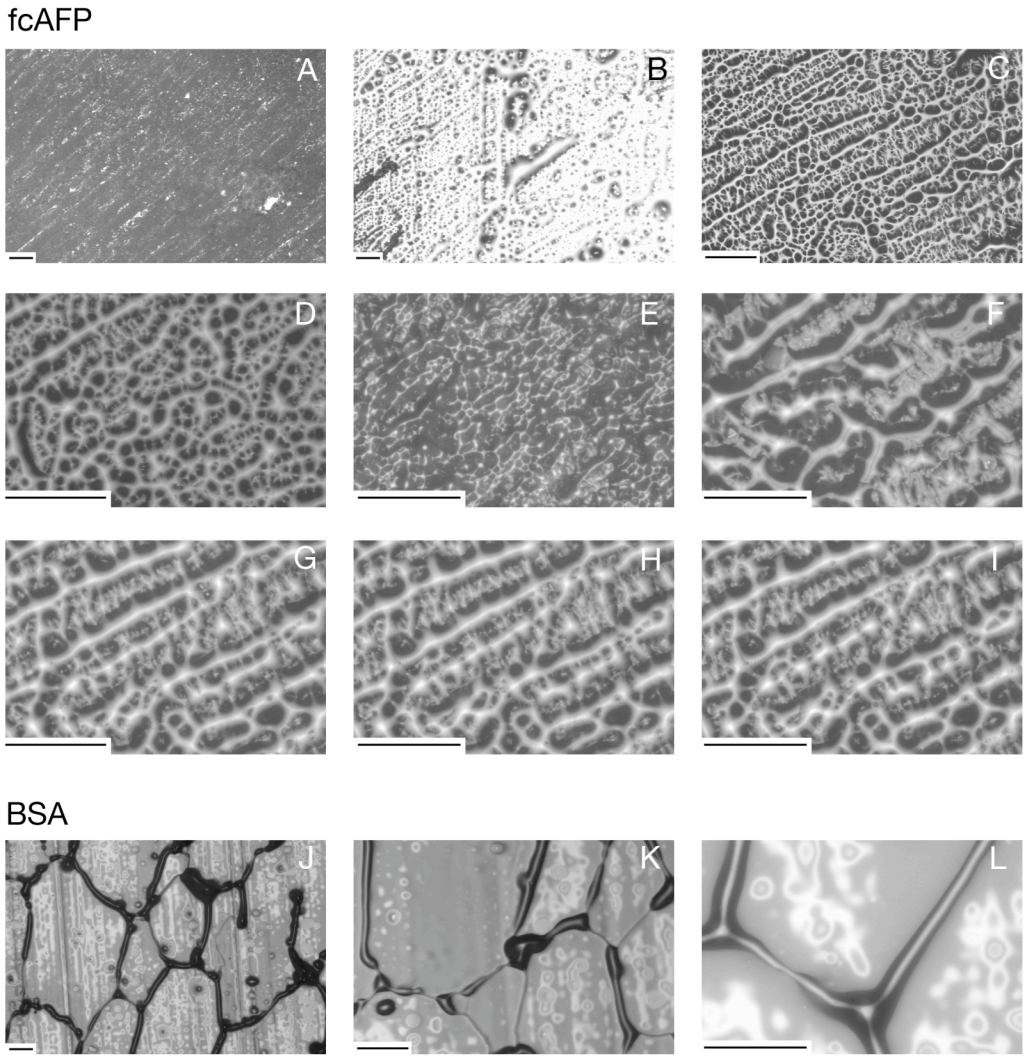


Figure 25: PBS solutions of fcAFP (12 µM; A-I) and BSA (5 µM; J-L) frozen overnight at -4°C, polished with a sled microtome and observed at light microscopy at different magnifications.
A-I: Different example of ice texture with characterized oriented striations. G-I were taken at time intervals of 30 seconds. The dark surfaces, interpreted as ice, were retreating (sublimation). J-L: Individual crystals with clear grain boundaries and brine inclusions between the grains developed in the negative control samples. Vertical white lines formed due to the effect of brine attached to the microtome knife. Scale bar: 100 µm.

This texture may be interpreted as inclusions within ice fibers. It is conceivable that diluted salts originating from the buffer, impurities and unbound fcAFPs accumulated between growing ice fronts. Ice grows explosively between bound AFPs when the freezing point is reached (Introduction, Figure 5), excluding from its lattice solutes that may concentrate between the growing ice fronts (Figure 26). Knowing the spacing

between proteins bound to ice would allow a theoretical estimate of the dimensions of the ice fibers and a comparison with the observations at light microscopy.

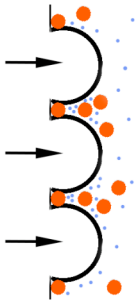

Figure 26: Ice „caps“ growing into the liquid phase (right) at the freezing point as indicated by the arrows, and AFPs (red dots) and other solutes (blue dots) excluded from the lattice accumulating between ice fronts.

The nature of striations can be verified by analysis with Raman microscopy. With this technique, which provides a molecular fingerprint of each material, ice could be distinguished from brine and from fcAFPs. Ice microscopy raises the need for a cryostage, which was not given when the experimental part of this work was concluded. However, it was possible to detect the spectrum of the dry fcAFPs (Figure A 5), which will allow further analysis for the detection of the protein in frozen samples.

Striations were also visible under crossed polarizers (Figure 27 A), and the automated fabric analyzer indicated c-axis perpendicular to striations (Figure 27 B) [Bayer-Giraldi et al., 2011]. It seems therefore that, in the presence of fcAFPs, fibers or layers of ice parallel to the basal plane alternated with inclusions perpendicular to the c-axis. Similar striations were not visible on the basal plane itself.

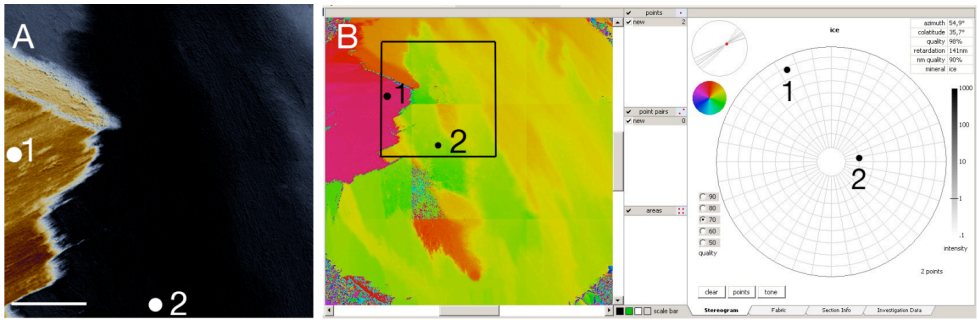


Figure 27: Ice with fcAFP (12 µM in PBS) seen between crossed polarizers of the fabric analyzer.
A: Detail of the sample (retardation image) with clear oriented striations in crystal 1.
B: Achsenverteilungsanalyse (AVA) map (left) with stereographic projection of the selected crystals 1 and 2 (right). Rectangle denotes the area of image A. The c-axis of crystal 1 is perpendicular to the striations, whereas it is approximatety perpendicular to the observation plane (therefore basal plane) in crystal 2 (See Figure 11 and Figure 12 for explanation on interpretation of AVA map and stereographic projection). Scale bar: 500 µm in A, 5 mm in B.

Also Krembs et al. [2011] reported chanes in sea ice microstructure related to brine channel surface topology and due to diatom exoloymeric substances (EPS; Introduction, page 7). The addition of EPS to artificial sea ice resulted in convoluted brine channels structure (Figure 28).

This complex microstructure resulted in a reduction in ice permeability and related desalination processes (Introduction, page 5). If brine drainage from ice is hindered, brine inclusions will maintain their dimensions, avoiding shrinking of pores and channels which would be fatal to sea ice organisms. Therefore, ice porosity in the presence of EPS is higher than without EPS. It is assumed that EPS released by sea ice organisms, mainly by diatoms, changes ice microstructure in order to conserve their living space. Furthermore, EPS attached to ice may change diffusive properties of salts, forcing the formation of brine inclusions in positions favorable to diatoms [Krembs et al., 2002] and may be responsible for incorporation and retention of organisms within brine inclusions by attachment to ice surfaces [Riedel et al., 2007; Ewert and Deming, 2011]. The effects of EPS on ice microstructure and on attachment to ice are related to its protein fraction [Ewert and Deming, 2011; Krembs et al., 2011]. It is therefore conceivable that fcAFPs, released from the cells, accumulate within EPS. The proteins, entrapped within the EPS matrix, may reach here high concentrations and locally influence ice microstructure, decreasing permeability and increasing porosity, thus positively influencing habitable space.

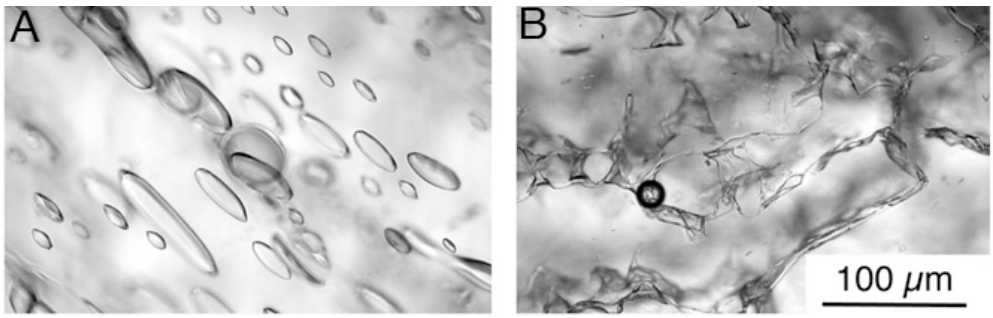


Figure 28: Photomicrographs of artificial sea ice without (A) and with (B) the addition of EPS form the diatom *Melosira arctica*. Images from Krembs et al. [2011], with permissions.

## 3.5.2. THE FABRIC OF ICE

The Achsenverteilungsanalyse (AVA) revealed a remarkable fabric pattern in the presence of fcAFPs (Figure 29). C-axis distribution within single ice crystals was not constant, but showed a gradual transition in axis direction. Furthermore, crystals were

not delimitated by straight grain boundaries seen in negative controls with BSA, but boundaries were intertwined with each other.

The low number of ice crystals in the frozen fcAFP solution, compared to the control (Figure 29, grain boundaries), suggests an effect of fcAFPs on nucleation. Ice crystallization proceeds by an initial nucleation event, followed by crystal growth. Several nucleation seeds (or embryos) may form in supercooled water, and their fluctuating size, due to attaching and detaching water molecules, may eventually result in the embryos reaching a critical size. At this size, seeds pass from a metastable to a stable state where it might be thermodynamically more favourable to grow rather than decay and dissipate into the melt again [Hobbs, 2010b]. AFPs could influence nucleation by different mechanisms. The proteins may hinder the formation of seeds by attaching to the active sites of ice nucleating agents (INA) or by disturbing the water structure [Nutt and Smith, 2008]. Furthermore, AFPs may attach to the seeds and poison their growth by the Kelvin effect [Du et al., 2002]. Only a few studies have concentrated on the nucleation inhibition by AFPs, reporting reduced nucleation temperature in the presence of AFGPs [Parody-Morreale et al., 1988; Wilson and Leader, 1995], fish AFP type I [Wilson et al., 2010] and type III [Du et al., 2002]. For IAFPs, Snider et al. [2000] reported no significant effect of the protein from T. ishikariensis on nucleation temperature. However, as shown in Figure 29, results suggest an inhibiting effect of fcAFPs on nucleation, either affecting the organization of water into lattice-like structures or by binding to new seeds.

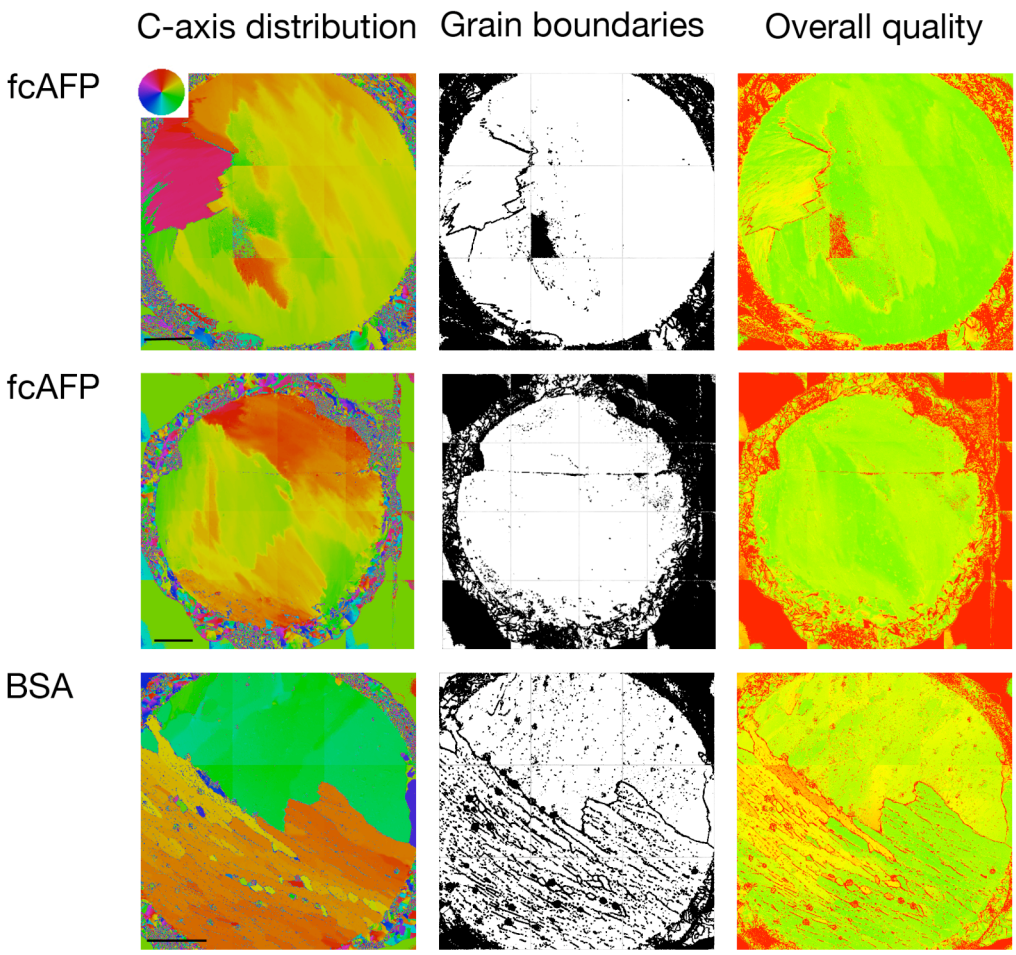


Figure 29: Ice samples seen at the automated fabric analyzer. Images show results for two frozen fcAFP solutions (12 µM) and one control BSA solution (5 µM) frozen in Petri dishes (3 cm diameter). Achsenverteilungsanalyse (AVA) map, grain boundaries and overall quality estimation of the results are shown here. AVA map: the color wheel shows the color coding in the stereographic projection (Figure 12 for explanation). Grain boundaries: Black lines denote grain boundaries as calculated by the Investigator software. Overall quality: Red dots mark points of bad resolution probably due to defects in the ice (grain boundaries among others). Green color denotes good measurement quality, due to good preparation and crystal quality. Here, the overall quality is shown to be high. Scale bar: 5 mm.

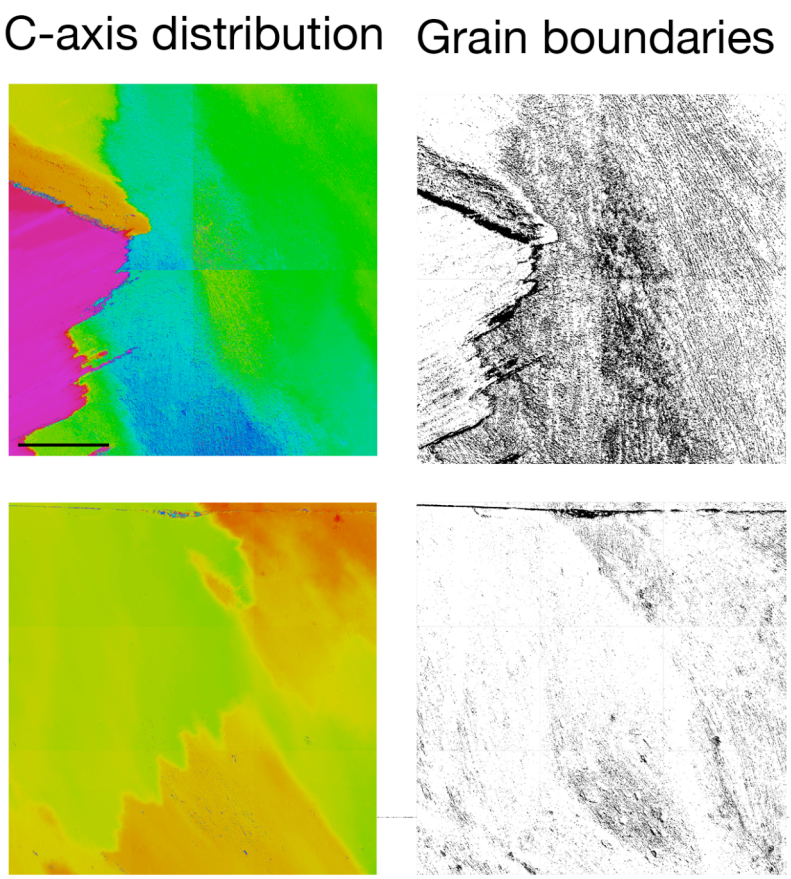


Figure 30: Magnified details of frozen fcAFP solutions (12 mM) shown in Figure 29. Grain boundaries appear interwoven and diffused. Scale bar: 500 µm.

**CONTRIBUTION TO OBJECTIVE 5:**

Results presented here focus on the topic of objective 5 (page 13) and show characteristic ice texture and fabric in the presence of fcAFPs.

The interaction with fcAFPs strongly influences ice microstructure, resulting in a fibrous texture with oriented striations. Striations, observed perpendicular to the c-axis, are interpreted as inclusions of liquid brine and unbound proteins.

Set in a broader frame, these results resemble observations on the effect of EPS on sea ice microstructure, and suggest that this effect may be due to fcAFPs accumulated within the EPS matrix changing the physical properties of ice. These results are presented in Publication 2.

Furthermore, the fabric of ice is strongly influenced by fcAFPs as seen in c-axis distribution and grain boundaries. The low number of crystals in the presence of fcAFPs indicate an inhibiting effect of the proteins of nucleation events either by affecting the formation of seed or by inhibiting their growth.

# 3.6.PUBLICATION 1

ANTIFREEZE PROTEINS IN POLAR SEA ICE DIATOMS:
DIVERSITY AND GENE EXPRESSION IN THE
GENUS *FRAGILARIOPSIS*

Maddalena Bayer-Giraldi, C. Uhlig, U. John, T. Mock, K. Valentin

Environmental Microbiology (2010)
12 (4): 1041-1052

Contributions:
Own contributions concern design research, performance of experiments with *F. cylindrus*, phylogenetic analyses, the discussion of the data and manuscript writing. C. Uhlig performed experiments with *F. curta*, U. John provided support in qPCR for expression analysis, K. Valentin and T. Mock provided general support.

environmental microbiology

Environmental Microbiology (2010) **12**(4), 1041–1052 doi:10.1111/j.1462-2920.2009.02149.x

# Antifreeze proteins in polar sea ice diatoms: diversity and gene expression in the genus *Fragilariopsis*

**Maddalena Bayer-Giraldi,[1]* Christiane Uhlig,[1] Uwe John,[1] Thomas Mock[2†] and Klaus Valentin[1]**
[1]*Alfred-Wegener-Institute for Polar and Marine Research, Bremerhaven, Germany.*
[2]*School of Oceanography, University of Washington, Seattle, WA, USA.*

## Summary

***Fragilariopsis* is a dominating psychrophilic diatom genus in polar sea ice. The two species *Fragilariopsis cylindrus* and *Fragilariopsis curta* are able to grow and divide below freezing temperature of sea water and above average sea water salinity. Here we show that antifreeze proteins (AFPs), involved in cold adaptation in several psychrophilic organisms, are widespread in the two polar species. The presence of AFP genes (*afp*s) as a multigene family indicated the importance of this group of genes for the genus *Fragilariopsis*, possibly contributing to its success in sea ice. Protein phylogeny showed the potential mobility of *afp*s, which appear to have crossed kingdom and domain borders, occurring in *Bacteria*, diatoms, crustaceans and fungi. Our results revealed a broad distribution of AFPs not only in polar organisms but also in taxa apparently not related to cold environments, suggesting that these proteins may be multifunctional. The relevance of AFPs to *Fragilariopsis* was also shown by gene expression analysis. Under stress conditions typical for sea ice, with subzero temperatures and high salinities, *F. cylindrus* and *F. curta* strongly expressed selected *afp*s. An E/G point mutation in the *Fragilariopsis* AFPs may play a role in gene expression activity and protein function.**

## Introduction

Polar diatoms have been described as being able not only to survive, but also to thrive under the extreme conditions found within sea ice, where temperatures range from about −1.8°C on the bottom to −20°C or less on the top (Maykut, 1986; Eicken, 1992), and brine salinities can be as high as 200 on the Practical Salinity Scale (Cox and Weeks, 1983). High diatom standing stocks of 1 mg chlorophyll per litre have been documented in marine ice (Arrigo *et al.*, 1995), and the total sea ice primary production (63–70 Tg C per year in the Southern Ocean) is crucial for the Antarctic trophic net (Thomas and Dieckmann, 2002). The diatoms *Fragilariopsis cylindrus* and *Fragilariopsis curta* play a key role in sea ice communities of the Southern Ocean, dominating the assemblages of both the platelet layer and within pack ice (Bartsch, 1989; Günther and Dieckmann, 2001; Lizotte, 2001; Thomas *et al.*, 2001; Roberts *et al.*, 2007).

The strategies adopted by *F. cylindrus* to cope with conditions of low temperatures and high salinities typical for sea ice have been analysed in several physiological and biochemical studies (Bartsch, 1989; Fiala and Oriol, 1990; Mock and Hoch, 2005). Recent efforts have focused on the molecular mechanisms of adaptation, with the set-up of expressed sequence tag (EST) libraries resulting in the identification of a variety of genes involved in the response to cold and salt stress in *F. cylindrus* (Mock and Valentin, 2004; Mock *et al.*, 2006; Krell *et al.*, 2008). Striking among these was the report of a new class of ice-binding proteins, which constituted the first molecular evidence for such proteins in diatoms (Janech *et al.*, 2006; Krell *et al.*, 2008). The nomenclature of these proteins varies, depending on authors, from antifreeze to ice binding or ice structuring. Here we use the term antifreeze proteins (AFPs), following Hoshino and colleagues (2003), who described the ability to depress the freezing point of water by proteins highly similar to those found by Janech and colleagues (2006) and Krell and colleagues (2008). We specify ice AFP (IAFP) when referring to this protein family, as found in organisms associated with sea ice.

Since the first isolation of a fish AFP in 1969 (DeVries and Wohlschlag), different families of ice structuring proteins have been found in polar and temperate organisms (Barrett, 2001; Venketesh and Dayananda, 2008). Even if at protein sequence or structure levels it seems impossible to find typical traits common to all the families, what defines AFPs is the ability to influence ice crystal growth. In the generally accepted adsorption–inhibition model (Raymond and DeVries, 1977), AFPs bind via hydrogen bonding and Van-der-Waals forces to the ice crystal lattice. The consequences are thermal hysteresis, i.e. the

Received 6 July, 2009; accepted 30 November, 2009. *For correspondence. E-mail maddalena.bayer@awi.de; Tel. (+49) 471 48311996; Fax (+49) 471 48311149. †Present address: School of Environmental Sciences, University of East Anglia, Norwich, UK.

lowering of the non-equilibrium freezing point below the melting point, and distortion of ice crystal habit. Moreover, AFPs pinned to ice immobilize crystal grain boundaries and thus inhibit recrystallization.

Until now, research on the new IAFP family has only focused on interspecific diversity, such that data about genetic diversity within single species are still scarce. IAFPs identified in *F. cylindrus* show remarkable similarity to proteins found in the snow mold *Typhula ishikariensis* and in the polar diatom *Navicula glaciei* (Hoshino *et al*., 2003; Janech *et al*., 2006). A molecular screening for IAFPs in other organisms revealed a broad distribution, as they were characterized also in a sea ice bacterium, a bacterium from Vostok ice core, in freeze-tolerant mushrooms from temperate regions and in a sea ice crustacean species (Raymond *et al*., 2007; 2008; Kiko, 2009; Raymond and Janech, 2009).

The broad spectrum of taxa with representatives of the IAFP family makes this protein interesting from an evolutionary point of view. This is the first time that we can observe an AFP family that passes kingdom borders and is found in *Bacteria*, diatoms, crustacean and fungi. Different AFP families are known from fishes, from insects and from plants, but they are restricted to a few classes inside the same phylum. However, little is known about the evolution of IAFPs. Janech and colleagues (2006) suggested that bacteria like *Shewanella* or *Cytophaga*-like species may have played a key role in phylogenetic history of these proteins. They proposed that sea ice representatives of these groups passed *iafp*s to diatoms via lateral gene transfer. Other origins and pathways of evolution could not be ruled out, but the close proximity of organisms inside the brine channel habitat of sea ice might have helped to facilitate lateral gene transfer.

In the following we report on intraspecific diversity of *iafp*s within *F. cylindrus* and *F. curta* and set our results in the framework of phylogenetic analyses of the new IAFP family. We concentrate on evolution of IAFPs in diatoms, but also speculate about possible origin of this protein family. Moreover, we extend the discussion to expression analysis of *iafp* isoforms, focused mainly on *F. cylindrus*. We analyse gene expression in cold and salt stress situations typical for sea ice and consider reasons of differential response of *iafp* isoforms. This is to our knowledge the first report on intraspecific diversity of IAFPs and their gene expression under environmentally relevant conditions.

## Results

### *Sequence analysis*

*Identification of isoforms.* We performed several PCR amplifications with different primer combinations for identification of *iafp* isoforms in *F. cylindrus* TM99 and *F. curta* TM99. For *F. cylindrus*, the amplification led to the isolation of 17 products. After cloning and sequencing we obtained 111 gene sequences, which were divided into 10 unique clades following the criteria described in *Experimental procedures*. Most of the sequences clustered with the three *iafp*s known from Janech and colleagues (2006) and Krell and colleagues (2008), initially taken as reference for primer design, but we could also identify seven new isoforms. For *F. curta* we obtained very similar results. After cloning eight amplicons, we obtained a total of 102 sequences that we divided into 11 clades.

*Phylogenetic analysis.* Similarity search with BLAST resulted in the identification of several putative homologues of IAFPs, belonging to 30 species and distributed between different phyla. Results are summarized in Table 1. Some of these organisms have manifold *iafp*s in their genome, and in the cases of *Flavobacteriaceae* bacterium and *Candidatus Methanoregula boonei*, single genes contain more than one *iafp* domain.

Instraspecific similarity search of *F. cylindrus* TM99 *iafp*s against the recently sequenced genome of *F. cylindrus* CCMP 1102 showed slight differences between the two strains. Whereas two isoforms of strain TM99 (GenBank: EL737280, DR026070) corresponded to sequences on the genome (GenBank: GU001153, GU001148), the remaining eight isoforms were unique and differed from genome data (GenBank: GU001149, GU001150, GU001151, GU001152) due to the presence of insertions or deletions (indels) of 3–15 nucleotides and/or more that 1% single point mutations.

We created a phylogenetic tree of all IAFP domains we had found in *Fragilariopsis* and the putative homologues found through similarity search (83 domains in total). Two independent groups could be identified, each of them supported by a high bootstrap value, as indicated in Fig. 1. Group I is taxonomically heterogeneous and includes fungi, diatoms, *Archaea* and *Bacteria*, whereas group II is clearly dominated by bacterial species. The remaining sequences are bacterial and too dissimilar to be grouped together.

The further phylogenetic analysis limited to group I resulted in five clusters with strong bootstraps support (Fig. 2). One cluster, designated sea ice eukaryotes, contains two distinct taxa, crustacaea and diatoms from sea ice. The other clusters are taxonomically well defined and consist separately of *Archaea*, *Bacteria*, fungi or diatoms from the genus *Fragilariopsis*.

Domain searches of all IAFPs and IAFP-like sequences against Pfam-A database showed five significant matches. Immunoglobulin-like domains (Ig-like) were found in the N-terminal region upstream of the IAFP domains in *Shewanella frigidamarina* (GenBank:

**Table 1.** Species name, taxonomical group and GenBank accession number of IAFPs and putative homologues included in the phylogenetic tree of Fig. 1.

| Species | Taxa | Accession No. |
|---|---|---|
| *Acidobacteria bacterium*, uncultured | *Acidobacteria* | AAP58537 |
| *Burkholderia xenovorans* LB400 | *Proteobacteria* | YP_552858 |
| | | YP_556507 |
| *Candidatus Methanoregula boonei* 6A8 | *Euryarchaeota* | YP_001404641 |
| | | YP_001404652 |
| | | YP_001403476 |
| *Candidatus Methanosphaerula palustris* E1-9c | *Euryarchaeota* | YP_002465308 |
| *Chaetoceros neogracile* KOPRI AnM0002 | *Bacillariophyceae* | EL622418 |
| *Clavibacter michiganensis* subsp. *michiganensis* NCPB 382 | *Actinobacteria* | YP_001223474 |
| | | YP_001711352 |
| *Colwellia* sp. SLW05 | *Proteobacteria* | ABH08428 |
| *Cytophaga hutchinsonii* ATCC 33406 | *Bacterioidetes* | YP_676864 |
| *Flammulina populicola* | Fungi-*Basidiomycota* | ACL27144 |
| *Flavobacteriaceae bacterium* 3519-10 | *Bacterioidetes* | ACD76102 |
| *Fragilariopsis curta* TM99 | *Bacillariophyceae* | GQ265833 |
| | | GQ265834 |
| | | GQ265835 |
| | | GQ265836 |
| | | GQ265837 |
| | | GQ265838 |
| | | GQ265839 |
| | | GQ265840 |
| | | GQ265841 |
| | | GQ265842 |
| | | GQ265843 |
| *Fragilariopsis cylindrus* CCMP 1102 | *Bacillariophyceae* | GU001149 |
| | | GU001150 |
| | | GU001151 |
| | | GU001152 |
| *Fragilariopsis cylindrus* TM99 | *Bacillariophyceae* | GQ232744 |
| | | GQ232745 |
| | | GQ232746 |
| | | GQ232747 |
| | | GQ232748 |
| | | GQ232749 |
| | | GQ232750 |
| | | DR026070 |
| | | EL737258 |
| | | EL737258 |
| *Frankia alni* ACN14a | *Actinobacteria* | YP_715224 |
| | | YP_712174 |
| *Lentinula edodes* | Fungi-*Basidiomycota* | ACL27145 |
| *Navicula glaciei* | *Bacillariophyceae* | AAZ76251 |
| | | AAZ76252 |
| | | AAZ76250 |
| | | AAZ76253 |
| *Phaeosphaeria nodorum* SN15 | Fungi-*Ascomycota* | XP_001806212 |
| *Polaribacter irgensii* 23-P | *Bacteriodetes* | ZP_01118128 |
| *Polaromonas naphthalenivorans* CJ2 | *Proteobacteria* | YP_981554 |
| *Psychromonas ingrahamii* 37 | *Proteobacteria* | YP_944155 |
| *Rhodococcus jostii* RHA1 | *Actinobacteria* | YP_703462 |
| *Rhodoferax ferrireducens* T118 | *Proteobacteria* | YP_523138 |
| *Rhodopseudomonas palustris* BisB18 | *Proteobacteria* | YP_532576 |
| *Shewanella denitrificans* OS217 | *Proteobacteria* | YP_562920 |
| | | YP_562921 |
| *Shewanella frigidamarina* NCIMB400 | *Proteobacteria* | YP_749708 |
| | | YP_749709 |
| *Stephos longipes* | *Arthropoda* | ACL00837 |
| | | ACL00838 |
| *Stigmatella aurantiaca* DW4/3-1 | *Proteobacteria* | ZP_01462925 |
| *Streptomyces* sp. Mg1 | *Actinobacteria* | YP_002184236 |
| | *Actinobacteria* | YP_002184267 |
| *Streptomyces avermitilis* MA-4680 | *Actinobacteria* | NP_825341 |
| Streptomyces sviceus ATCC 29083 | *Actinobacteria* | YP_002205477 |
| *Talaromyces stipitatus* ATCC10500 | Fungi-*Ascomycota* | EED17205 |
| *Typhula ishikariensis* | Fungi-*Basidiomycota* | BAD02891 |
| | | BAD02892 |
| | | BAD02895 |
| | | BAD02894 |
| | | BAD02896 |
| | | BAD02897 |
| | | BAD02893 |
| *Verrucomicrobium spinosum* DSM 4136 | *Verrucomicrobia* | ZP_02927694 |

 

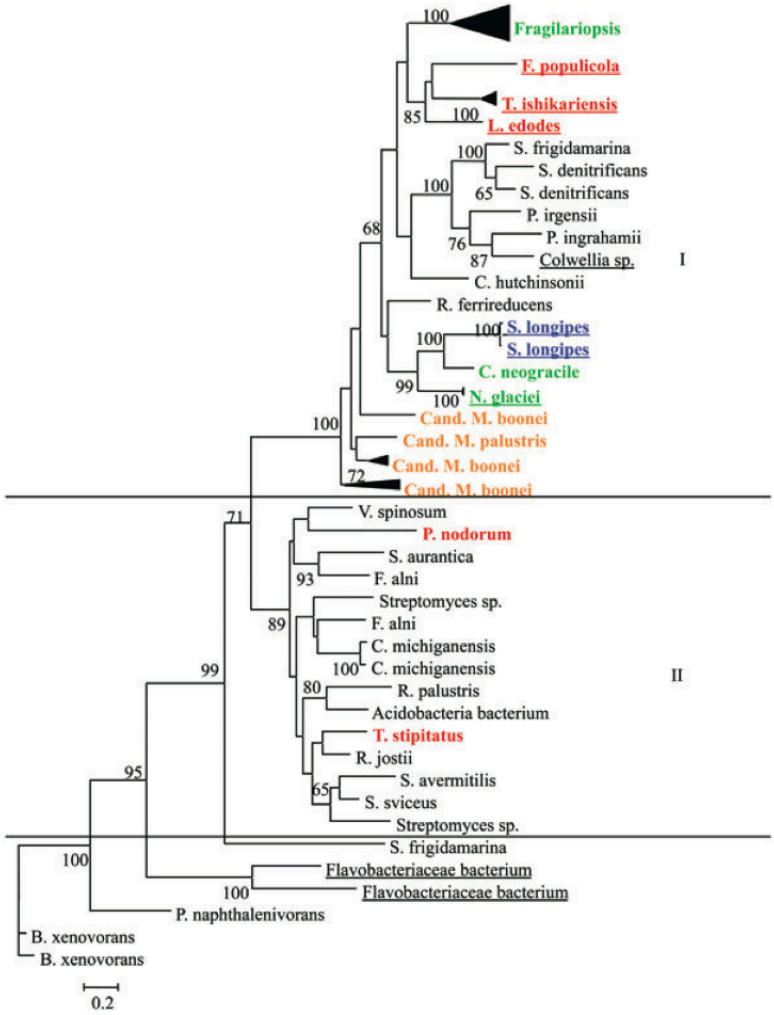


**Fig. 1.** Molecular phylogeny of IAFPs estimated by PhyML algorithm. The unrooted tree shows all known IAFP domains and their putative homologues inferred by similarity search. We applied the PhyML algorithm version 2.4.4 with the following settings: WAG model of amino acid substitution, initial tree BIONJ, gaps included, 100 bootstraps. For clarity, multiple isoforms of one species or genus are collapsed. Only nodal support values greater than 60 are shown. *Archaea* sequences are represented in orange, *Bacteria* are in black, diatoms in green, fungi in red and crustaceans in blue. Proteins known to have antifreeze function are underlined.

YP_749709), *Acidobacteria* bacterium and *Rhodoferax ferrireducens*. These domains belong to a superfamily whose proteins share structural features and mediate cell adhesion to other cells or a matrix (Kelly *et al.*, 1999). Moreover, C-terminal extensions with autotransporter domains were identified in *Rhodopseudomonas palustris* and *Verrucomicrobium spinosum* IAFP-like genes. Autotransporters are domains of Gram-negative bacteria that mediate the secretion of the protein they belong to. They consist of extensions that form beta-barrels in the outer membrane and transport the N-terminal passenger domain outside the cell (Henderson *et al.*, 1998).

Results of domain searches against the Pfam-B database evidenced no similarity to any protein family consistent in all sequences analysed. However, one IAFP domain from *S. frigidamarina* (GenBank: YP_749709)

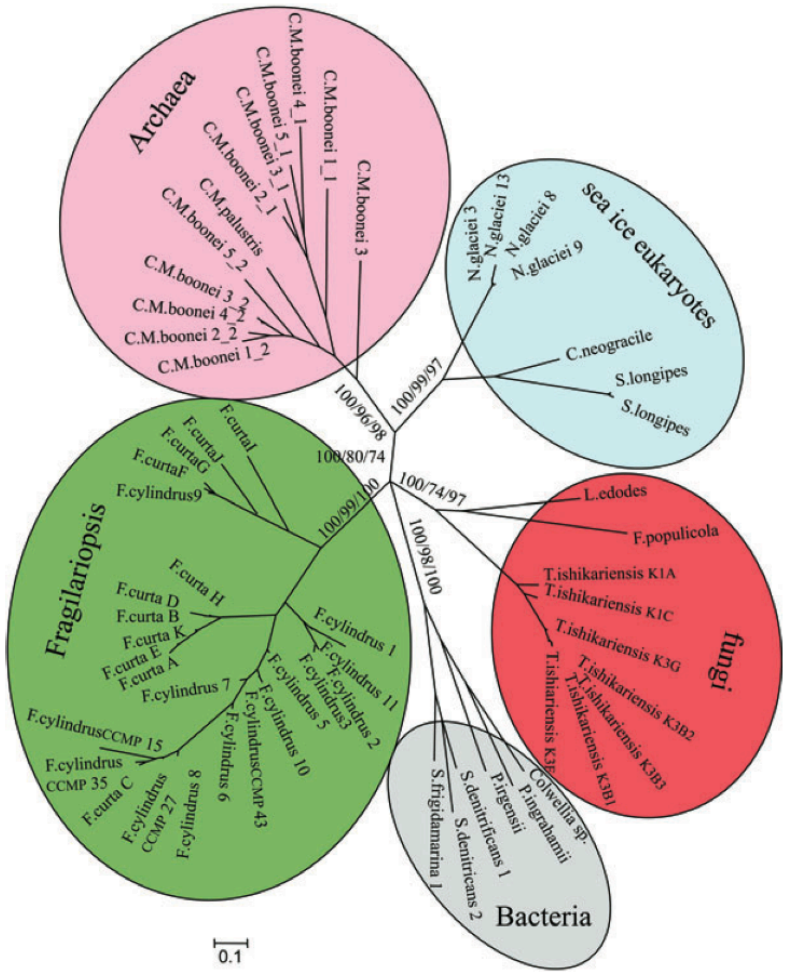


**Fig. 2.** Molecular phylogeny of selected IAFPs based on Bayesian inference. The unrooted tree shows phylogeny of selected sequences from group I. Bootstrap support at selected nodes is shown for Bayesian inference, Maximum Likelihood and Maximum Parsimony, which showed essentially the same topology. Algorithms and settings were as follows: MrBayes version 3.1.2 for Windows with posterior probabilities derived from 80 000 generations (four chains), random starting tree, sample frequency 100, WAG amino acid substitution model and discarding a burnin of 500; PAUP* 4.0b10 for Macintosh, simple weighting, 100 bootstraps; PhyML as in Fig. 1.

showed similarity ($E = 0.00120$) to domain PB098886, which appears to be related to adhesins, surface proteins specialized in bacterial adhesion.

### *Gene expression analysis*

In order to analyse *iafp* expression in response to multiple stressors, we exposed cultures of *F. cylindrus* TM99 and of *F. curta* TM99 to shock treatments of subzero temperature and high salinity characteristic for sea ice environment. In the middle of the logarithmic growth phase under optimal growth conditions (salinity 34, temperature 5°C), the different batches were separated for the following: salinity 70 and temperature 5°C (S), salinity 70 and temperature −4°C (ST). Control batches (C) were kept at optimal growth salinity (34) and temperature (5°C) throughout the experiment.

*Physiology.* Cultures of *F. cylindrus* and *F. curta* showed slight differences in growth before the treatments, which

 

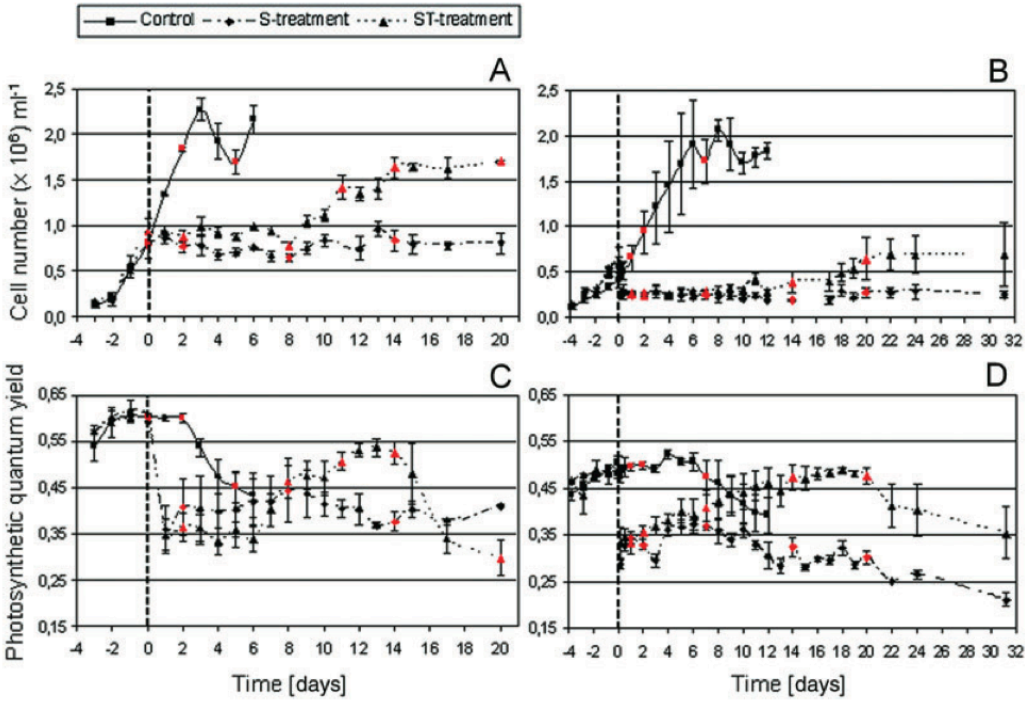


**Fig. 3.** Cell densities and photosynthetic quantum yield for photosystem II of experimental cultures. (A and C) *F. cylindrus*, (B and D) *F. curta*. Red marks represent sampling days for RNA. The dotted lines show the moment of shock, imposed immediately after sampling on day 0.

became more pronounced after the shock in response to increased salinity alone (S) and in combination with decreased temperature (ST).

Untreated cultures of *F. cylindrus* showed normal growth rates ($\mu = 0.56 \pm 0.05$, Fig. 3A) and photosynthetic quantum yield ($\Phi$ between $0.55 \pm 0.03$ and $0.61 \pm 0.01$, Fig. 3C), whereas *F. curta* showed a slower growth ($\mu = 0.3$, $\Phi = 0.45$–$0.5$, Fig. 3B and D). Control cultures reached the end of the exponential growth phase on day 2 (*F. cylindrus*) and day 6 (*F. curta*) after the day of S and ST shock treatments, and stayed in stationary phase until the batches were excluded from the experiment.

Salinity and temperature shocks arrested growth of *F. cylindrus* cells in both S- and ST-treatments (Fig. 3A). However, the cultures of the ST-treatments were able to recover beginning moderate growth 8 days after the shock and entering stationary phase around day 14. In contrast, the cultures of the S-treatments did not recover. Data of the photosynthetic quantum yield followed the same trend as those of cell numbers, occasionally preceding the latter by 1–2 days (Fig. 3C).

The consequences of the shock were more marked for *F. curta* than for *F. cylindrus*. After the shock, cell numbers of *F. curta* showed a precipitous drop and initially no recovery (Fig. 3B). After 1 week, cell numbers in the ST-treatments slowly increased and reached a maximum on day 22, whereas cultures of the S-treatment did not recover. The photosynthetic quantum yield results also showed a sudden decrease due to the shock, followed immediately in treatment ST by a slow and steady increase until day 18 (Fig. 3D).

*Gene expression.* Analysis of individual *iafp*s with qPCR showed expression of each gene, thus excluding pseudogenes from most of the sequences isolated by our approach. However, because some qPCR primers were designed to amplify more than one isoform due to their high sequence similarity, we could not rule out the possibility of pseudogenes for each sequence analysed.

Gene expression revealed significant differences between the several *iafp* isoforms in *F. cylindrus* and *F. curta*, with strongly divergent regulation patterns especially in the treated batches.

For *F. cylindrus*, we observed no significant change in expression of *iafp*s in the C-treatments. Our analysis of the initial, mid- and end-points of the logarithmic growth

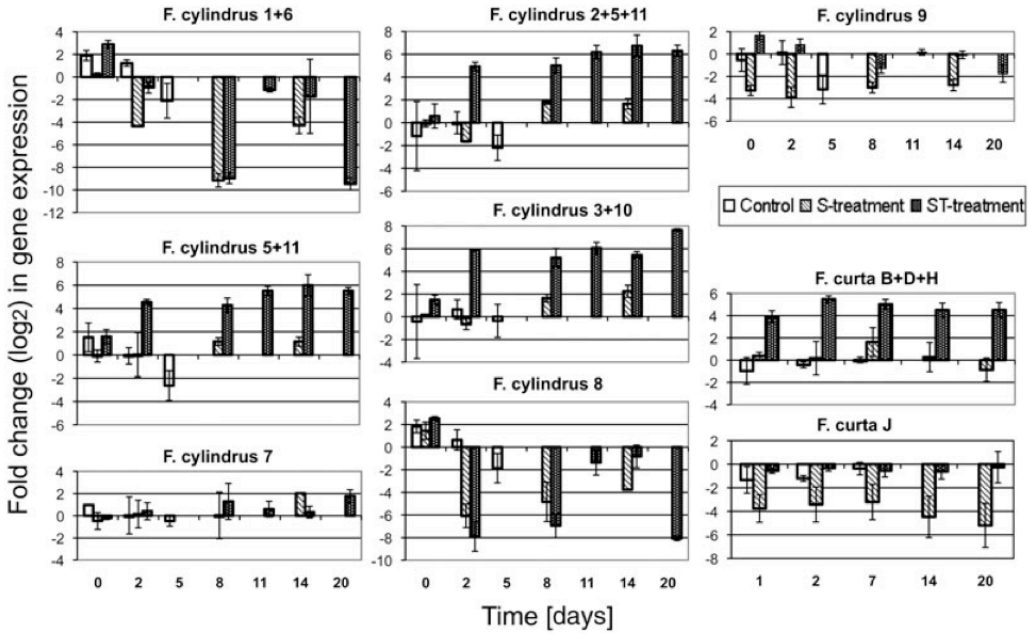


**Fig. 4.** qPCR analysis of *iafp* expression. Change in expression of single isoforms or a set of isoforms are shown. Results are represented as $\log_2$ of fold change values.

phase under control conditions revealed only fluctuations around the initial values of expression (Fig. 4). Downregulation appeared on day 5, when cultures started to slide from the stationary to the death phase, denoted by decreasing photosynthetic quantum yield values.

In the S-treatments, isoform groups 1 + 6 and 8 of *F. cylindrus* were downregulated immediately after the shock, reaching values of 20- and 56-fold reduction of the initial expression respectively [Fig. 4; fold changes of 20 and 56 correspond to a $\log_2$ (fold change) of 4.3 and of 5.8, respectively, on the figure]. Groups 3 + 10, 5 + 11 and 2 + 5 + 11 were slightly upregulated at the end of the experiment.

The most prominent feature of *F. cylindrus* gene expression was observed in the ST-treatment. Expression of *iafp* groups 1 + 6 and 8 decreased to minimal values approaching 0 after the shock (480- and 200-fold downregulation respectively), and groups 3 + 10, 5 + 11 and 2 + 5 + 11 were markedly upregulated. Expression of these genes was already pronounced 2 days after the shock, but peaked on day 14 (groups 5 + 11, 2 + 5 + 11) and 20 (group 3 + 10) with 70-, 120- and 200-fold upregulation respectively.

The two isoform groups investigated in *F. curta* also showed different expression patterns. In the control treatments both groups showed a slight downregulation at the beginning of the experiment.

The S-treatment resulted in an upregulation of group B + D + H up to fourfold on day 7 followed by a decrease just below the expression level before shock. In contrast group J was downregulated in this treatment by a factor of 10 directly after the shock, and decreased to a minimum of 20-fold reduction on day 20. The ST-treatment was followed by a distinct upregulation of *iafp* group B + D + H with its maximum of a 45-fold upregulation 2 days after the shock which levelled out at a value of about 25 until the end of the experiment, whereas in group J no distinct regulation was observed for this treatment.

## Discussion

### *Phylogenetic analysis*

The presence in *F. cylindrus* and *F. curta* of i*afp* multigene families suggests the importance of this gene for algal survival. Within the genus *Fragilariopsis*, *iafp*s probably evolved by repeated duplication events, a mechanism already described as important in adaptation to cold stress (Zhang, 2003; Carginale *et al*., 2004). Frequent replication of genes may compensate for reduced kinetic

efficiency of proteins due to low temperatures (Carginale *et al*., 2004), or induce the process of protein sub- or neofunctionalization, thus expanding the repertoire of cellular functions as adaptation to a new environment (Zhang, 2003).

The differences between isoforms of *F. cylindrus* TM99 and their most similar homologues in *F. cylindrus* CCMP 1102, revealed by interspecific analysis, may be explained by the different sources of these organisms. Although both strains were isolated from the Weddel Sea, they were collected in different environments and in separated points in time, strain TM99 isolated from sea ice in 1999, strain CCMP 1102 collected from sea water 20 years earlier.

In polar diatom species, acquisition of *iafp*s may have proceeded in at least two independent steps. The separation of diatom IAFP sequences into different clades, the genus *Fragilariopsis* in one group and the other polar diatoms in another (Fig. 2), casts doubt on a common origin of IAFPs in diatoms. *Fragilariopsis* IAFPs seem more related to fungal and bacterial sequences, whereas *N. glaciei* and *Chaetoceros neogracile* sequences are phylogenetically closer to *Archaea* than to other diatoms, indicating that diatoms acquired their *iafp*s from different ancestors. The results reinforce the hypothesis of horizontal gene transfer between sea ice microorganisms and the ice-dwelling crustacean *Stephos longipes* (Kiko, 2009), as they also appear phylogenetically closely related in our analysis. Our results thus suggest a high mobility of *iafp*s and underline their importance for polar organisms.

In the context of several potential horizontal gene transfers the identification of a path of protein evolution becomes more challenging. Moreover, little is known about the function of putative IAFP homologues. Proteins with demonstrated ice activity have been found in several polar and temperate, but cold-tolerant organisms (Hoshino *et al*., 2003; Janech *et al*., 2006). However, results from similarity search broaden this spectrum and extend the presence of putative IAFPs to a variety of species belonging to different phyla. While some of these organisms are polar, some others are mesophilic with no evident relationship to low temperature conditions, although information about their habitats is sparse. This diversity of sources suggests that not all sequences we extracted from the database may have a function related to cold adaptation, but rather that antifreeze activity may have arisen as a new function in organisms exposed to low temperatures.

Our results from phylogenetic analysis suggest that the bacterium *S. frigidamarina* played a key role in the evolution of IAFPs. *Shewanella frigidamarina* possesses two IAFP-like domains, which from genome analysis are observed to be adjacent to each other and thus most probably evolved by gene duplication. Other than in *Fragilariopsis* or in *Typhula ishikariensis*, where *iafp* paralogues are highly similar, the genes from *S. frigidamarina* do not cluster together in the phylogenetic tree: one is located in group I and the other is situated between the ungrouped sequences (Fig. 1). This divergence in sequence could be a signature for an early separation, but also for a divergence in function. After the duplication event, the new gene copy, eventually without functional constraints, was free to mutate and may have adopted new functions. This assumption is underlined by domain analysis.

From results of domain searches in the Pfam database, there seems to be a relation between IAFP genes and other extracellular proteins involved in adhesion mechanisms, adhesins in particular. Adhesins are surface proteins that mediate cell–cell interactions (Niemann *et al*., 2004). They are among the major virulence factors of pathogenic bacteria, since their function is to recognize and bind to the target. There are several kinds of evolutionarily related adhesins, many of which can be found in proteobacteria (*Escherichia coli*, *Bordatella pertussis*, *Yersinia*). Among the common traits of adhesins is that they frequently have an outer membrane beta-barrel domain (autotransporter). Moreover, several adhesins have Ig-like domains that do not mediate cell contact but rather serve as spacers or stabilizers. The description of these typical features of adhesin structure matches our results from domain search in Pfam. Therefore, it is conceivable that *S. frigidamarina*, a sea ice organism also belonging to the group of proteobacteria, evolved its adhesin-like domain to bind to ice.

### *Gene expression analysis*

The physiological response of *F. cylindrus* under salt shock treatment and at subzero temperatures reflects previous experiments with the same species (Mock and Valentin, 2004; Krell *et al*., 2007). The immediate stop of growth after the shock, followed by a restart after approximately 1 week, is characteristic for *F. cylindrus* and similar to the response in *F. curta*. Other than in previous experiments, where salt treatments were conducted at 0°C, our S-batches were kept at 5°C and did not recover from shock. Thus, *F. cylindrus* and *F. curta* appeared to cope better with a combination of high salt concentration and low temperatures than with high salinity at non-freezing temperatures. These results are perhaps not surprising, since they reflect adaptation to natural conditions in sea ice, where freezing always is accompanied by increasing brine salinities. Quantum yield data, slowly increasing after the shock, reveal an onset of response mechanisms that need 2–7 days to lead to an onset of growth.

Our gene expression analyses, in revealing strong differences in *iafp* regulation, clarified that the combined

conditions of high salt concentration and low temperature influence not only cell physiology, but also *iafp* expression. Because the strong gene regulation observed under subzero temperatures in our experiments was not observed under high salt conditions alone, we suggest that the observations by Krell and colleagues (2008), where salt was proposed as a major trigger for *iafp* gene expression, must have another explanation. For example, *iafp* expression may have been induced already by the temperature, set to 0°C in their experiment, in agreement with our result that moderate gene expression was observed even under control conditions of 5°C.

In nature, chilling events typically do not occur as abruptly as in our studies; nevertheless, under the conditions we imposed, expression of certain *iafp* isoforms seems to be a priority for sea ice diatoms analysed here, as they conspicuously increase gene expression while still in poor physiological conditions following the shock ($\Phi = 0.36 \pm 0.03$). The decided upregulation of isoform groups 3 + 10, 5 + 11 and 2 + 5 + 11 in *F. cylindrus* and group B + D + H in *F. curta* 1–2 days after the shock was only exceeded by the increase of these isoforms towards the end of the experiment. These results underline the relevance that IAFPs probably have for cold acclimation in polar diatoms.

It remains unclear why some *iafp*s are upregulated, while other isoforms stay constant or are strongly downregulated. One explanation could be a successive activation of different isoforms, with some genes responsible for early response and others for long-term acclimation. Another possibility is that *iafp*s, or at least some isoforms, code for proteins not primarily involved in antifreeze activity. IAFPs may have another (unknown) function that parallels cold acclimation. A comparison of the isoforms upregulated by *F. cylindrus* during cold and salt stress and those downregulated or kept constant reveals one base position that deserves further attention from this perspective. It shows a point mutation that is not silent but leads to an amino acid E/G replacement (Fig. S1). While an 18-E is present in all upregulated sequences, it is replaced by an 18-G in the other sequences. The same replacement was observed in *F. curta*. Since we lack protein structure analysis, the role of the amino acid in position 18 of the mature protein remains unclear. However, a substitution of glutamic acid in fish type III AFPs leads to a decrease in antifreeze activity (Li and Hew, 1991). Glutamic acid is a polar amino acid that forms hydrogen bonds, presumably the force that binds AFPs to their substrate. In contrast, glycine is not polar and not able to form hydrogen bonds. With these results we have established the molecular basis to further study this new IAFP family and to shed light on structural and functional aspects at the protein level.

## Experimental procedures

### *Material*

The cultures we used derive from isolates of *F. cylindrus* and of *F. curta* sampled in 1999 by Thomas Mock in sea ice from the Weddell Sea, Antarctica, during the Polarstern ANT XVI/3 expedition. We designated both strains TM99. Stock cultures were kept in ANT f/2 medium (Guillard and Ryther, 1962) at 5°C and continuous illumination of approximately 25 $\mu$E $m^{-2}$ $s^{-1}$.

### *Sequence analysis*

*Identification of isoforms.* For PCR amplification we isolated DNA from *F. cylindrus* and *F. curta* cultures using the DNeasy Plant Kit (Qiagen, Germany) following manufacturer's instructions. Oligonucleotides were designed manually, based on conserved features of *iafp* sequences from different diatom species reported in Janech and colleagues (2006) and Krell and colleagues (2008) (GenBank: DQ062566, DR026070, EL737258, EL737280). We ran PCRs using several combinations of forward and reverse primers (Tables S1 and S2). Reactions were performed using a Mastercycler (Eppendorf, Germany) with temperature settings as follows: 2 min at 94°C, 35 cycles with 5 s at 94°C, 30 s at 60°C, 1 min at 68°C and a single final elongation step for 5 min at 68°C.

Successful amplifications were visualized on agarose gels with SYBR Green staining, products excised and gel purified (MinElute from Qiagen). Amplicons were ligated into pCR 2.1-TOPO vector and cloned into ONE Shot TOP 10 *E. coli* cells according to the Topo TA Cloning Kit protocol (Invitrogen, USA). Plasmids were isolated (QIAprep Spin Miniprep Kit from Qiagen) and digested with EcoRI (New England BioLabs, USA), to check for inserts in clones. Samples were cycle-sequenced with an ABI Prism 3130xl Genetic Analyser (Applied Biosystems, Germany), sequence fragments assembled with the Lasergene SeqMan software (DNASTAR, GATC Biotech, Germany) after quality and vector clipping.

We sorted DNA sequences into clades of different isoforms. The presence of indels and/or more than 1% nucleotide mutations were considered criteria for differentiation between the clades. We selected one representative sequence for each clade, with point mutations typical for the corresponding clade, and used these for further analysis.

*Phylogenetic analysis.* We determined putative IAFP homologues by similarity search using the BLAST algorithm (*E*-value < $10^{-7}$) in the *F. cylindrus* CCMP 1102 genome portal at the DOE Joint Genome Institute (JGI) and in the protein database hosted by the National Center for Biotechnology Information (NCBI). We also used similarity search with BLAST to determine conserved IAFP domains for each sequence. Only these domains were included in the alignment, performed with the CLUSTALW algorithm of MEGA 4.0.2, while the N- and C-terminal regions of the proteins were not considered.

To infer the evolutionary relationship between the IAFP isoforms we used a Maximum Likelihood approach using the

 

PhyML algorithm (Guindon and Gascuel, 2003), based on the alignment results of all protein domains. For a more precise resolution of the resulting phylogenetic tree, we selected a subsample of closely related sequences, realigned them and applied various algorithms for estimation of phylogeny. We used the PhyML program, PAUP* for maximum parsimony estimation and MrBayes for Bayesian inference (Huelsenbeck *et al.*, 2001; Ronquist and Huelsenbeck, 2003; Dereeper *et al.*, 2008).

Moreover, we intended to characterize the functional regions of IAFPs and their putative homologues, in order to gain a better insight in the possible evolution of these sequences. Domains of full-length proteins were determined with search against the Pfam database (Finn *et al.*, 2008). We conducted our database search for IAFPs from *F. cylindrus*, *F. curta* and all putative IAFP homologues. Included in the search were both Pfam-A, a database with curated, manually created entries, and Pfam-B, with lower-quality, automatically generated sequences.

### *Gene expression analysis*

*Experimental set-up.* Experimental cultures of *F. cylindrus* and of *F. curta* were kept in 5 l flasks at 5°C, the optimal growth temperature for *F. cylindrus* (Fiala and Oriol, 1990), and constantly illuminated with 25 μE $m^{-2}$ $s^{-1}$. Cells were grown in ANT f/2 medium (Guillard and Ryther, 1962) with its characteristic salinity of 34, stirred and bubbled with sterile filtered air to ensure sufficient $CO_2$ supply. In the middle of the exponential growth phase we separated the different batches into the following treatments:

(i) salinity was increased from 34 to 70 (S-treatment);
(ii) salinity was increased to 70 and temperature lowered from 5°C to 4°C (ST-treatment); and
(iii) control cultures were not modified (C-treatment).

We used triplicate cultures for each treatment. Salinity change was achieved by addition of a concentrated brine of Sea Salts (Sigma, USA).

Samples to follow physiological conditions of the cultures were taken daily from the beginning of the experiment and over larger intervals after 14 days from the shock. On selected days we took samples for RNA extraction.

*Physiology.* Specific growth rate per day ($\mu$) was determined in triplicate by counts of cell numbers using a Multisizer 3 particle counter (Beckmann-Coulter Krefeld, Germany) with a 100 μm aperture capillary.

We also measured maximum quantum yield for photosystem II ($\Phi_{PSII}$) as a proxy for general cell fitness. Cells were dark adapted for 5–15 min at experimental temperature and then analysed using a Xenon-PAM-Fluorometer (WALZ GmbH, Germany). Measures of maximum ($F_m$) and minimum ($F_0$) fluorescence were used to calculate the following ratio that indicates maximum photochemical efficiency (Maxwell and Johnson, 2000): $\Phi_{PSII} = \frac{F_m - F_0}{F_m}$

*RNA extraction and cDNA synthesis.* For RNA isolation we applied the TRI Reagent extraction protocol (Sigma) followed by a DNase treatment and RNaesy Kit (Qiagen) clean-up. Purity of the RNA was checked by Nanodrop (Peqlab, Germany), integrity with an Agilent 2100 Bioanalyser (Santa Clara, USA). RNA was reversely transcribed using the Omniscript RT Kit (Qiagen). Five hundred nanograms of template RNA were incubated in 20 μl (1 h, 37°C) with 4 units of transcriptase and anchored oligo$(dT)_{20}$V primers (20 pmol). Control reactions to reveal presence of contaminating DNA were prepared by omitting transcriptase (no-RT controls). Immediately prior to transcription we added to all reactions defined amounts (10 pg) of RNA from the major allergen (MA) gene of the butterfly *Pieris rapae*, an organism considered alien to polar or marine diatoms, to provide an external standard for qPCR analysis.

*Gene expression analysis.* In samples from the *F. curta* experiment, we used qPCR assay with a SYBR Green approach, while in *F. cylindrus* samples we chose TaqMan chemistry for more precise gene detection. Oligonucleotides were designed manually (Sigma) or by Primer Express software (Applied Biosystems) in order to detect single isoforms or, when this was not possible due to the extreme similarity of sequences, a group of clades (Table S3). Primers and probe concentration was adjusted to reach an optimal efficiency ($E$) of 2 ± 0.05, with a reproducibility of replicates $R^2 > 0.98$. Assays were prepared with TaqMan Gene Expression or SYBR Green PCR Master Mixes and run on a 7500 Real-Time PCR System machine (all Applied Biosystems). Settings were as follows: initial heating at 50°C for 2 min, denaturation for 10 min at 95°C, amplification with 40 repetitions of 15 s at 95°C and 1 min at 60°C. No-RT reactions were controlled to give no signal or, if any, the difference between control and sample was ensured to be larger than 5 Ct (Nolan *et al.*, 2006). We calculated the expression of target genes relative to the standard gene MA, as described in the ΔΔCt method for data analysis (Pfaffl, 2001), defining data taken on the first day of the experiment as controls. We applied the following formula:

$$\text{ratio} = \frac{(E_{\text{target}})^{\Delta Ct_{\text{target}}(control-sample)}}{(E_{MA})^{\Delta Ct_{MA}(control-sample)}}$$

## Acknowledgments

Preparation of this work was partially supported by a scholarship of the 'Friedrich-Ebert-Stiftung', Bonn, to Maddalena Bayer-Giraldi. Authors would like to thank G. Dieckmann for support, S. Frickenhaus and L. Medlin for phylogenetic tree calculations and S. Sato for comments that improved the manuscript.

## References

Arrigo, K.R., Dieckmann, G.S., Gosselin, M., Robinson, D.H., Fritsen, C.H., and Sullivan, C.W. (1995) High resolution study of the platelet ice ecosystem in McMurdo Sound, Antarctica: biomass, nutrient, and production profiles within a dense microalgal bloom. *Mar Ecol Prog Ser* **127:** 255–268.

Barrett, J. (2001) Thermal hysteresis proteins. *IJBCB* **33:** 105–117.

Bartsch, A. (1989) Die Eisalgenflora des Weddelmeeres (Antarktis): Artenzusammensetzung und Biomasse sowie Ökophysiologie ausgewählter Arten. *Ber Polar Meeresforsch/Rep Polar Mar Res* **63**.

Bendtsen, J.D., Nielsen, H., Heijne, G., and Brunak, S. (2004) Improved prediction of signal peptides: SignalP 3.0. *J Mol Biol* **340:** 783–795.

Carginale, V., Trinchella, F., Capasso, C., Scudiero, R., and Parisi, E. (2004) Gene amplification and cold adaptation of pepsin in Antarctic fish. A possible strategy for food digestion at low temperature. *Gene* **336:** 195–205.

Cox, G.F.N., and Weeks, W.F. (1983) Equation for determining the gas and brine volumes in sea-ice samples. *J Glaciol* **29:** 306–316.

Dereeper, A., Guignon, V., Blanc, G., Audic, S., Buffet, S., Chevenet, F., *et al.* (2008) Phylogeny.fr: robust phylogenetic analysis for the non-specialist. *Nucleic Acids Res* **36:** W465–W469.

DeVries, A.L., and Wohlschlag, D.E. (1969) Freezing resistance in some Antarctic fishes. *Science* **163:** 1073–1075.

Eicken, H. (1992) The role of sea ice in structuring Antarctic ecosystems. *Polar Biol* **12:** 3–13.

Fiala, M., and Oriol, L. (1990) Light-temperature interactions on the growth of Antarctic diatoms. *Polar Biol* **10:** 629–636.

Finn, R.D., Tate, J., Mistry, J., Coggill, P.C., Sammut, S.J., Hotz, H.-R., *et al.* (2008) The Pfam protein families database. *Nucleic Acids Res* **36:** D281–D288.

Guillard, R.R.L., and Ryther, J.H. (1962) Studies of marine planktonic diatoms: I. *Cyclotella nana Hustedt* and *Detonula confervacea* (Cleve) Gran. *Can J Microbiol* **8:** 229–239.

Guindon, S., and Gascuel, O. (2003) A simple, fast and accurate algorithm to estimate large phylogenies by maximum likelihood. *Syst Biol* **52:** 696–704.

Günther, S., and Dieckmann, G.S. (2001) Vertical zonation and community transition of sea-ice diatoms in fast ice and platelet layer, Weddell Sea, Antarctica. *Ann Glaciol* **33:** 287–296.

Henderson, I.R., Navarro-Garcia, F., and Nataro, J.P. (1998) The great escape: structure and function of the autotransporter proteins. *Trends Microbiol* **6:** 370–378.

Hoshino, T., Kiriaki, M., Ohgiya, S., Fujiwara, M., Kondo, H., Nishimiya, Y., *et al.* (2003) Antifreeze proteins from snow mold fungi. *Can J Bot* **81:** 1175–1181.

Huelsenbeck, J.P., Ronquist, F., Nielsen, R., and Bolback, J.P. (2001) Bayesian inference of phylogeny and its impact on evolutionary biology. *Science* **294:** 2310–2314.

Janech, M.G., Krell, A., Mock, T., Kang, J.-S., and Raymond, J.A. (2006) Ice-binding proteins from sea ice diatoms (Bacillariophyceae). *J Phycol* **42:** 410–416.

Kelly, G., Prasannan, S., Daniell, S., Fleming, K., Frankel, G., Dougan, G., *et al.* (1999) Structure of the cell-adhesion fragment of intimin from enteropathogenic *Escherichia coli*. *Nat Struct Biol* **6:** 313–318.

Kiko, R. (2009) Acquisition of freeze protection in a sea-ice crustacean through horizontal gene transfer? *Polar Biol* (in press): doi: 10.1007/s00300-009-0732-0

Krell, A., Funck, D., Plettner, I., John, U., and Dieckmann, G. (2007) Regulation of proline metabolism under salt stress in the psychrophilic diatom Fragilariopsis cylindrus (Bacillariophyceae). *J Phycol* **43:** 753–762.

Krell, A., Beszteri, B., Dieckmann, G., Glöckner, G., Valentin, K., and Mock, T. (2008) A new class of ice-binding proteins discovered in a salt-stress-induced cDNA library of the psychrophilic diatom *Fragilariopsis cylindrus* (Bacillariophyceae). *Eur J Phycol* **43:** 423–433.

Li, X., and Hew, C.L. (1991) Structure and function of an antifreeze polypeptide from ocean pout, *Macrozoarces americanus*: role of glutamic acid residues in protein stability and antifreeze activity by site-directed mutagenesis. *Protein Eng* **4:** 1003–1008.

Lizotte, M.P. (2001) The Contributions of Sea Ice Algae to Antarctic Marine Primary Production. *Am Zool* **41:** 57–73.

Maxwell, K., and Johnson, G.N. (2000) Chlorophyll fluorescence – a practical guide. *J Exp Bot* **51:** 659–668.

Maykut, G.A. (1986) The surface heat and mass balance. In *NATO ASI Series*. Untersteiner, N. (ed.). New York, NY, USA: Plenum Press, pp. 395–463.

Mock, T., and Valentin, K. (2004) Photosynthesis and cold acclimation: Molecular evidence from a polar diatom. *J Phycol* **40:** 732–741.

Mock, T., and Hoch, N. (2005) Long-term temperature acclimation of photosynthesis in steady-state cultures of the polar diatom Fragilariopsis cylindrus. *Photosynthesis Res* **85:** 307–317.

Mock, T., Krell, A., Glöckner, G., Kolukisaoglu, Ü., and Valentin, K. (2006) Analysis of expressed sequence tags (ESTs) from the polar diatom Fragilariopsis cylindrus. *J Phycol* **42:** 78–85.

Niemann, H.H., Schubert, W.-D., and Hein, D.W. (2004) Adhesins and invasins of pathogenic bacteria: a structural view. *Microb Infect* **6:** 101–112.

Nolan, T., Hands, R.E., and Bustin, S.A. (2006) Quantification of mRNA using real-time RT-PCR. *Nat Protoc* **1:** 1559–1582.

Pfaffl, M.W. (2001) A new mathematical model for relative quantification in real-time RT-PCR. *Nucleic Acids Res* **29:** 2002–2007.

Raymond, J.A., and DeVries, A.L. (1977) Adsorption inhibition as a mechanism of freezing resistance in polar fishes. *Proc Natl Acad Sci USA* **74:** 2589–2593.

Raymond, J.A., and Janech, M.G. (2009) Ice-binding proteins from enoki and shiitake mushrooms. *Cryobiology* **58:** 151–156.

Raymond, J.A., Fritsen, C., and Shen, K. (2007) An ice-binding protein from an Antarctic sea ice bacterium. *FEMS Microbiol Ecol* **61:** 214–221.

Raymond, J.A., Christner, B.C., and Schuster, S.C. (2008) A bacterial ice-binding protein from the Vostok ice core. *Extremophiles* **12:** 713–717.

Roberts, D., Craven, M., Cai, M., Allison, I., and Nash, G. (2007) Protists in the marine ice of the Amery Ice Shelf, East Antarctica. *Polar Biol* **30:** 143–153.

Ronquist, F., and Huelsenbeck, J.P. (2003) Bayesian phylogenetic inference under mixed models. *Bioinformatics* **19:** 1572–1574.

Thomas, D.N., and Dieckmann, G.S. (2002) Antarctic sea ice – a habitat for extremophiles. *Science* **295:** 641–644.

Thomas, D.N., Kennedy, H., Kattner, G., Gerdes, D., Gough, C., and Dieckmann, G.S. (2001) Biogeochemistry of platelet ice: its influence on particle flux under fast ice in the Weddell Sea, Antarctica. *Polar Biol* **24:** 486–496.

 

Venketesh, S., and Dayananda, C. (2008) Properties, Potentials, and Prospects of Antifreeze Proteins. *Crit Rev Biotechnol* **28:** 57–82.
Zhang, J. (2003) Evolution by gene duplication: an update. *Trends Ecol Evol* **18:** 292–298.

**Supporting information**

Additional Supporting Information may be found in the online version of this article:

**Fig. S1.** Alignment of *F. cylindrus* and *F. curta* mature IAFP isoforms. The E/G point mutation at position 18 is highlighted in colour. Only mature protein sequences are shown. Signal peptides were predicted with SignalP 3.0 (Bendtsen *et al.*, 2004).

**Table S1.** GenBank accession numbers of *iafp* isoforms of *F. cylindrus* TM99 and *F. curta* TM99, and primer combinations used for PCR amplification of each gene.
**Table S2.** Primer sequences used for PCR.
**Table S3.** Primer and probe sequences used for qPCR. Some oligos bind multiple isoforms as shown here. Probes were labelled with 5′ FAM/3′ TAMRA. Bold letters denote LNA nucleotides.



Supplementary Information (Chapter A.2):

Figure A 1: Alignment of *F. cylindrus* and *F. curta* mature IAFP isoforms. The E/G point mutation at position 18 is highlighted in colour. Only mature protein sequences are shown. Signal peptides were predicted with SignalP 3.0 (Bendtsen et al., 2004).

Table A 1: GenBank accession numbers of iafp isoforms of *F. cylindrus* TM99 and *F. curta* TM99, and primer combinations used for PCR amplification of each gene.

Table A 2: Primer sequences used for PCR.

Table A 3: Primer and probe sequences used for qPCR. Some oligos bind multiple isoforms as shown here. Probes were labelled with 5′ FAM/3′ TAMRA. Bold letters denote LNA nucleotides.

# 3.7.PUBLICATION 2

## CHARACTERIZATION OF AN ANTIFREEZE PROTEIN FROM THE POLAR DIATOM *FRAGILARIOPSIS CYLINDRUS* AND ITS RELEVANCE IN SEA ICE

Maddalena Bayer-Giraldi[a], Ilka Weikusat[a], Hüseyin Besir[b], Gerhard Dieckmann[a]

[a] Alfred Wegener Institute for Polar and Marine Research, Am Handelshafen 12, 27570 Bremerhaven, Germany

[b] European Molecular Biology Laboratory, Meyerhofstr. 1, 69117 Heidelberg, Germany

Corresponding author:
Maddalena Bayer-Giraldi
Email: Maddalena.Bayer@awi.de
Telephone: +49-(0)471-48311996
Fax: +49-(0)471-48311149

Cryobiology (2011), doi: 10.1016/ j.cryobiol.2011.08.006
In press

Contributions:
Own contributions concern the design research, the performance of experiments on protein expression, antifreeze activity, ice microstructure, the discussion of the data and manuscript writing. I. Weikusat assisted ice microstructure measurements and contributed in data discussion, H. Besir performed the expression of the recombinant protein and G. Dieckman provided general support.

**ABSTRACT**

Antifreeze proteins (AFPs), characterized by their ability to separate the melting and growth temperatures of ice and to inhibit ice recrystallization, play an important role in cold adaptation of several polar and cold-tolerant organisms. Recently, a multigene family of AFP genes was found in the diatom *Fragilariopsis cylindrus*, a dominant species within polar sea ice assemblages. This study presents the AFP from *F. cylindrus* set in a molecular and crystallographic frame. Differential protein expression after exposure of the diatoms to environmentally relevant conditions underlined the importance of certain AFP isoforms in response to cold. Analyses of the recombinant AFP showed freezing point depression comparable to the activity of other moderate AFPs and further enhanced by salt (up to 0.9°C in low salinity buffer, 2.5°C at high salinity). However, unlike other moderate AFPs, its fastest growth direction is perpendicular to the c-axis. The protein also caused strong inhibition of recrystallization at concentrations of 1.2 mM and 0.12 mM at low and high salinity, respectively. Observations of crystal habit modifications and pitting activity suggested binding of AFPs to multiple faces of the ice crystals. Further analyses showed striations caused by AFPs, interpreted as inclusion in the ice. We suggest that the influence on ice microstructure is the main characteristic of these AFPs in sea ice.

Key words: Antifreeze proteins; AFP; sea ice; diatoms; *Fragilariopsis cylindrus*; antifreeze activity; salt; crystal habit; ice microstructure.

# 1. INTRODUCTION

Antifreeze proteins (AFPs) are defined by their ability to bind to ice and influence its growth [5; 16; 34; 74]. Several AFPs have been described, belonging to different protein families spread over a variety of taxa of polar and temperate, but cold-tolerant, organisms. Even if these proteins share no common feature at a sequence level, they resemble each other in their influence on ice growth. The thermal hysteresis (TH), i.e. the lowering of the freezing point of a solution below the melting point, is a typical effect of AFPs. Another characteristic feature of AFPs is the inhibition of recrystallization (RI), i.e. of the process of grain boundary migration by which large crystals grow at the expenses of small ones. Dependent on whether TH or RI is the dominant effect on ice, the proteins are also called thermal hysteresis, ice binding or ice structuring proteins, but the nomenclature of these proteins is still under discussion.

AFPs are thought to act on ice by an adsorption-inhibition mechanism [43; 59]. The proteins, attached to the crystal surface, force the ice front to grow between them as the temperature is lowered below the bulk freezing point. The resulting surface curvature, with the solid phase convex into the liquid phase, induces a shift in equilibrium vapor pressure, lowering the local freezing point (Kelvin or Gibbs-Thomson effect). Local ice growth is limited and stops when the surface reaches a characteristic curvature, which is related to the degree of supercooling, at which vapor pressure between ice and water is in equilibrium and no additional crystallization occurs. Lowering the temperature means an increase of the characteristic curvature. At the hysteresis freezing point, the curvature has reached its maximum convexity, and any further cooling will result in explosive ice growth.

Several factors contribute to the efficiency of AFPs. One factor influencing the antifreeze activity (TH, RI) is the specificity of the protein-ice interaction, which is limited to defined planes of the ice crystal characteristic for each protein [4; 20; 22; 48; 53; 70]. Hyperactive AFPs bind several planes of ice crystals and are highly effective, causing a freezing point depression of up to 3-6°C. Moderate AFPs lower the freezing point by no more than 1°C at millimolar protein concentration, and their interaction is limited to characteristic non-basal planes. Related to the specificity of the proteins, which inhibit growth on the crystallographic planes interacting with AFPs, is the characteristic ice crystal habit. Ice crystals in AFP solutions grow in the shapes of hexagonal bipyramids, hexagonal plates, lemons or arrowheads. Furthermore, the preferential direction of crystallization depends on the kind of AFPs. Scotter *et al.* [70]

suggested that moderate proteins cause crystallization bursts along the c-axis whereas hyperactive AFPs cause bursts perpendicular to it.

AFPs have a variety of potential industrial applications, for which it is crucial to understand their physical antifreeze mechanism. AFPs may be applied in the medical sector for cryopreservation of blood and organs [2; 11; 54], in the food industry [19; 23; 55], as additives in paint and varnish to protect surfaces [29] or as hydrate inhibitors to avoid the formation of plugs in oil and gas pipelines [21].

Little is known about the recently discovered AFPs from the polar diatom *Fragilariopsis cylindrus* (fcAFPs) [7; 30]. They belong to the same family as proteins from other sea ice organisms (diatoms, crustacean), polar bacteria and yeast and cold-adapted fungi [26; 28; 30; 32; 44; 58; 61; 62]. *F. cylindrus* is a dominant species within brine channels and pockets in polar sea ice [6; 25; 46; 57], where temperatures can reach values as low as –20°C and brine salinities up to 200 on a Practical Salinity Scale [13; 15; 49]. The mechanisms of adaptation and acclimation that sea ice diatoms have evolved to cope with their extreme environment are subject of several molecular [36; 51; 52] and physiological analyses [6; 50]. Furthermore, Krembs *et al.* [38] and Krembs *et al.* [39] focused on the interaction between sea ice and diatoms due to extracellular polymeric substances, which create a protective envelope around cells and may anchor them to the ice surface within brine inclusions [38; 39]. Molecular studies about fcAFP genes, showing that they constitute a multigene family and that *F. cylindrus* responds to cold and salt stress with a strong upregulation of selected isoforms (up to 200-fold compared to initial stress-free conditions), suggested their relevance for this polar species [7]. Based on these results and considering the extreme conditions *F. cylindrus* is exposed to, especially in winter sea ice, we would expect fcAFPs to be a main factor in adaptation of this species to its environment.

In the following we focus on the characterization of AFP from *F. cylindrus*. We analyzed the protein and its expression under environmentally relevant conditions. We isolated a recombinant fcAFP isoform and characterized its antifreeze activity in terms of TH and RI. Based on the analysis of ice crystal habit, protein ice pitting activity and crystallographic observations we speculate on protein-ice interaction and the possible role of fcAFP in sea ice.

## 2. MATERIALS & METHODS

### 2.1 STRAIN AND CULTURE CONDITIONS

The cultures we used derive from isolates of *F. cylindrus* designated strain TM99 (Figure 1). The organisms were collected from sea ice samples of the Weddell Sea by Thomas Mock during the Polarstern ANT XVI/3 expedition (1999). Stock cultures were kept in ANT f/2 medium [24] at 5°C and continuous illumination of approximately 25 µE $m^{-2}$ $s^{-1}$.

### 2.2 PROTEIN ANALYSIS

We performed analyses of the 10 protein isoforms obtained from conceptual translations of the fcAFP genes presented in Bayer-Giraldi *et al.* [7] (Table 1). Analyses of amino acid composition and pI were carried out with ProtParam [18]. Prediction of the presence of a signal peptide, a sequence which targets proteins as extracellular, was done with SignalP [8], but not carried out with all isoforms since some are not known as full length sequences and lack the relevant N-termini. N-glycosylation was predicted with NetNGlyc 1.0 (http://www.cbs.dtu.dk/services/NetNGlyc/).

### 2.3 FcAFP EXPRESSION

Expression of AFPs of *F. cylindrus* grown under different environmental conditions was analyzed with immunoblotting. The different *F. cylindrus* treatments were optimal growth conditions and conditions of low temperature and high salinity resembling those in sea ice brine. Experimental cultures of *F. cylindrus* were initially grown in ANT f/2 medium [24], with its characteristic salinity of 34, at 5°C and constant illumination of approximately 25 µE $m^{-2}$ $s^{-1}$. The cultures were stirred and bubbled with sterile filtered air to ensure sufficient $CO_2$ supply. In the middle of the exponential growth phase, cultures were separated into the following treatments: unchanged at temperature 5°C and salinity 34 (control treatment, C), shocked at temperature –4°C and salinity 70 (temperature and salinity treatment, ST). All treatments were set up as triplicates. For details on experimental conditions and data on cell numbers, cell fitness in terms of maximum quantum yield of photosystem II and gene expression analysis see Bayer-Giraldi *et al*. [7]. Samples for protein expression analysis were collected, filtering cell cultures (20 ml) on 1.2 µm polycarbonate membrane filters (Millipore, USA). We processed selected duplicates for each treatment and sampling point. Cells were washed from filter, resuspended in phosphate buffered saline (PBS) solution and lysed by sonication on ice (5x1 minute, 40% duty cycle, with cooling periods of 1-2 minutes). The lysate was concentrated in Amicon filter devices (Millipore, USA) and

mixed to lysis buffer. Defined sample volumes, which in all samples corresponded to the same cell numbers, were used for further analysis. The samples were electrophoresed on a 15% SDS-polyacrylamide gel [68] and blotted to PVDF membranes (BioRad, USA) at 100 V in transfer buffer (25 mM Tris, pH 8.3, 192 mM glycine, 20% MeOH, 0.1% SDS) for 4-5 h at 4°C. The membranes were blocked in TBS-T plus 5% bovine serum albumin (BSA). The blots were incubated overnight at 4°C with polyclonal rabbit IgG (BioGenes, Germany) generated against the recombinant fcAFP isoform 11 (GenBank Acc. Nr. DR026070) (see section 2.4), washed, incubated for 1 h at room temperature with ECL horseradish peroxidase (HRP)-linked anti-rabbit IgG from donkey (GE Healthcare, UK) diluted 1:10,000 and blocked again. The membranes were incubated for 5 minutes with ECL Advanced Western Blotting Detection Kit reagents (GE Healthcare, UK) with HRP chemiluminescent substrate. Chemiluminescence was revealed by visualization with a cooled CCD-camera system (LAS-1,000; Fujifilm, Japan).

Protein quantification was done by blotting selected experimental samples together with known amounts of recombinant fcAFP, following the protocol described above.

## 2.4 EXPRESSION AND PURIFICATION OF A RECOMBINANT fcAFP

The gene for signal sequence-free fcAFP isoform 11 (starting with Ser21 according to SignalP program) was chosen for expression in bacteria, since EST library [21; 54] and qPCR analyses [22] had suggested that in *F. cylindrus* the expression of this isoform is upregulated under cold and salt stress. We amplified the sequence by PCR and cloned it downstream of a modified version of the sumo3 gene in the SUMO3-fusion vector pET28M-Sumo3. SUMO fusions increase the expression of the recombinant protein and enhance solubility. The original SUMO3-vector [64] was kindly provided by Chris D. Lima (Sloan-Kettering Institute, USA). We modified it by introducing two restriction sites (AgeI, BamHI) at the 3'-end of the sumo3 gene by silent mutagenesis. Using BamHI/XhoI, the resulting AFP protein could be cleaved without additional amino acids at the N- or C-termini.

*Escherichia coli* BL21(DE3)RIL cells (Novagen, USA) were transformed with pET28M-S3AFP and plated on LB-Agar with kanamycin and chloramphenicol. A 30 ml preculture was inoculated, grown overnight at 37°C and used for inoculating (1:100) LB medium with kanamycin (30 µg/ml) and chloramphenicol (10 µg/ml). The culture was grown at 37°C with 250 rpm until OD600 was approximately 0.4 and further incubated at 18°C for 1h. The protein expression was induced with 0.2 mM IPTG and cells were grown overnight at 18°C with 250 rpm. After harvesting at 6,000

g (20 minutes), the cell pellet was washed with PBS solution and pelleted again.
The pellet was resuspended in 25 ml lysis buffer (50 mM Na-phosphate, pH8, 300 mM NaCl, EDTA-free complete protease inhibitor cocktail (Roche, Switzerland)) and 0.1 mg/ml DNase and 1 mg/ml lysozyme were added after resuspension. The cell suspension was incubated for 10 minutes at room temperature and 30 minutes on ice before sonication for 6x30 seconds on ice with a Branson sonifier (50% duty cycle, output level 7) with cooling periods of 1-2 minutes between the bursts.
The lysate was centrifuged at 4°C with 100,000 g (30 minutes) and the supernatant was filtered through a 0.45 µm sterile filter. About 20 ml of cleared lysate were loaded on a 5 ml NiNTA column mounted on an ÄKTA purifier (GE Healthcare, UK) and the column was washed with washing buffer (50 mM Na-phosphate, 300 mM NaCl, 20 mM imidazole) until baseline was reached. Bound protein was eluted with a gradient of imidazole in the same buffer and the fractions containing SUMO3-AFP were dialyzed against 2 L of PBS after addition of His-tagged SenP2 protease (1:500 w/w) for the cleavage of SUMO3. The dialyzate was filtered and loaded on the NiNTA column again to remove uncleaved fusion protein and the protease. The flow-through of the second NiNTA column was aliquoted, frozen in liquid nitrogen and stored at -80°C for further analysis of antifreeze function and for immunoblotting (see section 2.3). To control the purity of the protein sample, an electrophoresis was run on a 15% SDS-polyacrylamide gel [68] subsequently stained with Coomassie Blue for protein visualization.

## 2.5 ANTIFREEZE ACTIVITY TECHNIQUES

Recombinant fcAFP was concentrated in Microcon centrifugal filter columns (Millipore, USA) and adjusted to different concentrations in PBS (salinity 10) and in a NaCl-solution with salinity 60. Solutions of BSA, a protein known to have no antifreeze activity, were used as controls.
TH activity was analyzed with a nanoliter osmometer (Clifton Technical Physics, USA) as described in Chakrabartty and Hew [10], and the settings were modified to further analyze RI activity and crystal habit. A metal sample holder in contact with a cold plate controlled by a Peltier element was covered by immersion oil to avoid sample evaporation. Samples were loaded at least as triplicates. Droplets of about 10 nl were loaded into wells within the sample holder, deep frozen at –40°C and slowly adjusted to the melting point, which was defined as the highest temperature at which the last crystal of about 20 µm is stable, neither growing nor melting. To determine the freezing point, temperature was slowly lowered in steps of 0.0186°C (10 mOsm) every 30 seconds. Measurements were repeated 3-5 times. For RI analysis, after a first step of deep freezing to create polycrystalline ice, the temperature of the osmometer was set

for 7 hours at -4°C. Pictures were taken after 1h, 4h and 7h of annealing. Images were captured using a stereo microscope and a CCD camera. We defined the RI endpoint as the fcAFP concentration below which no RI activity was detected [73].

## 2.6 ICE PITTING ACTIVITY ASSAY

Ice pitting activity was analyzed as described previously [60] (J. Raymond, Univ. Nevada Las Vegas, USA). A pure ice single crystal, prepared as in Raymond *et al.* [63], was fixed to a glass plate and submerged into the solution to be assayed, placed in a viewing tube to allow observation from the front and the rear side. The tube was held in a temperature-controlled viewing chamber set to a temperature slightly lower than the freezing point. Samples were observed through a stereo microscope and photographed after a few minutes.

## 2.7 ICE MICROSTRUCTURE TECHNIQUES

The microstructure of frozen fcAFP solutions was analyzed to get insights into the protein-ice interaction. Recombinant fcAFP (12 µM) and BSA (5 µM) in PBS were frozen at −4°C overnight in small Petri dishes (diameter 3 cm). Analysis was performed in a temperature-controlled room at −20°C after Kipfstuhl *et al.* [33]. Ice was loosened from the Petri dish and fixed to a glass slide with freshwater droplets. The surface of each sample was smoothed with a sled microtome, the samples detached from the glass side, turned around with the smooth surface on the bottom and fixed again. The top surface was microtomed first roughly, then at intervals of approximately 2 mm to ensure pristine, polished surface. The sample was transferred and fixed to a microscope slide and observed by reflected light microscopy. Images were taken with an optical microscope and a CCD camera at different magnifications.

Crystal axes orientation (ice fabric) of the same frozen fcAFP and BSA samples as described above was determined with an automated G50 ice fabric analyzer (Russell-Head Instruments, Australia), based on the polarization microscope principle [75]. A CCD camera acquired images of a thin ice section located on a stationary sample stage between motorized rotating crossed polarizers and a motorised λ/4 retarder plate. Images were taken from 9 different viewing angles, approximately 200 in total. For each pixel and polarizers rotation step the light intensity in the images was determined and a fitted sine curve over the rotation angles gave the angle of extinction for a plane along each viewing direction. The intersection of all planes from the 9 viewing angles determined the c-axis orientation per pixel. For analyses, the frozen fcAFP and BSA samples were cut with a band-saw to a thickness of approximately 500 µm, fixed on a glass slide with freshwater droplets, again polished by microtome and finally observed

with the fabric analyzer. Images were captured at resolutions of 5 $\mu m^2$/pixel and 50 $\mu m^2$/pixel.

## 3. RESULTS AND DISCUSSION

### 3.1 PROTEIN ANALYSIS

The main protein features found in AFP from *F. cylindrus* are characteristic for AFPs in general. Amino acid composition analysis showed a high amount of alanine (10-13%), glycine (10-12%) and threonine (10-13%). The abundance of these amino acids is common for AFPs. Except for isoform 9, all isoforms are deficient in cysteine, which is consistent with the results from AFPs from the snow mold fungus *Typhula ishikariensis*, belonging to the same protein family [77]. All analyzed isoforms were predicted to have a signal peptide with low signal anchor probability, suggesting that the protein is neither intracellular nor transmembrane, but secreted into the extracellular space. Isoforms 1, 2, 3, 8, 9 and 11 have a potential N-glycosylation site. The predicted mean pI of all isoforms is 5.27± 1.14, and striking is the strong polarity of the proteins. N-terminal regions have an acidic and C-terminal regions a basic pI, with a maximum difference in isoform 10 with pI 3.91 at the N-terminus and 10.28 at the C-terminus.

### 3.2 FcAFP EXPRESSION

Immunoblotting confirmed fcAFP expression under several environmental conditions (Figure 2). A variety of isoforms were expressed, as already suggested by gene expression analysis carried out during the same experiment [7]. As a differential up- and downregulation of the several fcAFP genes was dependent on physiological and environmental conditions, also protein expression pattern changed over time and was related to temperature and salt stress. In immunoblotting, proteins of size around 29, 45 and 55 kDa dominated after cold and salt exposure, whereas the proteins of approximately 20 kDa size, dominant in the control sample, became weaker. This broad isoform size distribution is expected for fcAFP. The genome of the recently sequenced *F. cylindrus* strain CCMP 1102 (Joint Genome Institute, USA) revealed fcAFP isoforms in the same size range as seen in our results, from 20 kDa (fgenesh2_pg.3_#_146|Fracy1) to 56 kDa (fgenesh2_pg.17_#_101|Fracy1, fgenesh2_pg.8_#_409|Fracy1). Consistent with qPCR data, fcAFP concentration was highest when cultures of the ST-treatment had reached stationary phase (day 20) and the concentration of fcAFP was approximately 0.7 fg/cell.

### 3.2 RECOMBINANT fcAFP

The total yield of purified recombinant fcAFP from 3 L of culture was 97.1 mg.
The protein was expressed as mature protein thus lacking the signal peptide, with a molecular weight of 25,939 Da. The sample contained no contaminations (Figure 3).

### 3.3 ANTIFREEZE ACTIVITY

The recombinant fcAFP was confirmed to have marked antifreeze activity. The protein caused TH, with a hyperbolic relationship between fcAFP concentration and freezing point depression (Figure 4a). In concentrations of 1.2 µM in PBS, and above, single ice crystals were stable within the hysteresis gap and rapidly grew after bursting at the freezing point. At lower protein concentrations TH was below detection limit. TH reached saturation at 230 µM with 0.9°C freezing point depression. Concentrations higher than 345 µM could not be included in the measurements due to disturbed visibility (opacity) of the crystals at high protein contents. Compared to TH values of hyperactive proteins, TH of fcAFPs was lower and very similar to results from experiments with AFPs from *T. ishikariensis* [77], such that the fcAFP is classified as moderate. However, the hysteresis activity shown by the *F. cylindrus* protein, as that of *T. ishikariensis*, was clearly higher than the hysteresis of other moderate AFPs (Figure 4b).

RI activity was high compared to other AFPs. AFP from *F. cylindrus* showed strong RI at concentrations of 1.2 µM or higher, without observable crystal grain growth during annealing for 7 hours at –4°C (Figure 5). The endpoint of RI activity was detected at concentrations of 0.12 µM even if the effect was weak. Other AFP solutions showed RI endpoints between 200 nM and 1.3 µM, dependent on protein family and isoform, as well as the detection method used [35; 71; 72; 73].

### 3.4 THE EFFECT OF SALT

The addition of salt increased TH and RI activity. Freezing point depression at salinity of 60 was 2.4-3.4 times higher than in PBS solution (Figure 4a). Within the measured concentration range the TH effect did not reach saturation but a maximum at 345 µM AFP (TH 2.5°C). The RI endpoint in the high salt solution was shifted down by one order of magnitude compared to measurements with PBS, as due to the effect of salt, full RI activity was still present at a concentration of 0.12 µM and weak effect at 0.012 µM̃. The enhancement of antifreeze activity by salt, previously described by Li, Andorfer and Duman [45] and Hagikawa and Daichi [27], may be due to a salting-out effect [42]. The solubility of proteins in the water phase is influenced by salts and, in the specific case of AFPs, it is assumed that a liquid saline AFP solution would result

in protein precipitation on the ice surface region, and thus increase the antifreeze effect compared to a less saline solution [42]. The effect of salt is of relevance under natural conditions, since sea ice algae live in brine inclusions with salinities close to 34 at the ice-water interface, but of possibly 200 at the upper surface of the sea ice sheet.

### 3.5 ICE CRYSTAL HABIT

To understand the details of protein-ice interaction we observed the ice crystal habit, which was clearly influenced by fcAFPs. Whereas ice growing at low velocities from a control solution of BSA in PBS was a flat disc expanding in direction of the basal plane, fcAFPs clearly affected crystal habit already at a low concentration (0.12 μM in PBS solutions, 0.012 μM in brine of salinity 60), even if no TH and only weak RI could be measured. After 30 minutes of observation within the hysteresis gap, crystals developed no visible facets. However, slowly lowering the temperature below the freezing point, ice crystals in solutions of low protein concentration developed at first a hexagonal habit, which gradually turned into a star-like shape with a six-fold symmetry (Figure 6). Also at higher fcAFP concentrations no development of facets was visible within the hysteresis gap. Increasing concentrations of fcAFPs caused larger hysteresis gaps, stronger supercooling and thus higher crystal growth velocities below the hysteresis freezing point, such that the freezing burst was fast and difficult to follow in detail. Moreover, observation was in most of the cases limited to one plane, because sample crystals on the cold stage of the nanoliter osmometer tended to be oriented with their basal plane horizontal. After burst, the crystals expanded first parallel to the a-axes, later more slowly parallel to the c-axis, and eventually the solution droplet was frozen within seconds. Ice seemed to have a fibrous structure with lamellae perpendicular to the c-axis. The star-like habit of the crystal was not observable due to quick freezing, but the core of the crystal in dendritic form was still visible in the center of the grain.

### 3.6 SITES OF PROTEIN-ICE INTERACTION

FcAFPs appeared to bind to ice at multiple sites. Budke and Koop [9] studied the effect of poly(vinyl alcohol) (PVA) on ice growth habit. In the presence of PVA, ice crystals initially grew in hexagonal shape, eventually becoming star-like [9] (Figure 7a). The OH-spacing in the PVA segment adsorbed to ice matched the spacing of O atoms in different planes of the ice crystal. The best lattice fit was on the primary and secondary prism faces (Figure 7b), which is in agreement with the star-like shape of the crystal. This habit strongly resembles the habit we observed in the presence of fcAFPs, which suggests that fcAFPs bind to ice in a similar way, i.e., to the prismatic faces of the crystal. FcAFPs may also bind to other planes of ice, as demonstrated by pitting

experiments (Figures 8a, b). Pits were visible on the basal plane of a pure ice crystal submerged in a diluted solution of recombinant fcAFP (0.38 µM). After Raymond *et al.* [63], pits formed because of the growth of the ice crystal in the direction of the c-axis, exept in the areas where AFPs bound to ice. The binding of fcAFPs may have occurred on the basal plane or on some non-prismatic planes. At higher concentrations (3.8 µM) no pits were visible and fcAFPs completely inhibited growth in all directions, eventually allowing uniform growth on the basal plane and dendritic growth on the lateral planes (Figure 8c). These results suggest that fcAFPs bind not only to the prismatic faces, but also to other faces of the ice crystals.

In their crystallization pattern normal to the c-axes, and their interaction with multiple ice crystal planes fcAFPs resemble hyperactive AFPs. However, their TH effect is much lower and they are rather classified as moderate. This discrepancy cannot be explained by our data, but future insights into protein crystal structure and identification of residues interacting with ice will probably shed light on this aspect of fcAFPs.

### 3.7 MICROSTRUCTURE OF ICE WITH fcAFP

Fibrous structure of ice crystals in the presence of fcAFP was confirmed by microscope analysis of frozen ice samples. Whereas ice with a control protein showed clearly defined crystals with no striking internal structural pattern (Figure 9a), strong striation was visible in ice with fcAFPs (Figure 9b). It is conceivable that brine and unbound proteins accumulate as inclusions between ice fibers causing a porous ice texture.

Observations of ice fabric with the automated analyzer confirmed striation to be perpendicular to c-axis orientation (Figure 10), as supposed after analysis at the nanoliter osmometer. Ice fibers formed parallel to the basal plane. Other grains, with their basal plane oriented parallel to observation plane, showed no visible striation. Thus, fcAFPs strongly influence the microstructure of ice, creating fibrous ice with layers interpreted as inclusions.

### 3.8 WHAT COULD BE THE ROLE OF fcAFP IN SEA ICE?

The function of fcAFPs, released by *F. cylindrus* into the extracellular space, seems to be related to the extreme habitat of brine channels and the proteins most probably play an important role for other polar diatoms, too. They have been found in a variety of sea ice diatoms [30, Uhlig pers. comm.], but never in temperate diatom species. FcAFPs belong to a multigene family, and gene expression is higher under environmental conditions resembling sea ice brine [7]. This suggests that their occurrence is most probably related to the adjustment to this extreme environment, which might have influence on sea ice structure and formation processes and thus shall be considered

here briefly. As shown above, they clearly have antifreeze activity, with moderate TH and strong RI. However, these effects are unlikely to play a relevant role within sea ice.

*F. cylindrus* is a raphid diatom species, living in sea ice brine channels and pockets, most probably attached to the ice surface [39; 41; 65]. A high volume fraction of brine inclusions in ice (porosity) and large surface for attachment, determined by inclusions microstructure, are of vital importance to these organisms [41]. Ice porosity, and subsequently brine inclusions surface area, however, are lowered by cooling or desalination processes [56]. *F. cylindrus* has been found to be distributed throughout the ice column [6], where temperatures range from seawater freezing temperature (approx. -1.8°C) at the ice-water interface to a temperature at the surface possibly as low as -20°C. The moderate freezing point depression observed in the presence of fcAFPs would not be sufficient to avoid ice growth and consequent narrowing of the brine pore space. We also see no role of RI activity for diatom survival within brine inclusions. What might the function of AFPs in *F. cylindrus* then be?

FcAFPs secreted by *F. cylindrus* interact with the ice surface and will influence the local growth pattern of ice crystals. The interaction could change ice microstructure and create a texture as indicated in our experiments, increasing ice porosity and the potential attachment surface. Moreover, a diatom attached to ice would not be overgrown by the advancing ice interface, but survive in brine inclusions created locally due to fcAFPs. A comparable mechanisms of brine inclusion formation, due to extracellular polymeric substances (EPS), was already described by Krembs *et al.*[39]. However, fcAFP amounts within the cell are low, and even though we do not know expression rates or protein stability within sea ice, we suggest that fcAFPs would need to accumulate considerably before reaching effective amounts in ice. The accumulation would require long protein expression periods combined with stable conditions within the brine network to avoid a protein flux out of the ice.

Protein concentration in a sheath of EPS around the cells could increase the effectiveness of the proteins. Sea ice diatoms have repeatedly been shown to be producers of EPS [1; 40; 66], and there is a good correlation between the presence of EPS and of diatoms in brine pores [38; 39]. These substances, mainly polysaccharides and proteins, encapsulate and protect the cells. Krembs *et al.* [39] suggested that EPS could influence the growing ice crystal by changing the diffusive properties of salt at the ice interface, forcing the formation of brine pockets in a position favourable to the diatoms and increasing porosity such that the organisms would remain surrounded by

brine. Moreover, EPS changes the microstructure of ice within brine pores, creating angular and convoluted shapes [38]. A complex microstructure decreases ice permeability, and brine is retained within inclusions in the ice sheet and will not drain into the water column during desalination [38]. Furthermore, EPS have been suggested to provide a mechanism for preferential incorporation of bacteria [17] and algae [67] into sea ice and retention in brine inclusions, because of its properties to attach to ice surfaces [37].

The interaction of EPS with ice was shown to be linked to its heat-labile fraction [17] and more specifically to its protein fraction [38], suggesting that it may be related to AFPs. Kayitmazer *et al.* [31] showed that proteins embedded in protein-polysaccharide coacervates, as is EPS, show low mobility, entrapped within dense domains and at the dense/dilute domain interface. It is conceivable that fcAFPs, secreted from diatoms, may accumulate in the EPS matrix and reach here high concentrations effectively influencing attachment of organisms and shaping the microstructure of ice.
In order to shed light on the ice binding mechanisms and effects of fcAFP on ice, future work will focus on ice microstructure and clarify the nature of the observed striations. Furthermore, clarification on the interactions between fcAFPs and EPS coacervates will help to explain the adaptation of *F. cylindrus* to the sea ice environment. These combined investigations will improve the picture of how sympagic organisms shape their environment.

**AKNOWLEDGEMENTS**

Authors would like to thank Klaus Valentin, Sepp Kipfstuhl and Erika Allhusen (Alfred Wegener Institute) for support, and Jim Raymond (University Nevada Las Vegas) for experiments on ice pitting activity.

**BIBLIOGRAPHY**

[1] L. Aletsee, J. Jahnke, Growth and productivity of the psychrophilic marine diatoms *Thalassiosira antarctica* Comber and *Nitschia firgida* Grunow in batch cultures at temperatures below the freezing point of water, Polar Biology 11 (1992) 643-647.

[2] G. Amir, L. Horowitz, B. Rubinsky, B. Sheick Yousif, J. Lavee, A.K. Smolinsky, Subzero non freezing cryopreservation of rat hearts using antifreeze protein I and antifreeze protein III, Cryobiology 48 (2004) 273-282.

[3] J. Baardsnes, M. Jelokhani-Niaraki, L.H. Kondejewski, M.J. Kuiper, C.M. Kay, R.S. Hodges, P.L. Davies, Antifreeze protein from shorthorn sculpin: Identification of the ice-binding surface, Protein Science 10 (2001) 2566-2576.

[4] M. Bar, Y. Celik, D. Fass, I. Braslavsky, Interactions of β-helical antifreeze protein mutants with ice, Crystal Growth and Design 8 (2008) 2954-2963.

[5] J. Barrett, Thermal hysteresis proteins, The International Journal of Biochemistry and Cell Biology 33 (2001) 105-117.

[6] A. Bartsch, Die Eisalgenflora des Weddelmeeres (Antarktis): Artenzusammensetzung und Biomasse sowie Ökophysiologie ausgewählter Arten, Berichte zur Polar- und Meeresforschung/Reports on Polar and Marine Research 63 (1989).

[7] M. Bayer-Giraldi, C. Uhlig, U. John, T. Mock, K. Valentin, Antifreeze proteins in polar sea ice diatoms: diversity and gene expression in the genus Fragilariopsis, Environmental Microbiology 12 (2010) 1041-1062.

[8] J.D. Bendtsen, H. Nielsen, G.v. Heijne, S. Brunak, Improved prediction of signal peptides: SignalP 3.0, Journal of Molecular Biology 340 (2004) 783-795.

[9] C. Budke, T. Koop, Ice Recrystallization Inhibition and Molecular Recognition of Ice Faces by Poly(vinyl alcohol), ChemPhysChem 7 (2006) 2601-2606.

[10] A. Chakrabartty, C.L. Hew, The effect of enhanced α-helicity on the activity of a winter flounder antifreeze polypeptide, European Journal of Biochemistry 202 (1991) 1057-1063.

[11] H. Chao, P.L. Davies, J.F. Carpenter, Effects of antifreeze proteins on red blood cell survival during cryopreservation, Journal of Experimental Biology 199 (1996) 2071-2076.

[12] H. Chao, M.E.J. Houston, R.S. Hodges, C.M. Kay, B.D. Sykes, M.C. Loewen, P.L. Davies, F.D. Sönnichsen, A Diminished Role for Hydrogen Bonds in Antifreeze Protein Binding to Ice, Biochemistry 36 (1997) 14652-14660.

[13] G.F.N. Cox, W.F. Weeks, Equation for determining the gas and brine volumes in sea-ice samples., Journal of Glaciology 29 (1983) 306-316.

[14] C.I. DeLuca, R. Comley, P.L. Davies, Antifreeze Proteins Bind Independently to Ice, Biophysical Journal 74 (1998) 1502-1508.

[15] H. Eicken, The role of sea ice in structuring Antarctic ecosystems, Polar Biology 12 (1992) 3-13.

[16] K.V. Ewart, Q. Lin, C.L. Hew, Structure, function and evolution of antifreeze proteins, Cellular and Molecular Life Sciences 55 (1999) 271-283.

[17] M. Ewert, J.W. Deming, Selective retention in saline ice of extracellular polysaccharides prodiced by the cold-adapted marine strain bacterium *Colwellia psychrerythraea* strain 34H, Annals of Glaciology 52 (2011) 111-117.

[18] E. Gasteiger, C. Hoogland, A. Gattiker, S. Duvaud, M.R. Wilkins, R.D. Appel, A. Bairoch, Protein Identification and Analysis Tools on the ExPASy Server. in:

J.M. Walker, (Ed.), The Proteomics Protoclos Handbook, Humana Press, 2005, pp. 571-607.

[19] V.G. Gaukel, W.E.L. Spieß, EInfluss von Antigefrierproteinen auf die Rekristallisation von Eis in Modelllösungen für Eiskrem, Chemie Ingenieur Technik 76 (2004) 454-458.

[20] J.A. Gilbert, P.L. Davies, J. Laybourn-Parry, A hyperactive, $Ca^{2+}$-dependent antifreeze protein in an Antarctic bacterium, FEMS Microbiology Letters 245 (2005) 67-72.

[21] R. Gordienko, H. Ohno, V.K. Singh, Z. Jia, J.A. Ripmeester, V.K. Walker, Towards a Green Hydrate Inhibitor: Imaging Antifreeze Proteins on Clathrates, PLoS ONE 5 (2010) e8953.

[22] S.P. Graether, M.J. Kulper, S.M. Gagné, V.K. Walker, Z. Jia, B.D. Sykes, P.L. Davies, b-Helix structure and ice-binding properties of a hyperactive antifreeze protein from an insect, Nature 406 (2000).

[23] M. Griffith, V.K. Ewart, Antifreeze proteins and their potential use in frozen foods, Biotechnology Advances 13 (1995) 375-402.

[24] R.R.L. Guillard, J.H. Ryther, Studies of marine planktonic diatoms: I. *Cyclotella nana Hustedt* and *Detonula confervacea* (Cleve) Gran., Canadian Journal of Microbiology 8 (1962) 229-239.

[25] S. Günther, G.S. Dieckmann, Vertical zonation and community transition of sea-ice diatoms in fast ice and platelet layer, Weddell Sea, Antarctica, Annals of Glaciology 33 (2001) 287-296.

[26] I.G. Gwak, W.s. Jung, H.J. Kim, S.-H. Kang, E. Jin, Antifreeze Protein in Antarctic Marine Diatom, *Chaetoceros neogracile*, Marine Biotechnology 12 (2010) 630-639.

[27] Y. Hagiwara, D. Yamamoto, Cooperative Effect of Winter Flounder Antifreeze Protein and Ions on the Unidirectional Freezing of their Solution in a Narrow Space, Physics and Chemistry of Ice 2010, Hokkaido University Press, Sapporo, Japan, 2011, pp. 313-319.

[28] T. Hoshino, M. Kiriaki, S. Ohgiya, M. Fujiwara, H. Kondo, Y. Nishimiya, I. Yumoto, S. Tsuda, Antifreeze proteins from snow mold fungi, Canadian Journal of Botany/Revue Canadienne de Botanique 81 (2003) 1175-1181.

[29] IFAM, IFAM Jahresbericht 2006/2007, Fraunhofer-Institut für Fertigungstechnik und Angewandte Materialforschung Bremen.

[30] M.G. Janech, A. Krell, T. Mock, J.-S. Kang, J.A. Raymond, Ice-binding proteins from sea ice diatoms (Bacillariophyceae), Journal of Phycology 42 (2006) 410-416.

[31] A.B. Kayitmazer, H.B. Bohidar, K.W. Mattison, A. Bose, J. Sarkar, A. Hashidzume, P.S. Russo, W. Jaeger, P.L. Dubin, Mesophase separation and probe dynamics in protein-polyelectrolyte coacervates, Soft Matter 3 (2007) 1064-1076.

[32] R. Kiko, Acquisition of freeze protection in a sea-ice crustacean through horizontal gene transfer?, Polar Biology 33 (2010) 543-556.

[33] S. Kipfstuhl, I. Hamann, A. Lambrecht, J. Freitag, S.H. Faria, D. Grigoriev, N. Azuma, Microstructure mapping: a new method for imaging deformation-induced microstructural features of ice on the grain scale, Journal of Glaciology 52 (2006) 398-406.

[34] C.A. Knight, Adding to the antifreeze agenda, Nature 406 (2000) 249-250.

[35] C.A. Knight, J.A. Duman, Inhibition of Recrystallization of Ice by Insect Thermal Hysteresis Proteins: A possible Cryoprotective Role, Cryobiology 23 (1986) 256-262.

[36] A. Krell, D. Funck, I. Plettner, U. John, G. Dieckmann, Regulation of proline metabolism under salt stress in the psychrophilic diatom *Fragilariopsis cylindrus* (Bacillariophyceae), Journal of Phycology 43 (2007) 753-762.

[37] C. Krembs, J.W. Deming, The role of exopolymers in microbial adaptation to sea ice. in: R. Margesin, F. Schinner, J.-C. Marx, and C. Gerday, (Eds.), Psychrophiles: from biodiversity to biotechnology, Springer Verlag, Berlin, 2008, pp. 247-264.

[38] C. Krembs, H. Eicken, J.W. Deming, Exopolymer alterations of physical properties of sea ice and implications for ice habitability and biogeochemistry in a warmer Arctic, Proceedings of the National Academy of Science 108 (2011) 3653-3658.

[39] C. Krembs, H. Eicken, K. Junge, J.W. Deming, High concentrations of exopolymeric substances in Arctic winter sea ice: implications for the polar ocean carbon cycle and cryoprotection of diatoms, Deep Sea Research (Part I, Oceanographic Research Papers) 49 (2002) 2163-2181.

[40] C. Krembs, A. Engel, Abundance and variability of microorganisms and transparent exopolymer particles across ice-water interface of melting first-year sea ice in the Laptev Sea (Arctic), Marine Biology 138 (2001) 173-185.

[41] C. Krembs, R. Gradinger, M. Spindler, Implication of brine channels geometry and surface area for the interaction of sympagic organisms in Antarctic sea ice, Journal of Experimental Marine Biology and Ecology 243 (2000) 55-80.

[42] E. Kristiansen, S.A. Pedersen, K.E. Zachariassen, Salt-induced enhancement of antifreeze protein activity: A salting-out effect, Cryobiology 57 (2008) 122-129.

[43] E. Kristiansen, K.E. Zachariassen, The mechanism by which fish antifreeze proteins cause thermal hysteresis, Cryobiology 51 (2005) 262-280.

[44] J.K. Lee, K.S. Park, S. Park, H. Park, Y.H. Song, S.-H. Kang, H.J. Kim, An extracellular ice-binding glycoprotein from an Antarctic psychrophilic yeast, Cryobiology 60 (2010) 222-228.

[45] N. Li, C.A. Andorfer, J.A. Duman, Enhancement of insect antifreeze protein activity by solutes of low molecular mass, The Journal of Experimental Biology 201 (1998) 2243-2252.

[46] M.P. Lizotte, The Contributions of Sea Ice Algae to Antarctic Marine Primary Production, American Zoologist 41 (2001) 57-73.

[47] C.B. Marshall, M.E. Daley, B.D. Sykes, P.L. Davies, Enhancing the Activity of a β-Helical Antifreeze Protein by the Engineered Addition of Coils, Biochemistry 43 (2004) 11637-11646.

[48] C.B. Marshall, G.L. Fletcher, P.L. Davies, Hyperactive antifreeze protein in a fish, Nature 429 (2004) 153.

[49] G.A. Maykut, The surface heat and mass balance. in: N. Untersteiner, (Ed.), NATO ASI series, New York Plenum Pr., 1986, pp. 395-463.

[50] T. Mock, N. Hoch, Long-term temperature acclimation of photosynthesis in steady-state cultures of the polar diatom *Fragilariopsis cylindrus*, Photosynthesis Research 85 (2005) 307-317.

[51] T. Mock, A. Krell, G. Glöckner, Ü. Kolukisaoglu, K. Valentin, Analysis of expressed sequence tags (ESTs) from the polar diatom *Fragilariopsis cylindrus*, Journal of Phycology 42 (2006) 78-85.

[52] T. Mock, K. Valentin, Photosynthesis and cold acclimation: Molecular evidence from a polar diatom, Journal of Phycology 40 (2004) 732-741.

[53] Y.-F. Mok, F.-H. Lin, L.A. Graham, Y. Celik, I. Braslavsky, P.L. Davies, Structural Basis for the Superior Activity of the Large Isoform of Snow Flea Antifreeze Protein, Biochemistry 49 (2010) 2593-2603.

[54] J.A. Mugnano, T. Wang, J.R. Layne, A.L. DeVries, R.E.J. Lee, Antifreeze glycoproteins promote intracellular freezing of rat cardiomyocytes at high subzero temperatures, American Journal of Physiology: Regulatory, Integrative and Comparative Physiology 269 (1995) R474-R479.

[55] S.R. Payne, O.A. Young, Effects of pre-slaughter administration of antifreeze proteins on frozen meat quality, Meat Science 41 (1995) 147-155.

[56] C. Petrich, H. Eicken, Growth, Structure and Properties of Sea Ice. in: D.N. Thomas, and G. Dieckmann, (Eds.), Sea Ice, Wiley-Blackwell, Chichester, 2010, pp. 23-77.

[57] M. Poulin, Ice diatoms: the Arctic. in: L.K. Medlin, and J. Priddle, (Eds.), Polar Marine Diatoms, British Antarctic Survey, Cambridge, 1990, pp. 15-18.

[58] J.A. Raymond, B.C. Christner, S.C. Schuster, A bacterial ice-binding protein from the Vostok ice core, Extremophiles 12 (2008) 713-717.

[59] J.A. Raymond, A.L. DeVries, Adsorption inhibition as a mechanism of freezing resistance in polar fishes, Proceedings of the National Academy of Sciences, USA 74 (1977) 2589-2593.

[60] J.A. Raymond, C. Fritsen, Semipurification and Ice Recrystallization Inhibition Activity of Ice-Active Substances Associated with Antarctic Photosynthetic Organisms, Cryobiology 43 (2001) 63-70.

[61] J.A. Raymond, C. Fritsen, K. Shen, An ice-binding protein from an Antarctic sea ice bacterium, FEMS Microbiology Ecology 61 (2007) 214-221.

[62] J.A. Raymond, M.G. Janech, Ice-binding proteins from enoki and shiitake mushrooms, Cryobiology 58 (2009) 151-156.

[63] J.A. Raymond, P. Wilson, A.L. DeVries, Inhibition of growth of nonbasal planes in ice by fish antifreezes, Proceedings of the National Academy of Sciences, USA 86 (1989) 881-885.

[64] D. Reverter, C.D. Lima, Structural basis for SENP2 protease interactions with SUMO precursors and conjugated substrates, Nature Structural & Molecular Biology 13 (2006) 1060-1068.

[65] U. Riebesell, I. Schloss, V. Smetack, Aggregation of algae released from melting sea ice: implications for seeding and sedimentation, Polar Biology 11 (1991) 239-248.

[66] A. Riedel, C. Michel, M. Gosselin, Seasonal study of sea-ice exopolymeric substances on the Mackenzie shelf: implications for transport of sea-ice bacteria and algae, Aquatic Microbial Ecology 45 (2006) 195-206.

[67] A. Riedel, C. Michel, M. Gosselin, B. LeBlanc, Enrichment of nutrients, exoplymeric substances and microorganisms in newly formed sea ice on the Mackenzie shelf, Marine Ecology Progress Series 342 (2007) 55-67.

[68] H. Schägger, G. von Jagow, Tricine-sodium dodecyl sulfate-polyacrylamdie gel electrophoresis for the separation of protein in the range from 1 to 100 kDa, Analytical Biochemistry 166 (1987) 368-379.

[69] J.D. Schrag, S.M. O'Grady, A.L. DeVries, Relationship of amino acid composition and moleculra weight of antifreeze glycopeptides to non-colligative freezing point depression, Biochimica et Biophysica Acta 717 (1982) 322-326.

[70] A.J. Scotter, C.B. Marshall, L.A. Graham, J.A. Gilbert, C.P. Garnham, P.L. Davies, The basis for hyperactivity of antifreeze proteins, Cryobiology 53 (2006) 229-239.

[71] C. Sidebottom, S. Buckley, P. Pudney, S. Twigg, C. Jarman, C. Holt, J. Telford, A. McArthur, D. Worrall, R. Hubbard, P. Lillford, Phytochemistry: Heat-stable antifreeze protein from grass, Nature 406 (2000) 256.

[72] M. Smallwood, D. Worrall, L. Byass, L. Elias, D. Ashford, C.J. Doucet, C. Holt, L. Telford, P. Lillford, D.J. Bowles, Isolation and characterization of a novel antifreeze protein from carrot (*Daucus carota*), Biochemical Journal 340 (1999) 385-391.

[73] M.M. Tomczak, C.B. Marshall, J.A. Gilbert, P.L. Davies, A facile method for determining ice recrystallization inhibition by antifreeze proteins, Biochemical and Biophysical Research Communications 311 (2003) 1041-1046.

[74] S. Venketesh, C. Dayananda, Properties, Potentials, and Prospects of Antifreeze Proteins, Critical Reviews in Biotechnology 28 (2008) 57-82.

[75] L.A. Wilen, C.L. Diprinzio, R.B. Alley, N. Azuma, Development, Principles, and Applications of Automated Ice Fabric Analyzers, Microscopy Research and Technique 62 (2003) 2-18.

[76] Y. Wu, J. Banoub, S.V. Goddard, M.H. Kao, G.L. Fletcher, Antifreeze glycoproteins: relationship between molecular weight, thermal hysteresis and the inhibition of leakage from liposomes during thermotropic phase transition, Comparative Biochemistry and Physiology B: Biochemistry and Molecular Biology 128 (2001) 265-273.

[77] N. Xiao, K. Suzuki, Y. Nishimiya, H. Kondo, A. Miura, S. Tsuda, T. Hoshino, Comparison of functional properties of two fungal antifreeze proteins from *Antarctomyces psychotrophicus* and *Typhula ishikariensis*, FEBS Journal 277 (2010) 394-403.

| Isoform | 1 | 2 | 3 | 5 | 6 | 7 | 8 | 9 | 10 | 11 |
|---|---|---|---|---|---|---|---|---|---|---|
| Acc. Nr. | GQ23274 | GQ23274 | GQ23274 | GQ23274 | GQ23274 | GQ23274 | GQ23275 | EL737280 | EL737258 | DR026070 |
| Number of amino acids | 250 | 251 | 166 | 255 | 250 | 191 | 213 | 245 | 253 | 257 |
| Identities | 94% | 92% | 95% | 87% | 80% | 84% | 80% | 57% | 83% | - |

**Table 1:**
AFP isoforms of *F. cylindrus*TM99 used and corrisponding GenBank accession numbers. From Bayer-Giraldi *et al*. [7]. The number of amino acid residues and the identities between each isoform and isoform 11, calculated with the BLAST algorithm, are also shown.

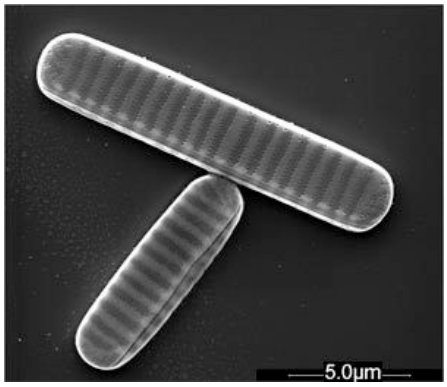


**Figure 1:**
*F. cylindrus* cells visualized by scanning electron microscopy (Image: courtesy of Henrik Lange and Friedel Hinz, Alfred Wegener Institute, Germany).

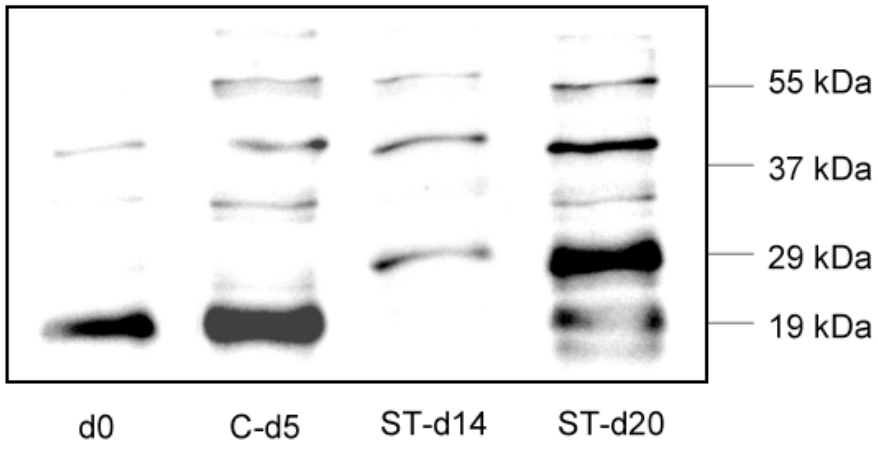


**Figure 2:**
Immunoblotting of fcAFP, with protein expression at the different stages of the experiment. d0: expression before separation of batches into C-and ST-treatments (day 0); C-d5: expression in the C-treatment at day 5, when cultures in control batches had reached stationary phase; ST-d14 and ST-d20: expression in the ST-treatment at days 14 and 20, respectively, when cells had reached the end of the logarithmic growth phase after recovery from the temperature and cold shock and fcAFP gene expression was highest.

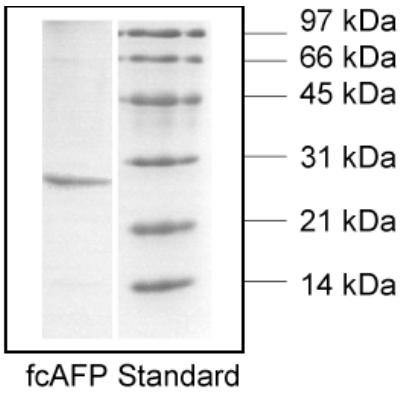


**Figure 3:**
SDS-polyacrylamide gel electrophoresis of the recombinant fcAFP (left) and a molecular weight standard (right). The electrophoresis showed no contamination of the protein.

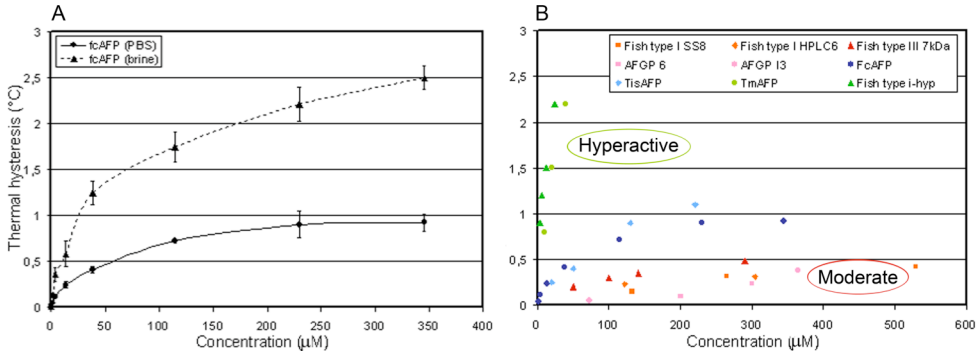


**Figure 4:**

A: Thermal hysteresis activity of FcAFP in PBS solution (salinity 10) and brine (salinity 60).

B: Thermal hysteresis activity of hyperactive and moderate AFPs. Hyperactive AFPs include ● *Tenebrio molitor* isoform 4-9 (TmAFP) [47] and ▲ fish type I-hyp [48]; moderate AFPs include fish type I, ■ isoforms SS8 [3] and ◆ HPLC6 [12], ▲ fish type III (7kDa) [14], ■ AFGP 6 [69], ● AFGP $I_3$ [76], ◆ *T. ishikariensis* wild type (TisAFP) [77] and ● fcAFP (in PBS).

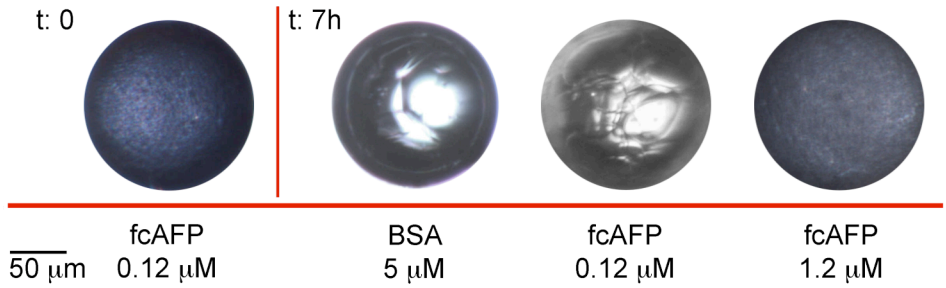


**Figure 5:**

RI in frozen solutions of BSA (5 µM) and fcAFP (0.12 µM and 1.2 µM) in PBS. Solutions were deep frozen (t0), annealed at –4°C and photographed after 7h. Sample of AFP (0.12 µM) at t0 is representative for all solutions after deep freezing. In samples at t0 and sample fcAFP (1.2 µM) t7 ice is polycrystalline and single ice crystals are not discernible individually. In samples BSA and fcAFP (0.12 µM) strong and limited ice recrystallization, respectively, has occurred, and grain became larger and visible individually.


**Figure 6:**

The habit of an ice single crystal growing in a solution of fcAFP (0.012 μM) at a temperature slightly below its freezing point. Pictures were taken at time intervals of approximately 10 seconds.

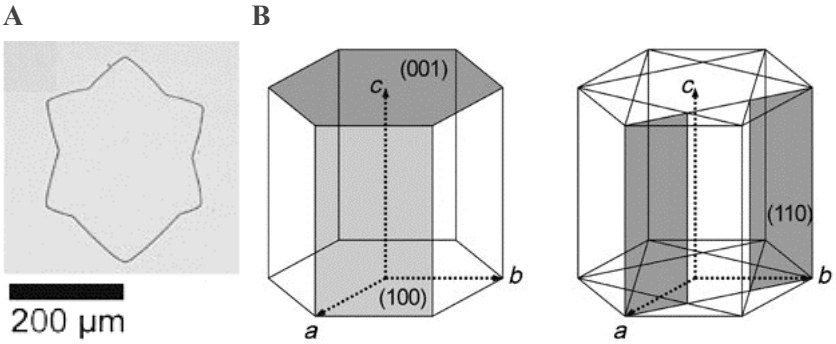


**Figure 7:**

A: The habit of an ice crystal grown in the presence of PVA27 (10 mg/ml).

B: Elementary cell of ice Ih. The picture shows primary (100) and secondary (110) prismatic faces as possible crystal planes for PVA (and fcAFP) binding.

Pictures from Budke and Koop [9], copyright Wiley-VCH Verlag GmbH & Co. KGaA, reproduced with permission.

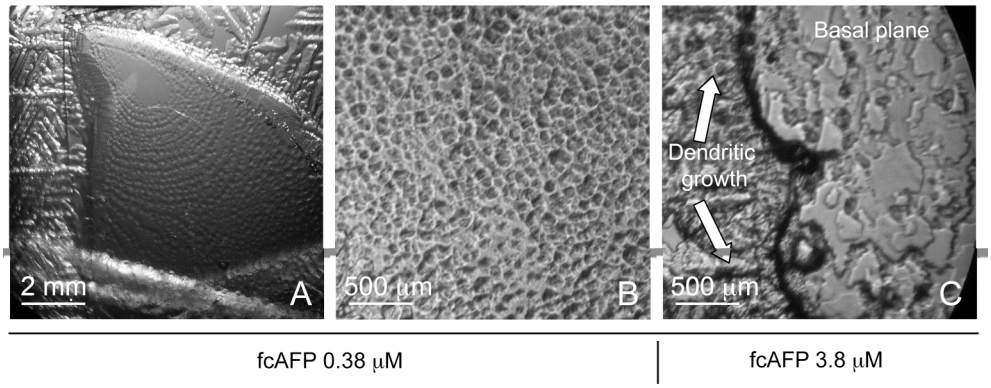


**Figure 8**:

Ice pitting activity in solutions of recombinant fcAFP at protein concentrations of 0.38 μM (A-B) and 3.8 μM (C). Observation was along the c-axes and pictures show the basal plane of the crystals. A: The pure ice single crystal at the center of the picture is

covered by pits on its basal plane. Around the original crystal, dendritic ice developed perpendicular to the c-axis. B: Basal plane covered by pits. C: Limited growth on the basal plane (right) and dendritic growth perpendicular to the c-axis (left). Pictures: courtesy of J. Raymond, Univ. Nevada Las Vegas, USA.

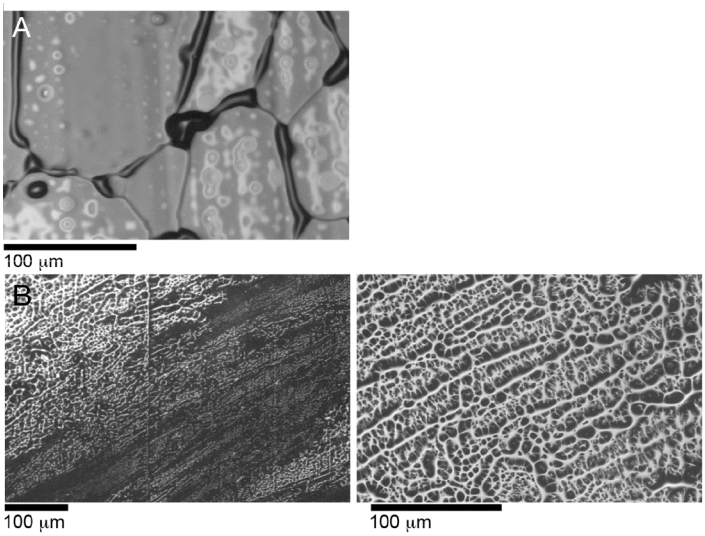


**Figure 9:**

Frozen and microtomed samples of protein solutions, observed by reflected light microscopy.

A: Frozen solution of BSA (5 µM)

B: Frozen solution of recombinant fcAFP (12 µM) in PBS buffer, at different magnifications.

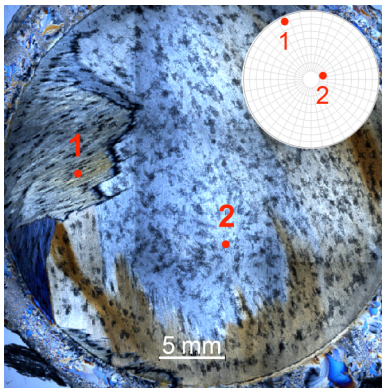


**Figure 10:**

Section of frozen solution of recombinant fcAFP (12 µM) observed under crossed polarizers. Single ice crystals can be distinguished. Crystal 1 shows striations, whereas crystal 2 is without striations. The stereographic projections shows c-axis direction of the selected ice crystals 1 and 2. Projection plane of the diagram is parallel to the observed section plane.

# 4. SUMMARY AND CONCLUSIONS

## 4.1.SUMMARY

The present work is aimed at improving the knowledge about AFPs recently discovered in the diatom *F. cylindrus*, including molecular understanding and protein activity analyses.

Chapters 3.1 and 3.2 set the molecular basis of fcAFPs. These chapters represent a crucial element and important tool for further work with fcAFPs, which relies on the knowledge about fcAFP gene diversity and activity. The chapters present the multigene family of fcAFPs and show their differential regulation under low temperature and high salinity stress. The number of isoforms detected in *F. cylindrus* and the strong upregulation in expression of selected fcAFPs suggest a great relevance of these proteins for this diatom species in response to sea ice conditions. Phylogenetic analysis indicates several events of HGT resulting in a broad taxonomic distribution never observed before in AFPs. Chapter 3.3 shows the heterologous expression of an fcAFP (isoform 11) in *E. coli*, whereas the protein purification resulted to be strongly dependent on the presence of the signal peptide.

The characterization of the antifreeze activity of the recombinant protein is of interest to understand the biological function and potential applications of fcAFPs. Chapter 3.4 presents the potential of fcAFPs regarding TH and RI, classified as moderate and high, respectively. These effects were further enhanced by the addition of salts. The proteins seem to bind multiple planes of ice crystals, presumably primary and secondary prismatic faces and some non-prismatic plane. Chapter 3.5 shows the marked influence fcAFPs have on ice microstructure, characterized by a fibrous texture with striations perpendicular to the c-axis. In this chapter I propose that inclusions of brine, with unbound fcAFPs and other solutes segregated from the ice lattice, are determinants for the striations. Chapter 3.5 also shows, to my knowledge for the first time in AFP research, the fabric of frozen fcAFP solutions, marked by gradual transitions in c-axis distribution and characteristic grain boundaries. Ice fabric in the presence of AFPs has not been analyzed in detail before, therefore no comparison is possible between the effect of fcAFPs and other AFPs. The characteristic fabric suggests that fcAFPs may also play a role as nucleation inhibitors.

## 4.2. WHAT COULD BE THE BIOLOGICAL ROLE OF fcAFPs?

The putative biological roles of AFPs are various and can be roughly divided into freeze avoidance and freeze tolerance. In fishes, AFPs are successful in inhibiting ice formation due to their nucleation inhibition and TH activity that compensate for differences in osmolarity between the organism and seawater. In plants, the TH effect of AFPs is weak compared to the low temperatures they have to withstand, but RI is effective in keeping ice crystals small, avoiding the mechanical damage of large ice grains to the cells.

The TH effect observed with fcAFPs is too weak to compensate for the low temperatures that *F. cylindrus* has to face within sea ice. Furthermore, an estimation of the fcAFP concentration of *F. cylindrus* cells suggests that protein amounts are too low to have a significant effect on freezing point depression or RI. Furthermore, sea ice crystals are already larger than *F. cylindrus* cells (Table 1) and most probably show no recrystallization, therefore I see no role of RI effect in sea ice. As for the effect of fcAFPs on ice nucleation, it is too early to make any assumption. However, the effect on ice microstructure, with a striated texture interpreted as fibrous ice with inclusions, is clear and may play an important role within sea ice. The data presented here seem to corroborate observations about the effect of exopolymeric substances (EPS), and its protein fraction, in sea ice. I suggest the main effect of fcAFPs in accumulation of proteins in the EPS matrix, attachment to the surface of brine inclusions, change of ice microstructure and related decrease of ice permeability and increase of porosity. In this way, *F. cylindrus* may influence local desalination processes and use fcAFPs to shape its environment and increase habitable space.

## 4.3. PROBLEMS AND LIMITATIONS

The main limitations of this work were given by the novelty of the subject, concerning both fcAFPs as a general frame of the work and in combination with the methodologies applied, which resulted in limited infrastructure and possibilities for discussion. Little was known about fcAFPs apart from 3 sequences found in a salt-stress induced cDNA library of *F. cylindrus*, and information about IAFP was also scarce. This aspect conferred freedom in the direction of research since most research topics were still unaddressed, but also raised several uncertainties about how to handle the subject. The need for basic information on the fcAFPs and their genes (gene

diversity, phylogeny, expression, protein activity) determined the focus of the first part of this work. However, in my opinion, the challenge was to avoid a mere descriptive work, but rather embed the proteins and their activity in a wider framework. The choice of a proper, promising context (i.e. evolution, sea ice biology, sea ice physical properties, potential applications) may constitute a problem when little information and experience in this field are given. I tried however to connect the subject to other fields, which may be of relevance for future work.

Concerning technical limitations in the presented work, problems were given by the search of fcAFP isoforms by PCR, which should result in less hits than *in silica* similarity search. However, the sequencing of the *F. cylindrus* genome, originally planned for 2005, was delayed and isoform detection had to be limited to PCR analyses. Furthermore, analysis of gene activity by qPCR was limited by the high similarity of the genes of interest, combined with the restrictions given by primer and probe design. For some isoforms, mentioned in detail in Publication 1, the detection was possible only for group of genes, and not for single sequences. The crystallographic observations presented a challenge because analyses like ice fabric determinations have never been reported before in the context of AFP research, but have raised interesting questions for further work.

# 5. OUTLOOK

Several questions have been raised in this work, which could lead further fcAFP research in different directions.
From a molecular point of view, the sequencing of the *F. cylindrus* CCMP 1102 genome at the JGI (USA) represents a large step forward. The annotation of the sequenced genome, expected to be published soon, will help to understand the diversity, evolution and regulation of fcAFPs.
Furthermore, important future research goals are deepening the knowledge of the distribution and interspecific diversity of IAFPs, in order to get a realistic picture of processes relevant within sea ice and also a basis for further evolutionary studies, and clarifying the process of ice nucleation in the presence of fcAFPs. However, in my eyes the main objectives for future works could be:

- **the development of an effective and fast method to extract fcAFPs from natural samples and from recombinant organisms.** Extraction could be based on affinity chromatography with activated sepharose attached to anti-fcAFP-antibodies. A less expensive, but also less effective, methodology could be based on the ice-finger technique [Kuiper et al., 2003]. This method, based on the affinity for ice inherent to fcAFPs, consists of treating a solution with multiple melt-freeze cycles. When a mixture of substances, as a filtered cell lysate, is frozen, fcAFPs remain attached to the ice due to their ice-binding properties. Impurities are segregated from the ice lattice, accumulate in the liquid phase and can be easily removed.

- **clarifying the localization of fcAFPs, and therefore their role for *F. cylindrus* within sea ice.** It has been suggested here that fcAFPs accumulate within EPS. This aspect can be further analyzed by improving knowledge of EPS dynamics of *F. cylindrus*. Cell culture experiments, focused on the possible triggers for EPS production (light, nutrient availability) and its distribution into a particulate and a dissolved fraction, are of interest in this context. These studies can be integrated by microscopic observations of *F. cylindrus* and EPS inside brine pockets of frozen samples, similarly to studies with natural sea ice in Krembs et al. [2002].
Alternatively to accumulation in EPS, proteins may be attached to the cell wall or dissolved in the medium. This topic can be addressed with immunoblotting.

- **deepen the understanding of ice microstructure and fabric.** Techniques presented here can be integrated with further methodologies. The nature of the

striations observed under light microscopy, assumed to be related to inclusions of brine, unbound proteins and other impurities, may be clarified by analyses with confocal Raman microscopy (improved by a cryostage). This method provides a fingerprint of each material, separating ice from solutes accumulated in the brine, with a spatial resolution of 10 µm. The spectrum of the dry fcAFP has been detected (Figure A 5) and serves as basis for future measurements in frozen protein solutions. Furthermore, X-ray computed tomography can present a detailed picture of ice porosity in the presence of fcAFPs, giving a spatial resolution of approximately 2 µm.
The clarification of these aspects is relevant for sea ice biology and for potential applications of fcAFPs. Higher ice porosity is important for the biological sea ice system, because it would increase the living space of organisms. Moreover, brine retention within sea ice, related to the complex microstructure of brine inclusions and decreased ice permeability (page 5), may have implications on the biogeochemical imprint of sea ice, since it will result in retention of further elements and substances relevant for chemical and biological processes [Krembs et al., 2011]. Higher porosity also changes the mechanical properties of ice. Mechanical strength of a volume of sea ice is largely determined by the brine volume fraction, and increased porosity results in lower strength [Petrich and Eicken, 2010]. In a context of possible applications of fcAFPs, if surface coatings with fcAFPs result in ice formations less resistant against mechanical pressure on these surfaces, ice could be easily removed without significant mechanical or chemical efforts [see for example Klein-Paste and Wåhlin, 2010]. Interesting applications could be on pavement surfaces, airplane decks and wind plant rotors among others.

This work has clearly shown that fcAFPs represent a key element in adaptation of *F. cylindrus* to conditions within sea ice. Phylogenetic observations have shifted the relevance of these proteins from a punctual, species-related issue to a broader picture involving several sea ice and cold-tolerant organisms. Crystallographic analyses have shown how *F. cylindrus* not only reacts to the conditions in its environment, but in turn uses fcAFPs to shape it, with consequences in the physical and possibly in the biochemical imprint of sea ice. The clarification of the points for future research mentioned above will help to shed further light on the ecology of *F. cylindrus* as a dominat sea ice species.

# BIBLIOGRAPHY


Ackley, S.F., and Sullivan, C.W. (1994) Physical controls on the development and characteristics of Antarctic sea ice biological communities - a review and synthesis. *Deep Sea Research I* 41: 1583-1604.

Amir, G., Horowitz, L., Rubinsky, B., Sheick Yousif, B., Lavee, J., and Smolinsky, A.K. (2004) Subzero non freezing cryopreservation of rat hearts using antifreeze protein I and antifreeze protein III. *Cryobiology* 48: 273-282.

Andersson, J.O. (2005) Lateral gene transfer in eukaryotes. *Cell. Mol. Life Sci.* 62: 1182-1197.

Apt, K.E., Kroth-Pancic, P.G., and Grossman, A.R. (1996) Stable nuclear transformation of the diatom *Phaeodactylum tricornutum*. *Mol. Genet. Genomics* 252: 572-579.

Armaleo, D., Ye, G.N., Klein, T.M., Shark, K.B., Sanford, J.C., and Johnston, S.A. (1990) Biolistic nuclear transformation of Saccharomyces cerevisiae and other fungi. *Curr. Genet.* 17: 97-103.

Arrigo, K.R., Worthen, D.L., Schnell, A., and Lizotte, M.P. (1998) Primary production in Southern Ocean waters. *JGR* 103C: 15587-15600.

Arrigo, K.R., and Thomas, D.N. (2004) Large scale importance of sea ice biology in the Southern Ocean. *Antarct. Sci.* 16: 471-486.

Baardsnes, J., Jelokhani-Niaraki, M., Kondejewski, L.H., Kuiper, M.J., Kay, C.M., Hodges, R.S., and Davies, P.L. (2001) Antifreeze protein from shorthorn sculpin: Identification of the ice-binding surface. *Protein Science* 10: 2566-2576.

Bar, M., Celik, Y., Fass, D., and Braslavsky, I. (2008) Interactions of β-helical antifreeze protein mutants with ice. *Cryst. Growth Des*. 8: 2954-2963.

Barrett, J. (2001) Thermal hysteresis proteins. *IJBCB* 33: 105-117.

Bartsch, A. (1989) Die Eisalgenflora des Weddelmeeres (Antarktis): Artenzusammensetzung und Biomasse sowie Ökophysiologie ausgewählter Arten. *Ber. Polar Meeresforsch./Rep. Polar Mar. Res.* 63.

Bayer-Giraldi, M., Uhlig, C., John, U., Mock, T., and Valentin, K. (2010) Antifreeze proteins in polar sea ice diatoms: diversity and gene expression in the genus Fragilariopsis. *Environ. Microbiol.* 12: 1041-1062.

Bayer-Giraldi, M., Weikusat, I., Besir, H., and Dieckmann, G. (2011) Characterization of an antifreeze protein from the polar diatom Fragilariopsis cylindrus and its relevance in sea ice. *Cryobiology* doi: 10.1016/ j.cryobiol.2011.08.006

Budke, C., and Koop, T. (2006) Ice Recrystallization Inhibition and Molecular Recognition of Ice Faces by Poly(vinyl alcohol). *ChemPhysChem* 7: 2601-2606.

Carginale, V., Trinchella, F., Capasso, C., Scudiero, R., and Parisi, E. (2004) Gene amplification and cold adaptation of pepsin in Antarctic fish. A possible strategy for food digestion at low temperature. *Gene* 336: 195-205.

Celik, Y., Drori, R., Graham, L.A., Mok, Y.-F., Davies, P.L., and Braslavsky, I. (2010a) *Freezing and melting hysteresis measurements in solutions of hyperactive antifreeze protein from an Antarctic bacteria*. Sapporo: Hokkaido University Press.

Celik, Y., Graham, L.A., Mok, Y.-F., Bar, M., Davies, P.L., and Braslavsky, I. (2010b) Superheating of ice crystals in antifreeze protein solutions. *Proc. Natl. Acad. Sci. USA* 107: 5423-5428.

Chao, H., Davies, P.L., and Carpenter, J.F. (1996) Effects of antifreeze proteins on red blood cell survival during cryopreservation. *J. Exp. Biol.* 199: 2071-2076.

Chao, H., Houston, M.E.J., Hodges, R.S., Kay, C.M., Sykes, B.D., Loewen, M.C. et al. (1997) A Diminished Role for Hydrogen Bonds in Antifreeze Protein Binding to Ice. *Biochemistry* 36: 14652-14660.

Cheng, A., and Merz, K.M.J. (1997) Ice-Binding Mechanism of Winter Flounder Antifreeze Proteins. *Biophys. J.* 73.

Cheng, C.-H.C. (1998) Evolution of the diverse antifreeze proteins. *Current Opinions in Genetics & Development* 8: 715-720.

Collins, E.R., Carpenter, S.D., and Deming, J.W. (2008) Spatial heterogenity and temporal dynamics of particles, bacteria, and pEPSin Arctic winter sea ice. *J. Mar. Syst.* 74: 902-017.

Collins, E.R., and Deming, J.W. (2011) Abundant dissolved genetic material in Arctic sea ice Part I: Extracellular DNA. *Polar Biol.* Online First 18 June 2011.

Cox, G.F.N., and Weeks, W.F. (1983) Equation for determining the gas and brine volumes in sea-ice samples. *J. Glaciol.* 29: 306-316.

Dayton, P.K., Robbiliard, G.A., and DeVries, A.L. (1969) Anchor Ice Formation in McMurdo Sound, Antarctica, and Its Biological Effects. *Science* 163: 273-274.

Decho, A.W. (1990) Microbial exoplymer secretions in ocean environments: their role(s) in food webs and marine processes. In *Oceanography and Marine Biology*. Barnes, M. (ed): Aberdeen University Press, pp. 73-153.

DeLuca, C.I., Chao, H., Sönnichsen, F.D., Sykes, B.D., and Davies, P.L. (1996) Effect of type III antifreeze protein dilution and mutation on the growth inhibition of ice. *Biophys. J.* 71: 2346-2355.

DeLuca, C.I., Comley, R., and Davies, P.L. (1998) Antifreeze Proteins Bind

Independently to Ice. *Biophys. J.* 74: 1502-1508.

DeVries, A.L. (1983) Antifreeze peptides and glycopeptides in cold-water fishes. *Ann. Rev. Physiol.* 45: 245-260.

Dieckmann, G., and Hellmer, H. (2010) The importance of Sea Ice: An Overview. In *Sea ice*. Thomas, D.N., and Dieckmann, G. (eds). Chichester: Wiley-Blackwell, pp. 1-22.

Dröge, M., Pühler, A., and Selbitschka, W. (1998) Horizontal gene transfer as a biosafety issue: A natural phenomena of public concern. *J. Biotechnol.* 64: 75-90.

Du, N., Liu, X.Y., and Hew, C.L. (2002) Ice Nucleation Inhibition - Mechanism of antifreeze by antifreeze protein. *J. Biol. Chem.* 27: 36000-36004.

Ebbinghaus, S., Meister, K., Born, B., DeVries, A.L., Gruebele, M., and Havenith, M. (2010) Antifreeze Glycoprotein Activity Correlates with Long-Range Protein-Water Dynamics. *J. Am. Chem. Soc.* 132: 12210-12211.

Eicken, H., and Lange, M.A. (1989) Development and Properties of Sea Ice in the Coastal Regime of the Southern Weddell Sea. *JGR* 94: 8193-8206.

Eicken, H. (1992) The role of sea ice in structuring Antarctic ecosystems. *Polar Biol.* 12: 3-13.

Ewert, M., and Deming, J.W. (2011) Selective retention in saline ice of extracellular polysaccharides prodiced by the cold-adapted marine strain bacterium *Colwellia psychrerythraea* strain 34H. *Ann. Glaciol.* 52: 111-117.

Fiala, M., and Oriol, L. (1990) Light-Temperature Interactions on the Growth of Antarctic Diatoms. *Polar Biol.* 10: 629-636.

Fletcher, G.L., Hew, C.L., and Davies, P.L. (2001) Antifreeze Proteins of Teleost Fishes. *Ann. Rev. Physiol.* 63: 359-390.

Frischer, M.E., Stewart, G.J., and Paul, J.H. (1994) Plasmid transfer to indigenous marine bacterial populations by natural transformation. *FEMS Microbiol. Ecol.* 15: 127-135.

Garcia-Vallvé, S., Romeu, A., and Palau, J. (2000) Horizontal Gene Transfer in Bacterial and Archaeal Complete Genomes. *Genome Res.* 10: 1719-1725.

Garrison, D.L., and Buck, K.R. (1985) Sea-ice algal communities in the Weddell Sea: Species composition in ice and plankton assemblages. In *Marine biology of polar regions and effects of stress on marine organisms*. Gray, J.S., and Christiansen, M.E. (eds). New York: John Wiley, pp. 103-122.

Garrison, D.L., and Buck, K.R. (1989) The Biota of Antarctic Pack Ice in the Weddell Sea and Antarctic Peninsula Regions. *Polar Biol.* 10: 211-219.

Garrison, D.L., and Close, A.R. (1993) Winter ecology of the sea ice biota in Weddell Sea pack ice. *Mar. Ecol. Prog. Ser.* 96: 17-31.

Gaukel, V.G., and Spieß, W.E.L. (2004) EInfluss von Antigefrierproteinen auf die Rekristallisation von Eis in Modelllösungen für Eiskrem. *Chemie Ingenieur Technik* 76: 454-458.

Golden, K.M., Eicken, H., Heaton, A.L., Miner, J., Pringle, D.J., and Zhu, J. (2007) Thermal evolution of permeability and microstructure in sea ice. *Geophys. Res. Lett.* 34: L16501.

Gordienko, R., Ohno, H., Singh, V.K., Jia, Z., Ripmeester, J.A., and Walker, V.K. (2010) Towards a Green Hydrate Inhibitor: Imaging Antifreeze Proteins on Clathrates. *PLoS ONE* 5: e8953.

Graham, L.A., Qin, W., Lougheed, S.C., Davies, P.L., and Walker, V.K. (2007) Evolution of Hyperactive, Repetitive Antifreeze Proteins in Beetles. *J. Mol. Evol.* 64: 387-398.

Griffith, M., and Ewart, V.K. (1995) Antifreeze proteins and their potential use in frozen foods. *Biotechnol. Adv.* 13: 375-402.

Griffith, M., and Yaish, M.W. (2004) Antifreeze proteins in overwintering plants: a tale of two activities. *Trends Plant Sci.* 9: 399-405.

Gwak, I.G., Jung, W.s., Kim, H.J., Kang, S.-H., and Jin, E. (2010) Antifreeze Protein in Antarctic Marine Diatom, *Chaetoceros neogracile*. *Mar. Biotechnol.* 12: 630-639.

Harding, M.M., Ward, L.G., and Haymet, A.D.J. (1999) Type I "antifreeze" proteins: Structure-activity studies and mechanisms of ice growth inhibition. *European Journal of Biochemistry* 264: 653-665.

Hobbs, P.V. (2010a) Growth of ice from the liquid phase. In *Ice Physics*. Oxford, UK: Oxford University Press, pp. 572-629.

Hobbs, P.V. (2010b) Nucleation of ice. In *Ice Physics*. Oxford, UK: Oxford University Press, pp. 461-523.

Hon, W.-C., Griffith, M., Chong, P., and Yang, D.S.C. (1994) Extraction and Isolation of Antifreeze Proteins from Winter Rye (*Secale cereale* L.) Leaves. *Plant Physiol.* 104: 971-980.

Hoshino, T., Kiriaki, M., and Nakajima, T. (2003a) Novel thermal hysteresis proteins from low temperature Basidiomycete, *Coprinus psychromorbidus*. *CryoLetters* 24: 135-142.

Hoshino, T., Kiriaki, M., Ohgiya, S., Fujiwara, M., Kondo, H., Nishimiya, Y. et al. (2003b) Antifreeze proteins from snow mold fungi. *Can. J. Bot./Rev. Can. Bot.* 81: 1175-1181.

IFAM (2006/2007) IFAM Jahresbericht. In. Bremen, F.-I.f.F.u.A.M. (ed): Fraunhofer-Institut für Fertigungstechnik und Angewandte Materialforschung Bremen.

Ikävalko, J., and Gradinger, R. (1997) Nanoflagellates and helizoans in the Arctic sea ice studied alive using light microscopy. *Polar Biol.* 17: 473-481.

Janech, M.G., Krell, A., Mock, T., Kang, J.-S., and Raymond, J.A. (2006) Ice-binding proteins from sea ice diatoms (Bacillariophyceae). *J. Phycol.* 42: 410-416.

Kang, S.-H., and Fryxell, G.A. (1992) Fragilariopsis cylindrus (Grunow) Krieger: The most abundant diatom in water column assemblages of Antarctic marginal ice-edge zones. *Polar Biology*
12: 609-627.

Kang, S.-J.L. (2005) *Sintering: Densification, grain growth and microstructure*. Amsterdam: Elsevier.

Kawahara, H., Iwanaka, Y., Higa, S., Muryoi, N., Sato, M., Honda, M. et al. (2007) A novel, intracellular antifreeze protein in an antarctic bacterium, *Flavobacterium xanthum*. *CryoLetters* 28: 39-49.

Kiko, R. (2010) Acquisition of freeze protection in a sea-ice crustacean through horizontal gene transfer? *Polar Biol.* 33: 543-556.

Kipfstuhl, S., Hamann, I., Lambrecht, A., Freitag, J., Faria, S.H., Grigoriev, D., and Azuma, N. (2006) Microstructure mapping: a new method for imaging deformation-induced microstructural features of ice on the grain scale. *JGlac* 52: 398-406.

Klein-Paste, A., and Wåhlin, J. (2010) Controlling the Properties of Thin Ice Layers on Pavement Surfaces - An Alternative Explanation for Anti-icing. In *Physicc and Chemistry of Ice*. Furukawa, Y., Sazaki, G., Uchida, T., and Watanabe, N. (eds). Sapporo, Japan: Hokkaido University Press, pp. 13-19.

Knight, C.A., and Duman, J.A. (1986) Inhibition of Recrystallization of Ice by Insect Thermal Hysteresis Proteins: A possible Cryoprotective Role. *Cryobiology* 23: 256-262.

Krell, A., Funck, D., Plettner, I., John, U., and Dieckmann, G. (2007) Regulation of proline metabolism under salt stress in the psychrophilic diatom *Fragilariopsis cylindrus* (Bacillariophyceae). *J. Phycol.* 43: 753-762.

Krell, A., Beszteri, B., Dieckmann, G., Glöckner, G., Valentin, K., and Mock, T. (2008) A new class of ice-binding proteins discovered in a salt-stress-induced cDNA library of the psychrophilic diatom *Fragilariopsis cylindrus* (Bacillariophyceae). *Eur. J. Phycol.* 43: 423-433.

Krembs, C., Gradinger, R., and Spindler, M. (2000) Implication of brine channels geometry and surface area for the interaction of sympagic organisms in Antarctic sea ice. *J. Exp. Mar. Biol. Ecol.* 243: 55-80.

Krembs, C., Mock, T., and Gradinger, R. (2001) A mesocosm study of physical-biological interactions in artificial sea ice: effects of brine channels surface evolution and brine movement on algal biomass. *Polar Biol.* 24: 356-364.

Krembs, C., Eicken, H., Junge, K., and Deming, J.W. (2002) High concentrations of exopolymeric substances in Arctic winter sea ice: implications for the polar ocean carbon cycle and cryoprotection of diatoms. *Deep Sea Res. (I Oceanogr. Res. Pap.)* 49: 2163-2181.

Krembs, C., Eicken, H., and Deming, J.W. (2011) Exopolymer alterations of physical properties of sea ice and implications for ice habitability and biogeochemistry in a warmer Arctic. *PNAS* 108: 3653-3658.

Kristiansen, E., and Zachariassen, K.E. (2005) The mechanism by which fish antifreeze proteins cause thermal hysteresis. *Cryobiology* 51: 262-280.

Kristiansen, E., Pedersen, S.A., and Zachariassen, K.E. (2008) Salt-induced enhancement of antifreeze protein activity: A salting-out effect. *Cryobiology* 57: 122-129.

Kröger, N., Bergsdorf, C., and Sumper, M. (1996) Frustulins: domain conservation in a protein family associated with diatom cell walls. *Eur. J. Biochem.* 239: 259-264.

Kröger, N., Lehmann, G., Rachel, R., and Sumper, M. (1997) Charakterization of a 200 kDa diatom protein that is specifically associated with a silica-based substructure of the cell wall. *Eur. J. Biochem.* 250: 99-105.

Kroth, P.G. (2007) Gene Transformation - a Tool to Study Protein Targeting in Diatoms. In *Methods in Molecular Biology - Protein Targeting Protocols*. Van der Giezen, M. (ed). Totowa, NJ: Humana Press, pp. 257-267.

Kuiper, M.J., Lankin, C., Gauthier, S.Y., Walker, V.K., and Davies, P.L. (2003) Purification of antifreeze proteins by adsorption to ice. *Biochem. Biophys. Res. Commun.* 300: 645-648.

Lake, R.A., and Lewis, E.L. (1970) Salt Rejection by Sea Ice during Growth. *JGR* 75: 583-597.

Lee, J.K., Park, K.S., Park, S., Park, H., Song, Y.H., Kang, S.-H., and Kim, H.J. (2010) An extracellular ice-binding glycoprotein from an Arctic psychrophilic yeast. *Cryobiology* 60: 222-228.

Legendre, L., Ackley, S.F., Dieckmann, G.S., Gulliksen, B., Horner, R., Hoshiai, T. et al. (1992) Ecology of sea ice biota - 2. Global significance. *Polar Biol.* 12: 429-444.

Li, X., and Hew, C.L. (1991) Structure and function of an antifreeze polypeptide from ocean pout, *Macrozoarces americanus*: role of glutamic acid residues in protein stability and antifreeze activity by site-directed mutagenesis. *Protein Eng.* 4: 1003-1008.

Lizotte, M.P. (2001) The Contributions of Sea Ice Algae to Antarctic Marine Primary Production. *Am. Zool.* 41: 57-73.

Lorenz, M.G., Aardema, B.W., and Wackernagel, W. (1988) Highly Efficient Genetic Transformation of *Bacillus subtilis* Attached to Sand Grains. *Journal of General Microbiology* 134: 107-112.

Low, W.-K., Lin, Q., Stathakis, C., Miao, M., Fletcher, G.L., and Hew, C.L. (2001) Isolation and Characterization of Skin-type, Type I Antifreeze Polypeptides from the Longhorn Sculpin, *Myoxocephalus octodecemspinosus*. *The Journal of Biological Chemistry* 276: 11582-11589.

Lundholm, N., Daugbjerg, N., and Moestrup, Ø. (2002) Phylogeny of the Bacillariaceae with emphasis on the genus *Pseudo-nitzschia* (Bacillariophyceae) based on partial LSU rDNA. *Eur. J. Phycol.* 37: 115-134.

Mangoni, O., Saggiomo, M., Modigh, M., Catalano, G., Zingone, A., and Saggiomo, V. (2009) The role of platelet ice microalgae in seeding phytoplankton blooms in Terra Nova Bay (Ross Sea, Antarctica): a mesocosm experiment. *Polar Biol.* 32: 311-323.

Marshall, C.B., Daley, M.E., Sykes, B.D., and Davies, P.L. (2004a) Enhancing the Activity of a β-Helical Antifreeze Protein by the Engineered Addition of Coils. *Biochemistry* 43: 11637-11646.

Marshall, C.B., Fletcher, G.L., and Davies, P.L. (2004b) Hyperactive antifreeze protein in a fish. *Nature* 429: 153.

McMinn, A., Pankowski, A., and Delfatti, T. (2005) Effect of hyperoxia on the growth and photosynthesis of polar sea ice microalgae. *J. Phycol.* 41: 732-741.

Middleton, A.J., Brown, A.M., Davies, P.L., and Walker, V.K. (2009) Identification of the ice-binding face of a plant antifreeze protein. *FEBS Lett.* 583: 815-819.

Mock, T., and Valentin, K. (2004) Photosynthesis and cold acclimation: Molecular evidence from a polar diatom. *J. Phycol.* 40: 732-741.

Mock, T., and Hoch, N. (2005) Long-term temperature acclimation of photosynthesis in steady-state cultures of the polar diatom *Fragilariopsis cylindrus*. *Photosynthesis Res*. 85: 307-317.

Mock, T., Krell, A., Glöckner, G., Kolukisaoglu, Ü., and Valentin, K. (2005) Analysis of expressed sequence tags (ESTs) from the polar diatom *Fragilariopsis cylindrus*. *J. Phycol.* 42: 78-85.

Mock, T., Krell, A., Glöckner, G., Kolukisaoglu, Ü., and Valentin, K. (2006) Analysis of expressed sequence tags (ESTs) from the polar diatom *Fragilariopsis cylindrus*. *J. Phycol.* 42: 78-85.

Mugnano, J.A., Wang, T., Layne, J.R., DeVries, A.L., and Lee, R.E.J. (1995) Antifreeze glycoproteins promote intracellular freezing of rat cardiomyocytes at high

subzero temperatures. *Am. J. Physiol. Regul. Integr. Comp. Physiol.* 269: R474-R479.

Notz, D., and Worster, G.M. (2009) Desalination processes og sea ice revisited. *JGR* 114: C05006.

Nutt, D., and Smith, J.C. (2008) Dual Function of the Hydration Layer around an Antifreeze Protein Revealed by Atomistic Molecular Dynamics Simulations. *J. Am. Chem. Soc.* 130: 13066-13073.

Oh, H.-Y., Cheon, J.-Y., Lee, J.H., Hur, S.B., and Ki, J.-S. (2010) Nuclear rDNA characteristics for DNA taxonomy of the centric diatom *Chaetoceros* (Bacillariophyceae). *Algae* 25: 65-70.

Pankowski, A., and McMinn, A. (2009) Iron availability regulates growth, photosynthesis, and production of ferredoxin and flavodoxin in Antarctic sea ice diatoms. *Aquat Biol* 4: 273-288.

Parody-Morreale, A., Murphy, K.P., Di Cera, E., Fall, R., DeVries, A.L., and Gill, S.J. (1988) Inhibition of bacterial ice nucleators by fish antifreeze glycoproteins. *Nature* 333: 782-783.

Payne, S.R., and Young, O.A. (1995) Effects of pre-slaughter administration of antifreeze proteins on frozen meat quality. *Meat Science* 41: 147-155.

Perey, F.G.J., and Pounder, E.R. (1958) Crystal orientation in ice sheets. *CaJPh* 36: 494-502.

Pertaya, N., Marshall, C.B., DiPrinzio, C.L., Wilen, L., Thomson, E.S., Wettlaufer, J.S. et al. (2007) Fluorescence Microscopy Evidence for Quasi-Permanent Attachment of Antifreeze Proteins to Ice Surfaces. *Biophys. J.* 92: 3663-3673.

Petrich, C., and Eicken, H. (2010) Growth, Structure and Properties of Sea Ice. In *Sea Ice*. Thomas, D.N., and Dieckmann, G. (eds). Chichester: Wiley-Blackwell, pp. 23-77.

Poulin, M. (1990) Ice diatoms: the Arctic. In *Polar Marine Diatoms*. Medlin, L.K., and Priddle, J. (eds). Cambridge: British Antarctic Survey, pp. 15-18.

Raymond, J.A., and DeVries, A.L. (1977) Adsorption inhibition as a mechanism of freezing resistance in polar fishes. *Proc. Natl. Acad. Sci. USA* 74: 2589-2593.

Raymond, J.A., Wilson, P., and DeVries, A.L. (1989) Inhibition of growth of nonbasal planes in ice by fish antifreezes. *Proc. Natl. Acad. Sci. USA* 86: 881-885.

Raymond, J.A., Sullivan, C.W., and DeVries, A.L. (1994) Release of ice-active substances by Antarctic sea ice diatoms. *Polar Biol.* 14: 71-75.

Raymond, J.A., and Knight, C.A. (2003) Ice binding, recrystallization inhibition, and cryoprotective properties of ice-active substances associated with Antarctic sea ice diatoms. *Cryobiology* 46: 174-181.

Raymond, J.A., Fritsen, C., and Shen, K. (2007) An ice-binding protein from an Antarctic sea ice bacterium. *FEMS Microbiol. Ecol.* 61: 214-221.

Raymond, J.A., Christner, B.C., and Schuster, S.C. (2008) A bacterial ice-binding protein from the Vostok ice core. *Extremophiles* 12: 713-717.

Raymond, J.A., and Janech, M.G. (2009) Ice-binding proteins from enoki and shiitake mushrooms. *Cryobiology* 58: 151-156.

Riebesell, U., Schloss, I., and Smetack, V. (1991) Aggregation of algae released from melting sea ice: implications for seeding and sedimentation. *Polar Biol.* 11: 239-248.

Riedel, A., Michel, C., Gosselin, M., and LeBlanc, B. (2007) Enrichment of nutrients, exoplymeric substances and microorganisms in newly formed sea ice on the Mackenzie shelf. *Mar. Ecol. Prog. Ser.* 342: 55-67.

Robin, G.d.Q. (1979) Formation, Flow and Disintegration of Ice Shelves. *J. Glaciol.* 24: 259-271.

Schrag, J.D., O'Grady, S.M., and DeVries, A.L. (1982) Relationship of amino acid composition and moleculra weight of antifreeze glycopeptides to non-colligative freezing point depression. *Biochim. Biophys. Acta* 717: 322-326.

Sidebottom, C., Buckley, S., Pudney, P., Twigg, S., Jarman, C., Holt, C. et al. (2000) Phytochemistry: Heat-stable antifreeze protein from grass. *Nature* 406: 256.

Smallwood, M., Worrall, D., Byass, L., Elias, L., Ashford, D., Doucet, C.J. et al. (1999) Isolation and characterization of a novel antifreeze protein from carrot (*Daucus carota*). *Biochemical Journal* 340: 385-391.

Snider, C.S., Hsiang, T., Zhao, G., and Griffith, M. (2000) Role of Ice Nucleation and Antifreeze Activities in Pathogenesis and Growth of Snow Molds. *Phytopathology* 90: 354-361.

Sumper, M., and Kröger, N. (2004) Silica formation in diatoms: the function of long-chain polyamines and silaffins. *JMCh* 14: 2059-2065.

Thomas, D.N., and Dieckmann, G.S. (2002) Antarctic Sea Ice - a Habitat for Extremophiles. *Science* 295: 641-644.

Tomczak, M.M., Marshall, C.B., Gilbert, J.A., and Davies, P.L. (2003) A facile method for determining ice recrystallization inhibition by antifreeze proteins. *Biochem. Biophys. Res. Commun.* 311: 1041-1046.

Understeiner, N. (1967) Natural desalination and equilibrium salinity profiles of old sea ice. In *Physics of Snow and Ice, International Conference on Low Temperature Science*. Oura, H. (ed). Sapporo: Hokkaido University, Sapporo, Japan, p. 569.

Venketesh, S., and Dayananda, C. (2008) Properties, Potentials, and Prospects of Antifreeze Proteins. *Crit. Rev. Biotechnol.* 28: 57-82.

Wang, Y. (1999) The development of an automatic analyzer for fabrics and textures of polar ice cores. In. Nagaoka, Japan: University of Technology.

Weeks, W.F., and Ackley, S.F. (1982) *The growth, structure, and properties of sea ice* Hanover.

Werner, I., Ikävalko, J., and Schünemann, H. (2007) Sea-ice algae in Arctic pack ice during late winter. *Polar Biol.* 30: 1493-1504.

Wilen, L.A., Diprinzio, C.L., Alley, R.B., and Azuma, N. (2003) Development, Principles, and Applications of Automated Ice Fabric Analyzers. *Microsc. Res. Tech.* 62: 2-18.

Wilson, C.J.L., Russell-Head, D.S., Kunze, K., and Viola, G. (2007) The analysis of quartz c-axis fabrics using a modified optical microscope. *J. Microsc.* 227: 30-41.

Wilson, P., and Leader, J.P. (1995) Stabilization of Supercooled Fluids by Thermal Hysteresis Proteins. *Biophys. J.* 68: 2098-2107.

Wilson, P., Osterday, K.E., Heneghan, A.F., and Haymet, A.D.J. (2010) Type 1 antifreeze proteins enhance ice nucleation above certain concentrations. *J. Biol. Chem.* 285: 34741-34745.

Wilson, P.W. (1994) A Model for Thermal Hysteresis Utilizing the Anisotropic Interfacial Energy of Ice Crystals. *Cryobiology* 31: 406-412.

Wu, Y., Banoub, J., Goddard, S.V., Kao, M.H., and Fletcher, G.L. (2001) Antifreeze glycoproteins: relationship between molecular weight, thermal hysteresis and the inhibition of leakage from liposomes during thermotropic phase transition. *Comp. Biochem. Physiol. B: Biochem. Mol. Biol.* 128: 265-273.

Xiao, N., Suzuki, K., Nishimiya, Y., Kondo, H., Miura, A., Tsuda, S., and Hoshino, T. (2010) Comparison of functional properties of two fungal antifreeze proteins from *Antarctomyces psychotrophicus* and *Typhula ishikariensis*. *FEBS J.* 277: 394-403.

Zaslavskaia, L.A., Lippmeier, J.C., Kroth, P.G., and Grossman, A.R. (2000) Transformation of the diatom Phaeodactylum tricornutum (Bacillariophyceae) with a variety of selectable marker and reporter genes. *J. Phycol.* 36: 379-386.

Zepeda, S., Yokoyama, E., Uda, Y., Katagiri, C., and Furukawa, Y. (2008) In Situ Observation of Antifreeze Glycoprotein Kinetics at the Ice Interface Reveals a Two-Step Reversible Adsorption Mechanism. *Cryst. Growth Des.* 8: 3666-3672.

Zhang, J. (2003) Evolution by gene duplication: an update. *Trends Ecol. Evol.* 18: 292-298.

# A. APPENDIX

## A.1. PUBLICATION 3

### RECRYSTALLIZATION INHIBITION IN ARCTIC AND ANTARCTIC DIATOM ISOLATES

C. Uhlig, T. Eberlein, A. Seidler, A. Krell, B. Beszteri, M. Bayer-Giraldi, G. S. Dieckmann

Alfred Wegener Institute for Polar and Marine Research, Am Handelshafen 12, 27570 Bremerhaven, Germany

Draft version

Contributions:
Own contributions concern the supply of fcAFP for measurements and support in draft revision.

**Abstract**

Diatoms constitute one of the major fractions of biological assemblages in sea ice. They contribute significantly to polar primary production and serve as important food source for higher trophic organisms. Diatoms are able to thrive in sea ice due to a suit of adaptation mechanisms including the production of antifreeze proteins (AFPs). Subjecting a set of Arctic and Antarctic diatom species to high salinity and subzero temperature, we studied the abundance and activity of AFPs in polar diatom species spread over the whole diatom phylogeny and from both polar regions. AFP activity, measured as recrystallization inhibition, was regulated by temperature and salinity stress in *Entomoneis sp*., *Navicula* sp. sensu lato III and *Porisira glacialis*. Twelve other species did not show a clear regulation, but however showed antifreeze activity. Recrystallization measured with the optical recrystallometer showed an exponential decay function relative to the protein concentration for a *F. nana* Ant cell extract and a recombinant AFP. This correlation allowed us to estimate the AFP concentration as AFP equivalents per cell. Concentrations of 0.3 to 68.5 µM AFP equivalent approve intracellular function of diatom AFPs as recrystallization inhibitor, but also lie in the range of concentrations required for thermal hysteresis.

## Introduction

Subjected to a seasonally changing extent, sea ice expands up to $20*10^6$ $km^2$ in Antarctica and $15*10^6$ $km^2$ in the Arctic, thus constituting one of the largest ecosystems in the world [1]. When sea ice forms in winter, pelagic organisms become incorporated into microscopic channels and pockets [2, 3] inside the ice matrix. In the ice the organisms encounter subzero temperatures as low as -20°C and corresponding brine salinities of over 200 [4]. Although the organisms are exposed to rapid changes and extremes in abiotic conditions compared to the relatively stable seawater system, biomass within the sea ice exceeds that in the water column below by as much as a factor of $10^3$ [3, 1]. In polar Antarctic oceans, photosynthetic sea ice organisms contribute to up to 5% of the annual primary production [5]. Diatoms frequently dominate sea ice assemblages, contributing significantly to primary production [5] and serving as food source for higher trophic levels (e. g. krill, metazoans) [6, 1, 7].

Organisms inhabiting brine channels and pores in sea ice are successful due to a whole suite of physiological and biochemical adaptations [8]. By accumulation of salts as well as compatible solutes such as glycerol, sorbitol or proline [9] cells regulate osmolality and thus turgor pressure, when subjected to elevated salinity. Through formation of poly-unsaturated fatty acids, membrane fluidity is maintained under low temperatures [10]. Exopolymeric substances produced by bacteria and diatoms (e.g. *Melosira arctica*) can alter brine pore morphologies [11] and create a microenvironment that protects the cells from dehydration and potentially harmful ice crystals [12]. Raymond et al. [13, 14] previously reported the release of ice active proteins by sea ice diatoms. These proteins can inhibit recrystallization, which is the growth of larger ice crystals at the expense of smaller ones, and thus circumvent or reduce mechanical damage caused by ice crystals [14, 15]. The proteins were reported to bind to the ice, thus causing pitting on ice surfaces [16]. The *in situ* function of ice active proteins produced by diatom is still under discussion but strongly depends on the *in situ* concentrations. Recrystallization inhibition (RI) requires only 100 to 500 times less protein than thermal hysteresis (TH) [19]. Due to the different character and effect, the nomenclature of these proteins varies and a multitude of methods has been developed to study AFPs. Compliant with Bayer-Giraldi [20] we will use the term antifreeze proteins (AFPs). In this study we assessed the recrystallization inhibition activity of AFPs with two different methods. A Clifton Nanoliter Osmometer was used to measure AFP activity in terms of RI and crystal deformation and compared to RI measured by an optical recrystallometer [21].

Up to now information on AFP activity in diatoms are rather patchy. Several studies report AFPs from single Antarctic diatom species like *Navicula glacei* [15], *Fragilariopsis cylindrus* and *F. curta* [22, 20], *Chaetoceros neogracile* [17], and ice

associated diatom assemblages [13, 23, 14]. Raymond et al. [23] report ice pitting activity in a sample dominated by pennate diatom from Resolute, Canada, Arctic. The presence of diatom AFPs thus seems to be a bipolar phenomenon. Anyhow there is no information available on the broad phylogenetic distribution of AFPs in Bacillariophyta.

Demonstrating the presence of AFPs in several new diatom genera and families, especially from the Arctic, this study contributes to the knowledge on the phylogenetic and local distribution of AFPs in diatoms. The optical recrystallometer and a calibration with a recombinant AFP, allowed us to estimate AFP equivalent concentrations within the cell. Concentrations calculated are well within the range necessary for intracellular recrystallization inhibition and come close to concentrations required for thermal hysteresis.

## Material and Methods

Recrystallization inhibition and crystal deformation assays

The presence of AFPs in cell extracts was measured using an optical recrystallometer (Otago Instruments, New Zealand) [21] and a nanoliter osmometer (Clifton Technical Physics). Both instruments can be used to measure recrystallization. A freshly frozen sample appears opaque due to the formation of a multitude of small crystals, since little light will pass through the sample. Recrystallization causes the growth of lager crystals, the scatter inside the sample decreases, more light passes through and the sample appears brighter or transparent. In the presence of a recrystallization inhibitor (e.g. AFP) the opacity does not or hardly decrease.

For measurements with the optical recrystallometer 150 µL sample was transferred to the bottom of a glass tube that serves as sample holder and frozen for 1 h at -20 °C in a freezer. The tube was transferred on ice to the instrument, quickly wiped with paper to remove condensation and inserted into the measuring block. The sample was kept at -4 °C ± 0.2 °C for one hour and the transmission of light was logged with a frequency of 10 s. An index of recrystallization (R) was calculated as follows:

(1) $R=T_{60}-T_{10}$

with $T_t$: transmission (in mV) at time t (in min).

Dilution series of *F. nana* Ant cell extract (5 – 200 µg $mL^{-1}$) and of a recombinant AFP (fcAFP) [24] (0.02 – 20 µg $mL^{-1}$) were assayed in the optical recrystallometer. The calibration curve resulting from fcAFP was used to calculate the concentration of AFP equivalents ($c_{AFPeq}$) in cell extracts. AFP fraction of total protein (AFPeq) was calculated by division of cAFPeq by the total protein concentration used for the measurement (approximately 150 µg $µL^{-1}$).

(2) $c_{AFPeq}(µg\ µL^{-1})=10^{((R-4,6)/(-3,2))}$

(3) AFPeq (of total protein) = $c_{AFPeq} / c_{total} * 100$

In the nanoliter osmometer the sample was loaded in duplicates to the sample holder and deep frozen to approx. -40 °C. After reaching the annealing temperature of -4 °C the turbidity of samples were documented after 0 and 20 min incubation. In addition, the deformation of crystals caused by the presence of AFPs was determined. For this purpose the crystals were melted until only one small crystal remained. Subsequently, the temperature was lowered slowly to initiate crystal growth. Without AFP activity crystals grow as circular disks, whereas they show deformations to hexagons or stars, or other sharper edges in presence of AFP [25]. We developed a scheme to classify results for recystallization and crystal deformation, in order to compare nanoliter osmometer results from different samples. Numbers denote respective observations: (1) presence of RI and deformed crystals in both samples, (2) RI in one of both

samples and deformed crystals, (3) no RI but deformed crystals and (4) neither RI nor deformed crystals.

Diatom cultures

All arctic diatom cultures, except of *Thalassiosira nordenskioeldii* CCMP 997, were isolated from sea ice collected in Kongsfjord from 2nd till 8th May 2009 (for details see table 1.) Antarctic cultures were kindly supplied from the UTS Sydney, University of East Anglia or were available at the Alfred Wegener Institute for Polar and Marine Research. Previous studies by Mock and Valentin [26] and Krell *et al.* [27, 22] were done with *F. nana* Ant (isolated by Mock, 1999), in those studies, however, denoted as *F. cylindrus*. Lundholm and Hasle (2008) [28] identified this culture as *F. nana* and hence it will be referred to accordingly in our study.

Stock cultures were grown in ANT F/2 medium [29] at 5 °C under continuous illumination of approximately 25 µmol photons $m^{-2}$ $s^{-1}$. Cultures were clonal but non-axenic. Stock cultures were treated sterile while experimental cultures were treated as clean as possible but non-sterile. A culture of the temperate diatom *Phaeodactylum tricornutum* was kept in ANT F/2 medium under continuous illumination of 25 µmol photons $m^{-2}$ $s^{-1}$ and 20 °C and used as negative control.

Taxonomy

Cells were harvested on polycarbonate filters (pore size 1.2 µm) (Millipore), immediately frozen in liquid nitrogen and stored at -80 °C. Genomic DNA was isolated using the DNeasy Kit Plant Mini Kit (Qiagen) according to the manufactures protocol except for the following modification. For lysis, cells were washed off the filter with 400 µL AP1 buffer and incubated for 1 h at 65 °C after adding RNAse and Proteinase K to final concentrations of 1 µg $\mu L^{-1}$ and 0.01 µg $\mu L^{-1}$, respectively. 18S rDNA was amplified using the Phusion Polymerase (Finzymes) and primers EukA (1F) and EukB (1528R) [30] with the following cycling conditions: initial denaturation at 98 °C for 2 min, followed by 34 cycles each comprising 98 °C for 5 sec, 62 °C for 30 sec and 72 °C for 90 sec; and finally 72 °C for 5 min. PCR products were purified with the MinElute PCR Purification Kit (Qiagen) and amplified with each of the primers 1F EukA (1F), E528F (528F) [31] or 1055R [32] and 1528R (EukB) [30] using ABI Prism BigDye Terminator v3.1 Cycle Sequencing Kit (Applied Biosystems) in a temperature program of one initial step of 96 °C for 1 min followed by 30 cycles of 96 °C for 10 sec, 60 °C for 5 sec and 60 °C for 3 min. Products were prepared with the DyeEx Kit (Qiagen) and analyzed on an ABI Prism 3130xl Genetic Analyzer (Applied Biosystems).

Vector clipping and assembly of partial sequences was accomplished in Gap v4.10 from the Staden Package [33]. Assembled sequences were aligned in the SILVA Web Aligner [34] SSU database release version 103 including the ten nearest neighbor sequences of each sequence into the result. This database was merged in ARB [35] with the SILVA SSUref database release version 102, which was previously reduced to all diatom sequences and three bolidohytes as outgroup.
Additionally, taxonomy was assessed by light and scanning electron microscopy (SEM) (Fig. S1). Living samples were studied in Uthermöhl Chambers using an Axiovert inverted microscope (Carl Zeiss). Raw material and frustules, cleaned according to Simonsen [36], were dried onto circular glass coverslips. After coating samples with gold/palladium, SEM pictures were taken in a Quanta FEG 200 (FEI).

Experimental procedures

Six replicate cultures of each species were grown in 2 L Erlenmeyer flasks filled with 1.3 L ANT F/2 medium [29] aerated with sterile filtered air. Temperature and light regime was kept at 5 °C and continuous illumination of 25 µmol photons $m^{-2}$ $s^{-1}$ in Rumed light thermostats (Rubarth Apparate GmbH). During the exponential growth phase the replicates were split into three replicates of control cultures, that were kept at 5 °C and a salinity of 34, and three replicates of cultures treated with lowered temperature of -4°C and elevated salinity of 70. Salinity was elevated by addition of approx. 200 mL brine (25 g Sea Salts (Sigma) in 100 mL ANT F/2) into the culture flask at a rate of 1 mL $min^{-1}$ (Ismatec REGLO Digital, Ismatec). To account for dilution effects the same amount of F/2 medium was added to the non-treated cultures. The temperature of the thermostats was lowered to -4 °C simultaneously to the start of the brine addition. Cultures were monitored at respective conditions for 5 to 8 days after this treatment.
Samples for determination of cell densities were taken every other day, preserved with a final concentration of approx. 5% Lugol´s solution [37] and stored at 5 °C in the dark for later enumeration. Additional samples were preserved with a final concentration of 5% buffered Formalin (Merck) and stored at 5 °C for later determination of potential bacterial contamination. Samples were stained with DAPI (4',6-diamidino-2-phenylindole-dichloride (Merck)) at 5 µg $µL^{-1}$ final concentration, filtered on respective filters used for sampling, and studied with fluorescent light (365nm) under an Axioskop 2 (Carl Zeiss) microscope.
To determine the presence of AFPs, samples were taken just before the treatment, two days after the treatment and at the end of the experiment. Approximately 250 mL culture volume was filtered on polycarbonate filters (Millipore) with a pore size between 1.2 and 5.0 µm, depending on the cell size of the species. Filters were flushed

with approximately 100 mL sterile filtered seawater to reduce bacterial contamination, before they were transferred into cryo vials and flash frozen in liquid nitrogen. Samples were stored at -80 °C until processing.

*Physiology:* Maximum photosynthetic quantum yield of photosystem II ($F_v/F_m$) was monitored daily or every other day as a proxy for general cell fitness [38]. Cells were dark adapted at experimental temperature for 15 min and subsequently analyzed using a Xenon-PAM-Fluorometer (Walz, Germany). Cell densities were determined from Lugol preserved samples using Sedgwick-Rafter Cells (S50, Graticules) and a stereomicroscope (Carl Zeiss).

*Preparation of cell extracts:* Cells were washed off the filter with 1 mL homogenization buffer (10 mM Tris, 100 mM NaCl, pH 8.0 at 4 °C) and transferred to a microcentrifuge tube. Disruption of cells was achieved by 5 cycles of 1 min continuous sonication at a power setting of 15 to 20% (Sonopuls HD 2070 sonicator, Bandelin). The samples were kept on ice during the complete treatment. The homogenate was centrifuged at 20000 g at 4 °C for 15 min and the supernatant collected for further analysis. In cases of low protein concentration in the supernatant, sonication was repeated after adding 1 mL homogenization buffer to the pellet produced during centrifugation.
Protein concentrations of supernatants were determined with the modified Bradford assay described by Zor and Selinger [39] measuring at wavelengths of 450 and 600 nm (instead of 590 nm) in a Synergy HT plate reader photometer (BioTek). A standard curve was prepared with BSA for each plate. Total protein concentration of the lysates was adjusted to a concentration of 150 µg $mL^{-1}$ by concentration over Amicon Ultra-0.5 Centrifugal filter devices (10K) (Millipore) or dilution with the homogenization buffer. For sample concentration the columns were used according to the manufactures recommendations with centrifugation steps of 14000 g at 4 °C for 8 min and a prior wash step with 400 µL buffer used for preparation of cell extracts. The presence of AFPs in cell extracts was measured using an optical recrystallometer [21] and a nanoliter osmometer (Clifton Technical Physics) as described above.

*Stability to temperature and protease:* The effect of temperature and protease on antifreeze activity was tested for one sample of each species. Protein concentration in cell extracts was 150 µg $mL^{-1}$. Protease E (Sigma) was added to a final concentration of 1 mg $mL^{-1}$. Negative controls were run with BSA at 1 mg $mL^{-1}$ instead of Pronase E. Samples were incubated for 1 h at 20 °C and tested for activity with the nanoliter osmometer. Subsequently samples were incubated for additional 20 min at 95°C and

the activity assayed. Selected samples were digested at higher protein concentration and analyzed on SDS-PAGE [40] with Coomassie staining to verify successful digest.

## Results

Comparison of methods for determination of recrystallization inhibition

In the Clifton Nanoliter Osmometer the buffer control and the BSA negative controls did not show recrystallization inhibition (RI) activity (Fig. 1a). The presence of a non-AFP protein (BSA or *P. tricornutum* cell extract) resulted in some recrystallization inhibition measured in the optical recrystallometer compared to the buffer control without protein (Fig. 1a). Low protein content or low activity resulted in high variability in the optical recrystallometer (i.e. buffer without BSA, all BSA concentrations, all *P. tricornutum* cell extracts and 5 and 10 µg $\mu L^{-1}$ *F. nana* cell extract)(Fig 1a).

For the *F. nana* cell extracts we defined two different categories in the Clifton Nanoliter Osmometer, lower activity (category 2) for 5-50 µg $mL^{-1}$ protein and higher activity (category 1) at 100-200 µg $mL^{-1}$ protein (Fig. 1a). Recrystallization (R) measured with the optical recrystallometer shows an inverse linear correlation to the protein concentration (µg $mL^{-1}$) on $\log_{10}$ scale for a *F. nana* cell extract and the recombinant AFP (fcAFP). For the *F. nana* cell extract the correlation was linear in a concentration range of 5-50 µg $mL^{-1}$. At 5 mg $mL^{-1}$ protein *F. nana* cell extract showed recrystallization inhibition comparable to the negative control *P. tricornutum* (R=7.48 (±1.00) at 150 µg $mL^{-1}$). Above 50 µg $mL^{-1}$ protein in *F. nana* cell extract, with R=2.44 (±0.50), no further decrease of recrystallization was observed. For the recombinant fcAFP the correlation was linear from 0.02 to 20µg $mL^{-1}$, with values between R=10.23 (±1.32) and R=0.45 (±0.27), respectively. The slopes of both regressions do not differ significantly with -3.95 (±0.89) for *F. nana* cell extract and -3.24 (±0.36) for fcAFP. Comparing both calibrations we set a valid calibration range of $2.44 < R > 7.48$ to calculate fcAFP equivalents of total protein in the cell extracts.

Taxonomy

Taxonomic classification of the Arctic isolates was based on 18S rDNA sequences, light microscopy and SEM (S1, S2-S7). Results of all methods matched well except for isolate KFVC1, which groups into the *Nitzschia* clade based on 18S analysis, whereas microscopic observations clearly indicate its classification to Naviculaceae. Species investigated in this study are listed in table 1.

Physiology and AFP activity under temperature and salinity stress

*Navicula sp.* sensu lato I showed exponential growth rates of 0.49 (±0.06) (control) and 0.44 (±0.08) (treated) (table S8). Regardless of the change of temperature and salinity, treated cultures maintained a similar growth than the controls. Photosynthetic quantum yield of the treated cultures decreased upon treatment from 0.65 (±0.05) to 0.46 (±0.08), while control cultures were stable at 0.66 (±0.01) up to day 4 (Fig. 2a), subsequently declining until the end of the experiment. Recrystallization inhibition activity was present in all measured *Navicula sp.* sensu lato I cultures, yet activity increased for the treated cultures after the stress induction while the activity of the non-treated culture stayed constant (Fig. 2a and 3).

*Fragilairopsis nana* Ark showed exponential growth rates of 0.49 (±0.04) (control) and 0.55 (±0.04) (treated) (table S8). Upon stress induction treated cultures show a decrease in cell number stabilizing until the end of the experiment. The control cultures first continued growing until reaching a stationary phase followed by a decrease in the last two days of the experiment. Photosynthetic quantum yield of the treated cultures declined upon treatment from 0.60 (±0.03) to 0.27 (±0.04), while control cultures were stable at 0.59 (±0.02) up to day 2 (Fig. 2b), subsequently slightly decreasing until the end of the experiment. Prior to treatment (T0) control cultures did not show recrystallization inhibition activty. All other cultures of *Fragilairopsis nana* Ark show RI, with the maximal value for the treated cultures 7 days after the treatment (T2) (Fig. 2b and 3).

*Navicula sp.* sensu lato II showed exponential growth rates of 0.44 (±0.02) (control) and 0.41 (±0.02) (treated) (table S8). Regardless of the change temperature and salinity treated cultures maintained a slow growth until day 3 after the treatment. The control cultures also reached their maximum cell number 3 days after T0, followed by a steep decrease. Photosynthetic quantum yield of the treated cultures decreased upon treatment from 0.56 (±0.05) to 0.21 (±0.04), whereas control cultures increased from 0.54 (±0.06) to 0.70 (±0.01) (Fig. 2c). High recrystallization inhibition activity was present in all measured *Navicula sp.* sensu lato II cultures, yet activity increased for the treated cultures after the stress induction. Maximal RI values were obtained for the non-treated cultures at T2 (Fig. 2c and 3).

*Entomoneis sp.* showed exponential growth rates of 0.49 (±0.02) (control) and 0.48 (±0.01) (treated) (table S8). The change temperature and salinity arrested growth in the treated cultures. Control cultures reached a maximum 3 days after T0 and stayed in stationary phase. Photosynthetic quantum yield of the treated cultures decreased upon stress induction from 0.74 (±0.01) to 0.44 (±0.04), subsequently recovering to 0.57

(±0.05) till the end of the experiment (Fig. 2d). Control cultures showed a stable photosynthetic quantum yield of 0.73 (±0.02). Reasonable recrystallization inhibition activity was only found in *Entomoneis sp.* cultures after the change of temperature and salinity, while only a slight activity was also found for the control samples at T2 (Fig. 2d and 3).

*Navicula sp.* sensu lato III showed exponential growth rates of 0.44 (±0.03) (control) and 0.43 (±0.02) (treated) (table S8). The change in temperature and salinity caused a slight decrease in cell numbers and arrested growth in the treated cultures, whereas control cultures continued growing. Photosynthetic quantum yield of the treated cultures decreased upon stress induction from 0.68 (±0.01) to 0.48 (±0.05), subsequently recovering to 0.54 (±0.01) (Fig. 2e). In control cultures photosynthetic quantum yield slightly decreased from day 3 until end of the experiment. Recrystallization inhibition activity was elevated in *Navicula sp.* sensu lato III cultures after the change of temperature and salinity, yet some activity was also found for the control samples except for T0 (Fig. 2e and 3).

*Nitzschia sp.* showed exponential growth rates of 0.47 (±0.03) (control) and 0.46 (±0.04) (treated) (table S8). The change of temperature and salinity caused a decrease in cell numbers in treated cultures, with a subsequent slight recovery. Control cultures reached their maximum 1 day after T0 merging into stationary phase. Photosynthetic quantum yield of the treated cultures decreased upon treatment from 0.66 (±0.01) to 0.46 (±0.03), subsequently recovering to 0.54 (±0.01). Control cultures had a stable photosynthetic quantum yield of 0.67 (±0.01) upon day 3 after stress induction, followed by a slight decrease until the end of the experiment (Fig. 2f). High recrystallization inhibition activity was present in all measured *Nitzschia sp.* cultures. In control cultures activity increased over the course of the experiment, whereas it was not triggered by the change in temperature and salinity (Fig. 2f and 3).

*Thalassiosira nordenskioeldii* showed exponential growth rates of 0.55 (±0.05) (control) and 0.49 (±0.05) (treated) (table S8). The change temperature and salinity arrested growth in the treated cultures. Control cultures reached a maximum cell density 3 days after T0 and stayed in stationary phase till end of the experiment. Photosynthetic quantum yield of the treated cultures decreased upon stress induction from 0.72 (±0.01) to 0.49 (±0.05) (Fig. 2g) whereas control cultures showed a stable photosynthetic quantum yield of 0.72 (±0.01). Recrystallization inhibition activity was absent (control) or low (treated) at T0 in *Thalassiosira nordenskioeldii* cultures, whereas it increased after for treated and non-treated cultures at the later sampling points (Fig. 2g and 3).

*Fragilairopsis nana* Ant showed exponential growth rates of 0.68 (±0.09) (control) and 0.61 (±0.08) (treated) (table S8). Upon stress induction cell numbers of treated and non-treated cultures dropped until day 3 after the treatment. Both treatments resumed growth reaching a stationary phase at day 6. The salinity and temperature stressed cultures showed maximum cell numbers of approx. 60% of the controls. Photosynthetic quantum yield of the treated cultures declined upon stress induction from 0.60 (±0.02) to 0.33 (±0.08), while control cultures were stable at 0.59 (±0.01) until day 2 (Fig. 2h), subsequently slightly decreasing until the end of the experiment. Recrystallization inhibition activity was present in all *Fragilairopsis nana* Ant cultures, yet continuously increased for the treated cultures after the temperature and salinity stress (Fig. 2h and 3).

*Eucampia antarctica* showed exponential growth rates of 0.33 (±0.04) (control) and 0.36 (±0.06) (treated) (table S8). Due to change in temperature and salinity cell numbers of treated cultures slightly dropped and stayed constant, whereas the control continued growing exponentially after one day. Photosynthetic quantum yield of the treated cultures declined upon stress induction from 0.61 (±0.01) to 0.10 (±0.03), while control cultures were stable at 0.63 (±0.03) until the end of the experiment (Fig. 2i). Recrystallization inhibition activity was found in *Eucampia antarctica* cultures, yet protein concentration in the stressed cultures was too low to exhibit activity (Fig. 2i).

*Proboscia inermis* showed exponential growth rates of 0.45 (±0.06) (control) and 0.50 (±0.02) (treated) (table S8) after a short lag phase (Fig. 2j). Upon stress induction growth of treated cultures arrested. At the same time the control cultures decreased and resumed growing after day 1. Photosynthetic quantum yield of the treated cultures declined upon stress induction from 0.59 (±0.08) to 0.10 (±0.02), while control cultures were stable at 0.56 (±0.03) until the end of the experiment (Fig. 2j). Recrystallization inhibition activity was found in *Proboscia inermis* cultures and increased in control cultures over the course of the experiment (Fig. 2j).

*Porisira glacialis* showed exponential growth rates of 0.29 (±0.01) (control and treated) (table S8). Upon change in temperature and salinity growth of treated cultures arrested, whereas the control cultures continued growing exponentially. Photosynthetic quantum yield of the treated cultures declined upon stress induction from 0.55 (±0.01) to 0.37 (±0.06). Control cultures showed a maximum quantum yield values of 0.66 (±0.03) (Fig. 2k). Recrystallization inhibition activity was not present in control cultures of *Porisira glacialis* and increased in the treated cultures due to the temperature and salinity treatment (Fig. 2k).

AFPeq content estimation

The slight recrystallization inhibition in the negative control (*P. tricornutum)* at a protein concentration of 150 µg $mL^{-1}$ (Fig. 1a) resulted in a calculated value of 0.11% (±0.07%) AFPeq of total protein (cf. Eq. 2, 3; Fig. 3). This value was considered as a baseline and no predication on AFP activity or presence can be drawn from optical recrystallometer data below this baseline. Nevertheless additional observations from the Clifton Nanoliter Osmometer did provide evidence on AFP activity in some cases (Fig. 2a, b, d). AFPeq in all control cultures (T0, T1, T2) and cultures prior to treatment (T0) range from 0.05% (±0.03%) to 7% (±1%), whereas subsequently to treatment cultures (T1 and T2) had 0.6% (±0.2%) to 5.6% (±4.7%) AFPeq (Fig. 3). Minimal values of AFPeq are thus about ten times higher after treatment (0.6%) than prior to treatment (0.05%), whereas maximal values cannot be separated (7% before vs. 5.6% after).

Total AFPeq per cell increased with increasing cell size. For the small species *F. nana* Ant (45$\mu m^3$) total AFPeq $cell^{-1}$ was lowest with values of 0.02 to 0.08 pg total AFPeq $cell^{-1}$. In comparison, the large *Nitzschia sp*. sl II (18000$\mu m^3$) contained 10 to 58 pg total AFPeq per cell. Taking into account the total protein concentration in the cells AFPeq in both species is about 0.3 to 8%. *Entomoneis sp*. did not follow this trend and had rather low total AFPeq concentrations of 0.05 (±0.03) to 1.57 (±1.17).

The presence of notable AFP contamination of bacterial origin can be excluded as samples were filtered and washed to reduce bacterial contamination and checked with DAPI staining (data not shown).

Stability to temperature and protease

Eight out of eleven protein extracts were susceptible to incubation for 1 h at moderate temperature of 20 °C with or without additional protease treatment (Fig. 4). The protein extract of *P. glacialis* completely lost AFP activity while the other 7 samples showed only a reduced activity. Additional incubation at 95 °C resulted in a loss of activity for five more species (Fig. 4). For two species the activity was only lost after incubation at 95 °C and protease (*Navicula sp*. sensu lato II, *T. nordenskioeldii*). For cell extracts of *F. nana* Arc, *Entomoneis sp*. and *P. inermis* no loss in activity was observed upon treatments at 20 °C, but activity was completely abolished when incubated at 95 °C with either BSA or protease. A protease treatment and subsequent SDS-PAGE analysis with Coomassie staining showed that digests were successful. A sample of Ovalbumin as well as cell extracts from *F. nana* Ant and *P. tricornutum* were degraded after incubation with PronaseE for 1h at 20°C (data not shown).

## Discussion

Methods for RI and AFP measurement

In comparison to the Clifton Nanoliter Osmometer, where microscopical observations are biased by the experimentator, data acquired with the optical recrystallometer is objective as readouts are done by the device [21]. The optical recrystallometer produces quantitative results indicated by the logarithmic function of standard curves (Fig. 1b), whereas the Clifton Nanoliter Osmometer is half quantitative, enabling the classification of results in no, low or high recrystallization inhibition. The higher sensitivity of the nanoliter osmometer was advantageous for our study, e.g. the low protein content sample (5 µg $mL^{-1}$) of *F. nana* ANT cell extract clearly showed activity (category 2), but was not distinguishable from the negative control in the optical recrystallometer (Fig. 1a). AFP concentrations in some cell extracts were low, thus failing to produce RI at the optical recrystallometer. Nevertheless in those samples we were often able to determine crystal deformation with the nanoliter osmometer, which indicates the activity of AFPs as well. A combination of both methods allowed us to draw conclusions on the fraction of AFP present in the cell extracts (optical recrystallometer), as well as to obtain information on samples with low AFP content (nanoliter osmometer).

AFP-independent recrystallization inhibition activity was found for BSA and *P. tricornutum* cell extracts with the optical recrystallometer (Fig. 1a). As explained by Knight et al. (1988) [41], molecules, especially large ones, stabilize grain boundaries by reducing the grain boundary energy and disturb grain boundary migration by forcing water molecules to diffuse around them. This results in a weak inhibition of recrystallization. The RI observed for BSA and *P. tricornutum* thus constitutes a baseline or background activity. AFP independent recrystallization inhibition was not observed in the nanoliter osmometer, which thus appears to be a valuable method to verify negative controls.

In samples with high protein concentration and high RI activity we observed an effect of the sample matrix on RI activity. Increasing the protein concentration of *F. nana* calibration cell extract did not lead to any further decrease in R (no values below R=2.44 (±0.50)), whereas for other cell extracts and fcAFP we observed values as low as 1.33 (±0.21) and 0.45 (±0.27), respectively (Fig. 1, 2). Solutes like salts, sugars, amino acids, peptides change the osmolality of a sample, thus leading to different amounts of liquid water molecules available for ice restructuring [21]. For samples containing a complex matrix, like cell extracts, this might result in an elevated recrystallization activity compared to pure samples of single proteins in a defined buffer. To study the effect of matrices in detail, further experiments should include tests of different non-active matrices (e.g. BSA or *P. tricornutum* cell extracts) at fixed

protein concentration (e.g. 150µg/mL), spiked with changing concentrations of RI active protein (e.g. fcAFP). It is important to consider both effects interpretation of the results (AFP independent recrystallization inhibition activity and the recrystallization caused by the matrix) for and to include appropriate negative controls, providing a similar matrix as present the samples.

Taxonomy and ecology

AFPs were only found in organisms subjected to subzero temperature and ice formation for at least limited periods of their lifespan [19, 13]. All Arctic species investigated like *Nitzschia spp*., *Navicula spp*., *Entomoneis spp*. and *Thalassiosira spp*. were reported as commonly found in Kongsfjord sea ice [42]. *Thalassiosira nordenskioeldii, Fragilariopsis spp.*, *Navicula spp*. and *Nitzschia spp*. were also frequently found in the water column in the Kongsfjord [42, 43]. All Antarctic species investigated here were reported in sea ice samples in the Weddell Sea in different frequencies ranging from regular (*E. antarctica, P. glacialis, P. inermis*) to dominant (*F. nana*) [44, 45]. We additionally identified sequences with high similarities of 97.6% for *P. inermis* and above 99.5% for *E. antarctica* and *F. cylindrus* in an environmental 18S library from East Antarctica (110-130°E) (not published). Sequences with high similarities (>99.5%) to *F. nana* were also present in an 18S library from the Weddell Sea (not published).

Physiology and AFP activity under salinity and temperature stress

Physiological data from this study fit well with the ecological habitat of the Antarctic species. The species *E. antarctica*, *P.* inermis and P. *glacialis,* which are less frequently found [44] in sea ice samples, were most severely damaged by the stress conditions indicated by arrested cell growth, a severe drop of quantum yield and low total protein concentration (Fig 2l, j, k). A similar stress response (reduction of total protein per cell) was also reported for *P. tricornutum* under heat stress [46]. The low protein concentrations in several samples of *E. antarcica* and *P. inermis* do not allow any conclusions on RI activity regulation, but it is apparent, that these species are able to produce AFPs (Fig. 2i, j). In contrast *F. nana* Ant, reported as dominant in Weddell Sea ice, shows a smaller drop in photosynthetic quantum yield and cell numbers and an up-regulation of AFPs under temperature and salinity stress (Fig. 2h and [20]).

From the arctic species, although not isolated from the ice, *T. nordeskioeldii* (Fig. 2g) copes equally well with the stress conditions than the species isolated from the ice. *Navicula sp*. sensu lato I (Fig. 2a) appeared to be the most robust of all investigated species. The decrease in photosynthetic quantum yield is rather small and the cultures show positive cell growth after only five days of acclimation to the stress conditions.

Anyhow cell numbers of treated cultures cannot be statistically distinguished from untreated cultures at any time in the course of the experiment, due the late exponential phase at time of treatment and early decline of the control culture [42].
AFP activity was clearly triggered by temperature and salinity stress in *Entomoneis sp*., *Navicula* sp. sensu lato III and *P. glacialis*. For all other species freezing and salinity stress did not result in a clear pattern of AFP activity. This was probably caused by the differences in growth phases between the species when applying the stress. Moreover, high deviations between the replicates of every species and treatment distort clear trends.
In all control cultures and cultures prior to treatment (non-induced) AFP activity was low for *Entomoneis sp*., *Navicula sp*. sl III and *T. nordenskioeldii* (Fig. 2d, e, g), whereas *Navicula sp*. sl II and *Nitzschia sp*. (2c, f) showed quite high levels. No correlation to higher stress tolerance in respect to photosynthetic quantum yield or growth was observed for the species with higher non-induced AFP activity compared to the ones with low non-induced AFP activity.
Increasing AFP activity in the control treatments (5°C, S=70) at T1 and T2 (Fig. 4) can be explained by the late stage of the growth phase. Some cultures had already reached the stationary phase on T2 (Fig. 2). An up-regulation of AFP genes under senescence (due to nutrient limitation) was already observed in prior experiments for *F. nana* Ant [47].

Content and function of AFPs in diatoms

Temperature and protease sensitivity of the cell extracts indicate that recrystallization inhibition activity i.e. antifreeze activity is mainly of proteinaceous nature. Although the digest was proven to be successful (shown by the examples *F. cylindrus* and *P. tricornutum*), some activities were however rather stable to temperature and Pronase E treatment. Doucet *et al*. [48] reported previously that antifreeze activity from some plant and lichen samples remained although proteins were degraded and hypothesize than some activities might be caused by non-protein components.
Species tested contained a calculated amount of 0.1-5% AFPeq of total cell protein, which is rather high. It is comparable to or even higher than the content of the photosystem II proteins PsbA and PsbD in diatoms. Under growth at low light (30 µmol photons $cm^{-2}$ $s^{-1}$) values of 0.15% and 0.42% were reported for *Thalassiosira pseudonana* and 0.07 and 0.08% for *Coscinodiscus radiatus*, respectively [49]. Total AFPeq amount per cell was found to increase with increasing cell size. Smaller cells like *F. nana* Ant contain about 500 times less AFP than the 400 times bigger *Navicula sp*. sl II cells. Since total protein per cell also increases with diatom cell size [50], the fraction of AFPeq per total protein is not affected (Fig. 3).

Cellular AFP levels estimated in this study indicate high AFP concentrations for some cultures tested. For *F. nana* Ant 0.02 to 0.08 pg AFP equivalent per cell were calculated from R in this study, which is 30 to 120 times higher than AFP content determined by Bayer-Giraldi et al. [24] using immunoblot (0.7 fg per cell). Several aspects can lead to the discrepancy observed between both methods. Experiments showed that the antibody raised against one AFP isoform binds to several of the of AFP isoforms in *F. nana* Ant, but due to sequence differences between isoforms it does not bind to all, i.e. two out of three tested recombinant AFPs (Fig. S9). The immunoblot will underestimate total AFP concentration for that reason. In contrast RI assessed in this study will encompass all RI active substances which might be even more single proteins or other compounds than the actual AFP isoforms identified. Also RI measurements will overestimate AFP concentration (in the low concentration range), since some RI is caused by non-AFP compounds, like e.g. observed for *P. tricornutum* cell extracts. The intracellular AFP content is likely to be between a minimum of 0.7 fg per cell (immunoblott) and a maximum of 8 fg per cell (RI measurements). These concentrations (0.016 mg $mL^{-1}$ to 1.8 mg $mL^{-1}$) are however still 5 to 2000 times lower than those reported for fish blood with 10 to 35 mg $mL^{-1}$ [51, 52, 53].

Apart from having an possible extracellular function [24], AFPs may already be active inside the cells It is still unknown if AFPs in diatoms only act as recrystallization inhibitor, which requires 100 - 500 times less AFP than TH [19], or if they also cause TH at *in situ* concentrations. We used a set of data available from this study and from studies on recombinant AFPs from *F. nana* Ant [24, 18] to gain information on the *possible* function of AFPs in diatoms. Considering AFP contents of 0.7 fg [24], 0.02 pg and 0.08 pg per cell and protein sizes of 25.9 kDa [24], 41.3 kDa and 52.8 kDa [18], we calculated concentrations of 0.3 to 68.5 µM AFP inside the cells. Thermal hysteresis activity of three recombinant *F. nana* Ant AFP isoforms was reported for concentrations of 1.2 µM or higher [24, 18], whereas RI was detected at concentrations down to 0.012 µM for fcAFP in saline solution [24]. At the concentrations calculated (0.3 to 68.5 µM), AFPs in *F. cylindrus* will clearly act as recrystallization inhibitor. Since the immunoblot is likely to underestimate cellular total AFP content we assume that AFPs might even account for low thermal hysteresis at *in situ* concentrations. Both functions might protect the cells from intracellular ice formation or mechanical damage through ice crystals grown.

The intracellular activity of the AFPs might potentially be higher than estimated in this study due to the chemical composition of our extraction buffer. Antifreeze activity (RI as well as TH) was reported to increase with salinity at constant AFP concentration [24, 18]. Potential intracellular [18] as well as extracellular AFPs [15, 13] will

encounter inside the cells conditions that are iso-osmolar to the surrounding brine. Subjected to elevated salinities, diatoms regulate turgor pressure by accumulation of salts as well as compatible solutes such as glycerol, sorbitol or proline [9, 44, 27], substances not used in our buffer composition. Low molecular mass solutes were shown to increase activity of a thermal hysteresis protein from the beetle *Dendroides canadensis*. Even though the effects were small in comparison to the other solutes tested, sodium chloride, sorbitol and proline caused an increase in TH activity [56, 57]. Activity (ice pitting) of AFP preparations from sea ice samples that were dominated by diatoms was shown to be solute dependent as well. All solutes tested (NaCl, LiCl, NaPO3, mannitol, urea) had the same enhancing effect on activity [23]. The extraction buffer with a salinity of 8.72 and no low molecular mass solutes used in our study will most likely yield in an underestimation of AFP activity.

The *in situ* function of diatom AFPs is thus dependent on the AFP concentration as well as other ambient conditions and will have to be investigated in more detail. Our study confirms that the presence of AFPs in diatoms is a bipolar phenomenon with a broad phylogenetic distribution throughout the whole diatom phylogeny in species from cold habitats. This fact and the high cellular AFP levels highlight the importance of AFPs for polar diatoms.

## References


[1] D. N. Thomas, G. S. Dieckmann, Antarctic Sea Ice–a Habitat for Extremophiles, Science 295 (5555) (2002) 641–644. http://www.sciencemag.org/cgi/-content/abstract/295/5555/641

[2] M. Gleitz, D. N. Thomas, Physiological responses of a small Antarctic diatom (sp.) to simulated environmental constraints associated with sea-ice formation, Marine Ecology Progress Series 88 (1992) 271–278.

[3] H. Eicken, The role of sea ice in structuring Antarctic ecosystems, Polar Biology V12 (1) (1992) 3–13, tY - JOUR. http://dx.doi.org/10.1007/BF00239960

[4] G. F. N. Cox, W. F. Weeks, Equations for determining the gas and brine volumes in sea-ice samples, Journal of Glaciology 29 (102) (1983) 306–316.

[5] M. P. Lizotte, The contributions of sea ice algae to Antarctic marine primary production, American Zoologist 41 (2001) 57–73.

[6] C. Krembs, R. Gradinger, M. Spindler, Implications of brine channel geometry and surface area for the interaction of sympagic organisms in Arctic sea ice, Journal of Experimental Marine Biology and Ecology 243 (1) (2000) 55 – 80. http://-www.sciencedirect.com/science/article/B6T8F-3XXCXYP-4/2/-4e445853a74208e863ade514d9f71af6

[7] V. Loeb, V. Siegel, O. Holm-Hansen, R. Hewitt, W. Fraser, W. Trivelpiece, S. Trivelpiece, Effects of sea-ice extent and krill or salp dominance on the antarctic food web, Nature 387 (6636) (1997) 897–900.

[8] T. Mock, D. N. Thomas, Recent advances in sea-ice microbiology, Environmental Microbiology 7 (5) (2005) 605–619. http://dx.doi.org/10.1111/j.1462-2920.2005.00781.x

[9] G. O. Kirst, Salinity tolerance of eukaryotic marine algae, Annual Review of Plant Physiology and Plant Molecular Biology 41 (1) (1990) 21–53. http://-www.annualreviews.org/doi/abs/10.1146/annurev.pp.41.060190.000321

[10] D. S. Nichols, P. D. Nichols, T. A. McMeekin, Ecology and physiology of psychrophilic bacteria from Antarctic saline lakes and sea-ice, Science Progress 78 (1995) 311.

[11] C. Krembs, H. Eicken, J. W. Deming, Exopolymer alteration of physical properties of sea ice and implications for ice habitability and biogeochemistry in a warmer Arctic, Proceedings of the National Academy of Sciences. http://-www.pnas.org/content/early/2011/02/11/1100701108.abstract

[12] C. Krembs, H. Eicken, K. Junge, J. W. Deming, High concentrations of exopolymeric substances in Arctic winter sea ice: implications for the polar ocean carbon cycle and cryoprotection of diatoms, Deep Sea Research Part I: Oceanographic Research Papers 49 (12) (2002) 2163–2181, tY - JOUR. http://-www.sciencedirect.com/science/article/B6VGB-47S5NKV-4/2/-4f0202a8a76b0270380a7792d33f745e

[13] J. A. Raymond, C. W. Sullivan, A. L. DeVries, Release of an ice-active substance by Antarctic sea ice diatoms, Polar Biology 14 (1) (1994) 71–75. http://-dx.doi.org/10.1007/BF00240276

[14] J. A. Raymond, C. A. Knight, Ice binding, recrystallization inhibition, and cryoprotective properties of ice-active substances associated with Antarctic sea ice diatoms, Cryobiology 46 (2) (2003) 174 – 181. http://www.sciencedirect.com/science/-article/B6WD5-487DHNB-5/2/5bd949f2f00aaa196e190ee154a20c6c

[15] M. G. Janech, A. Krell, T. Mock, J.-S. Kang, J. A. Raymond, Ice-binding proteins from sea ice diatoms *(Bacillariophyceae)*, Journal of Phycology 42 (2) (2006) 410–416. http://dx.doi.org/10.1111/j.1529-8817.2006.00208.x

[16] J. A. Raymond, P. Wilson, A. L. DeVries, Inhibition of growth of nonbasal planes in ice by fish antifreezes, Proceedings of the National Academy of Sciences of the United States of America 86 (3) (1989) 881–885. http://www.pnas.org/content/86/-3/881.abstract

[17] I. Gwak, W. sic Jung, H. Kim, S.-H. Kang, E. Jin, Antifreeze protein in antarctic marine diatom, *Chaetoceros neogracile*, Marine Biotechnology 12 (2010) 630–630. http://dx.doi.org/10.1007/s10126-009-9250-x

[18] C. Uhlig, J. Kabisch, G. J. Palm, K. Valentin, T. Schweder, A. Krell, Heterologous expression, refolding and functional characterization of two antifreeze proteins from *Fragilariopsis cylindrus* (bacillariophyceae), Cryobiology In Press, Uncorrected Proof (2011) –. http://www.sciencedirect.com/science/article/pii/-S0011224011001283

[19] K. V. Ewart, Q. Lin, C. L. Hew, Structure, function and evolution of antifreeze proteins, Cellular and Molecular Life Sciences 55 (2) (1999) 271–283. http://-dx.doi.org/10.1007/s000180050289

[20] M. Bayer-Giraldi, C. Uhlig, U. John, T. Mock, K. Valentin, Antifreeze proteins in polar sea ice diatoms: diversity and gene expression in the genus *Fragilariopsis*, Environmental Microbiology 12 (4) (2010) 1041–1052. http://dx.doi.org/10.1111/-j.1462-2920.2009.02149.x

[21] D. A. Wharton, P. W. Wilson, J. S. Mutch, C. J. Marshall, M. Lim, Recrystallization inhibition assessed by splat cooling and optical recrystallometry, CryoLetters 28 (1) (2007) 61–68.

[22] A. Krell, B. Beszteri, G. Dieckmann, G. Glöckner, K. Valentin, T. Mock, A new class of ice-binding proteins discovered in a salt-stress-induced cDNA library of the psychrophilic diatom *Fragilariopsis cylindrus* (Bacillariophyceae), Journal of Phycology 43 (4) (2008) 423 – 433.

[23] J. A. Raymond, Distribution and partial characterization of ice-active molecules associated with sea-ice diatoms, Polar Biology 23 (10) (2000) 721–729. http://dx.doi.org/10.1007/s003000000147

[24] M. Bayer-Giraldi, I. Weikusat, H. Besir, G. Dieckmann, Characterization of an antifreeze protein from the polar diatom *Fragilariopsis cylindrus* and its relevance in sea ice, Cryobiology In Press, Accepted Manuscript (2011) –. http://-www.sciencedirect.com/science/article/pii/S0011224011001313

[25] L. A. Bravo, M. Griffith, Characterization of antifreeze activity in Antarctic plants, Journal of Experimental Botany 56 (414) (2005) 1189–1196. http://-jxb.oxfordjournals.org/cgi/content/abstract/56/414/1189

[26] T. Mock, K. Valentin, Photosynthesis and cold acclimation: molecular evidence from a polar diatom, Journal of Phycology 40 (4) (2004) 732–741. http://-dx.doi.org/10.1111/j.1529-8817.2004.03224.x

[27] A. Krell, D. Funck, I. Plettner, U. John, G. Dieckmann, Regulation of proline metabolism under salt stress in the psychrophilic diatom *Fragilariopsis cylindrus*

(*Bacillariophyceae*), Journal of Phycology 43 (4) (2007) 753–762. http://dx.doi.org/-10.1111/j.1529-8817.2007.00366.x

[28] N. Lundholm, G. Hasle, Are *Fragilariopsis cylindrus* and *Fragilariopsis nana* bipolar diatoms?—morphological and molecular analyses of two sympatric species, Nova Hedwig Beih 133 ((2008)) 231–250.

[29] R. R. L. Guillard, J. H. Ryther, Studies of marine planktonic diatoms: I. *Cyclotella nana* Hustedt, and *Detonula confervacea* (Cleve) gran., Canadian Journal of Microbiology 8 (2) (1962) 229–239.

[30] L. K. Medlin, H. J. Elwood, S. Stickel, M. L. Sogin, The characterization of enzymatically amplified eukaryotic i16S-like rRNA coding regions, Gene 71 (1988) 491–499.

[31] V. P. Edgcomb, D. T. Kysela, A. Teske, A. de Vera Gomez, M. L. Sogin, Benthic eukaryotic diversity in the Guaymas Basin hydrothermal vent environment, Proceedings of the National Academy of Sciences of the United States of America 99 (11) (2002) 7658–7662. http://www.pnas.org/content/99/11/7658.abstract

[32] H. Elwood, G. Olsen, M. Sogin, The small-subunit ribosomal RNA gene sequences from the hypotrichous ciliates *Oxytricha nova* and *Stylonychia pustulata*, Mol Biol Evol 2 (5) (1985) 399–410. http://mbe.oxfordjournals.org/cgi/content/-abstract/2/5/399

[33] R. Staden, The staden sequence analysis package, Molecular Biotechnology 5 (3) (1996) 233–241. http://dx.doi.org/10.1007/BF02900361

[34] E. Pruesse, C. Quast, K. Knittel, B. M. Fuchs, W. Ludwig, J. Peplies, F. O. Glockner, SILVA: a comprehensive online resource for quality checked and aligned ribosomal RNA sequence data compatible with ARB, Nucl. Acids Res. 35 (21) (2007) 7188–7196. http://nar.oxfordjournals.org/cgi/content/abstract/35/21/7188

[35] W. Ludwig, O. Strunk, R. Westram, L. Richter, H. Meier, Yadhukumar, A. Buchner, T. Lai, S. Steppi, G. Jobb, W. Förster, I. Brettske, S. Gerber, A. W. Ginhart, O. Gross, S. Grumann, S. Hermann, R. Jost, A. König, T. Liss, R. Lüßmann, M. May, B. Nonhoff, B. Reichel, R. Strehlow, A. Stamatakis, N. Stuckmann, A. Vilbig, M. Lenke, T. Ludwig, A. Bode, K.-H. Schleifer, Arb: a software environment for sequence data, Nucleic Acids Research 32 (4) (2004) 1363–1371. http://nar.oxfordjournals.org/content/32/4/1363.abstract

[36] R. Simonsen, The diatom plankton of the Indian Odean expedition of RV "Metero" 1964- 1965, in: Forschungsergebnisse, no. 19 in Reihe D, Deutsche Forschungsgesellschaft, 1974.

[37] J. Throndsen, Phytoplankton manual, UNESCO, Paris, 1978, Ch. Preservation and storage, pp. 69–74.

[38] K. Maxwell, G. N. Johnson, Chlorophyll fluorescence–a practical guide, J. Exp. Bot. 51 (345) (2000) 659–668. http://jxb.oxfordjournals.org/cgi/content/abstract/-51/345/659

[39] T. Zor, Z. Selinger, Linearization of the Bradford protein assay increases its sensitivity: theoretical and experimental studies, Analytical Biochemistry 236 (2) (1996) 302 – 308. http://www.sciencedirect.com/science/article/B6W9V-45N4PDS-CG/2/6f0bdd3c1f5d07a2d9f0eb178fca72e7

[40] U. K. . Laemmli, Cleavage of structural proteins during the assembly of the head of bacteriophage T4, Nature 227 (5259) (1970) 680–685. http://dx.doi.org/-10.1038/227680a0

[41] C. A. Knight, J. Hallett, A. L. Devries, Solute effects on ice recrystallization: An assessment technique, Cryobiology 25 (1988) 55–60.

[42] H. Hop, T. Pearson, E. N. Hegseth, K. M. Kovacs, C. Wiencke, S. Kwasniewski, K. Eiane, F. Mehlum, B. Gulliksen, M. Wlodarska-Kowalczuk, C. Lydersen, J. M. Weslawski, S. Cochrane, G. W. Gabrielsen, R. J. G. Leakey, O. J. Lønne, M. Zajaczkowski, S. Falk-Petersen, M. Kendall, S.-k. Wängberg, K. Bischof, A. Y. Voronkov, N. A. Kovaltchouk, J. Wiktor, M. Poltermann, G. Prisco, C. Papucci, S. Gerland, The marine ecosystem of Kongsfjorden, Svalbard, Polar Research 21 (1) (2002) 167–208. http://dx.doi.org/10.1111/j.1751-8369.2002.tb00073.x

[43] G. R. Hasle, B. R. Heimdal, The net phytoplankton in Kongsfjorden, Svalbard, July 1988, with general remarks on species composition of arctic phytoplankton, Polar Research 17 (1) (1998) 31–52. http://dx.doi.org/10.1111/j.1751-8369.1998.tb00257.x

[44] A. Bartsch, Die Eisalgenflora des Weddellmeeres (Antarktis): Artenzusammensetzung und Biomasse sowie Ökophysiologie ausgewählter Arten, Ph.D. thesis (1989).

[45] J. Hager, Winterliche Meereislebensgemeinschaft im nordwestlichen Weddellmeer, Master's thesis, Universität Bremen (2008).

[46] J. M. Rousch, S. E. Bingham, M. R. Sommerfeld, Protein expression during heat stress in thermo-intolerant and thermo-tolerant diatoms, Journal of Experimental Marine Biology and Ecology 306 (2) (2004) 231 – 243. http://-www.sciencedirect.com/science/article/pii/S0022098104000759

[47] C. Uhlig, Anti-freeze-proteine in meereis-diatomeen - ihre diversität und expression am beispiel von *Fragilariopsis curta*, Master's thesis, Fachhochschule Aachen, Abteilung Jülich (2006).

[48] C. J. Doucet, L. Byass, L. Elias, D. Worrall, M. Smallwood, D. J. Bowles, Distribution and characterization of recrystallization inhibitor activity in plant and lichen species from the UK and maritime antarctic, Cryobiology 40 (3) (2000) 218 –

227. http://www.sciencedirect.com/science/article/B6WD5-45FCN13-1T/2/-f7eeeac1c10da8d34ba6419d3490f6cd

[49] H. Wu, A. M. Cockshutt, A. McCarthy, D. A. Campbell, Distinctive PSII photoinactivation and protein dynamics in marine diatoms, Plant Physiology. http://-www.plantphysiol.org/content/early/2011/06/03/pp.111.178772.abstract

[50] G. L. Hitchcock, A comparative study of the size-dependent organic composition of marine diatoms and dinoflagellates, Journal of Plankton Research 4 (2) (1982) 363–377. http://plankt.oxfordjournals.org/content/4/2/363.abstract

[51] F. D. Sönnichsen, C. I. DeLuca, P. L. Davies, B. D. Sykes, Refined solution structure of type III antifreeze protein: hydrophobic groups may be involved in the energetics of the protein-ice interaction, Structure 4 (11) (1996) 1325–1337. http://-linkinghub.elsevier.com/retrieve/pii/S0969212696001402

[52] J. Barrett, Thermal hysteresis proteins, The International Journal of Biochemistry & Cell Biology 33 (2) (2001) 105–117, tY - JOUR. http://-www.sciencedirect.com/science/article/B6TCH-42GDGD7-1/2/-e438fdd5167453e04d9b39ec9c20f6df

[53] P. L. Davies, J. Baardsnes, M. J. Kuiper, V. K. Walker, Structure and function of antifreeze proteins, Philosophical Transactions of the Royal Society of London. Series B: Biological Sciences 357 (1423) (2002) 927–935. http://-rstb.royalsocietypublishing.org/content/357/1423/927.abstract

[54] J. G. Duman, Antifreeze and ice nucleation proteins in terrestrial arthropods, Annual Review of Physiology 63 (1) (2001) 327–357. http://www.annualreviews.org/-doi/abs/10.1146/annurev.physiol.63.1.327

[55] M. E. Urrutia, J. G. Duman, C. A. Knight, Plant thermal hysteresis proteins, Biochimica et Biophysica Acta (BBA) - Protein Structure and Molecular Enzymology 1121 (1-2) (1992) 199 – 206. http://www.sciencedirect.com/science/article/B6T21-488CFHV-3J/2/1001663519ead5440b1203ecf29fca32

[56] J. G. Duman, D. W. Wu, T. M. Olsen, M. Urrutia, D. Tursman, Advances in low-temperature biology, JAi Press Ltd, 1993, Ch. Thermal hysteresis proteins, pp. 131–182.

[57] N. Li, C. A. Andorfer, J. G. Duman, Enhancement of insect antifreeze protein activity by solutes of low molecular mass., Journal of Experimental Biology 201 (15) (1998) 2243–51. http://jeb.biologists.org/content/201/15/2243.abstract

[58] E. V. Armbrust, J. A. Berges, C. Bowler, B. R. Green, D. Martinez, N. H. Putnam, S. Zhou, A. E. Allen, K. E. Apt, M. Bechner, M. A. Brzezinski, B. K. Chaal, A. Chiovitti, A. K. Davis, M. S. Demarest, J. C. Detter, T. Glavina, D. Goodstein, M. Z. Hadi, U. Hellsten, M. Hildebrand, B. D. Jenkins, J. Jurka, V. V. Kapitonov, N. Kroger, W. W. Y. Lau, T. W. Lane, F. W. Larimer, J. C. Lippmeier, S. Lucas,

M. Medina, A. Montsant, M. Obornik, M. S. Parker, B. Palenik, G. J. Pazour, P. M. Richardson, T. A. Rynearson, M. A. Saito, D. C. Schwartz, K. Thamatrakoln, K. Valentin, A. Vardi, F. P. Wilkerson, D. S. Rokhsar, The genome of the diatom *Thalassiosira pseudonana*: ecology, evolution, and metabolism, Science 306 (5693) (2004) 79–86. http://www.sciencemag.org/cgi/content/abstract/306/5693/79

[59] C. Bowler, A. E. Allen, J. H. Badger, J. Grimwood, K. Jabbari, A. Kuo, U. Maheswari, C. Martens, F. Maumus, R. P. Otillar, E. Rayko, A. Salamov, K. Vandepoele, B. Beszteri, A. Gruber, M. Heijde, M. Katinka, T. Mock, K. Valentin, F. Verret, J. A. Berges, C. Brownlee, J.-P. Cadoret, A. Chiovitti, C. J. Choi, S. Coesel, A. De Martino, J. C. Detter, C. Durkin, A. Falciatore, J. Fournet, M. Haruta, M. J. J. Huysman, B. D. Jenkins, K. Jiroutova, R. E. Jorgensen, Y. Joubert, A. Kaplan, N. Kroger, P. G. Kroth, J. La Roche, E. Lindquist, M. Lommer, V. Martin-Jezequel, P. J. Lopez, S. Lucas, M. Mangogna, K. McGinnis, L. K. Medlin, A. Montsant, M.-P. O.-L. Secq, C. Napoli, M. Obornik, M. S. Parker, J.-L. Petit, B. M. Porcel, N. Poulsen, M. Robison, L. Rychlewski, T. A. Rynearson, J. Schmutz, H. Shapiro, M. Siaut, M. Stanley, M. R. Sussman, A. R. Taylor, A. Vardi, P. von Dassow, W. Vyverman, A. Willis, L. S. Wyrwicz, D. S. Rokhsar, J. Weissenbach, E. V. Armbrust, B. R. Green, Y. Van de Peer, I. V. Grigoriev, The *Phaeodactylum* genome reveals the evolutionary history of diatom genomes, Nature 456 (7219) (2008) 239–244. http://dx.doi.org/-10.1038/nature07410

## Tables

**Table 1 – Diatom species under investigation in this study.** Listed are the isolate name and species, an abbreviation for each species that will be used throughout the manuscript, isolation site, position and a closer description if the isolates were taken from water or ice, as well as the source i.e. person and date who isolated the clone or who supplied the culture.

| Name / *Species* | Abbrenv. | Isolation site Position | Ice / Water column | Source |
|---|---|---|---|---|
| KFI B2 – *Navicula sp.* sensu lato I | Na.sp sl I | Arctic, Kongsfjord 78.8910N 12.3627E | ice | C. Uhlig, 2009 |
| KFII A4 – *Fragilariopsis nana* | F.nana Arc | Arctic, Kongsfjord 78.9653N 12.3339E | ice | C. Uhlig, 2009 |
| KFIII A2 – *Navicula sp.* sensu lato II | Na.sp sl II | Arctic, Kongsfjord 78.9653N 12.3339E | ice | C. Uhlig, 2009 |
| KFV B4 – *Entomoneis sp.* | En.sp | Arctic, Kongsfjord 78.8539N 12.4661E | ice | C. Uhlig, 2009 |
| KFV C1 – *Navicula sp.* sensu lato III | Na.sp sl III | Arctic, Kongsfjord 78.8539N 12.4661E | ice | C. Uhlig, 2009 |
| KFV C2 – *Nitzschia sp.* | Ni.sp | Arctic, Kongsfjord 78.8539N 12.4661E | ice | C. Uhlig, 2009 |
| *Thalassiosira nordenskioeldii* CCMP 997 | T.nor | Arctic, North Atlantic, Tromsø 69.6667N 18.9667E | n.A. | E. Syvertsen, 1978 |
| *Fragilariopsis nana* | F.nana Ant | Antarctic, Weddell Sea n.A. | ice | T. Mock, 1999 |
| *Eucampia antarctica* CCMP 1452 | E.ant | Antarctic, McMurdo Sound 77.8333S 163.0000E (approx.) | n.A. ice edge 25m | G. Fryxell, 1991 |
| *Porosira glacialis* | P.gla | Antarctic n.A. | n.A. | S. Chollet, University of East Anglia, UK |
| *Proboscia inermis* (Castracane) Jordan & Ligowski, *comb. nov.* | P.ine | Antarctic n.A. | n.A. | Katherina Petrou, UTS Sydney, Australia |

**Figure 1** a)

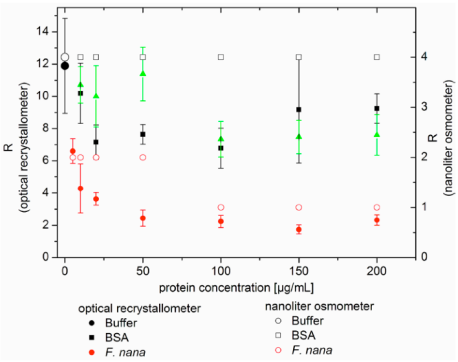


b)

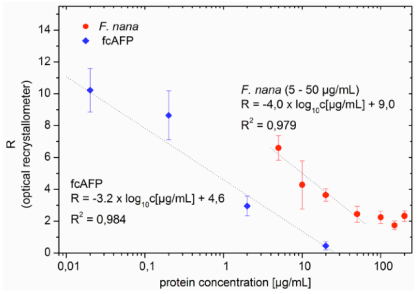


**Figure 1: Recrystallization (R) vs. protein concentration** of BSA (black squares) and cell extracts of *F. nana* Ant (red circles), *P. tricornutum* (green triangles), recombinant *F. nana* AFP (fcAFP) [1] (blue squares) and buffer without protein (black circles). (a) Comparison of R against protein concentrations measured with the optical recrystallometer (closed symbols) and the Clifton Nanoliter Osmometer (open symbols). (b) Linear inverse correlation of R to $\log_{10}$ of the protein concentration.

**Figure 2 a) KFI B2**

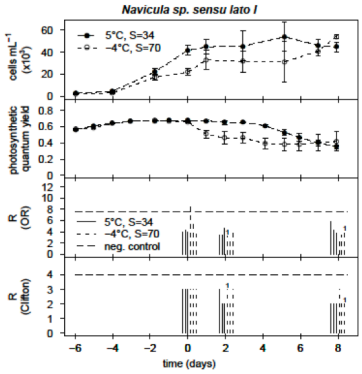


**c) KFIII A2**

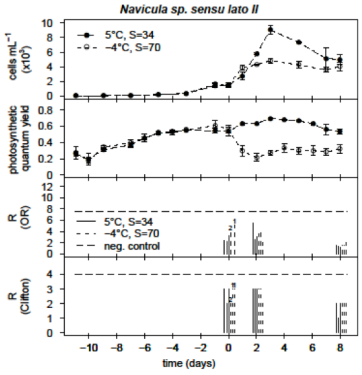


**b) KFII A4**

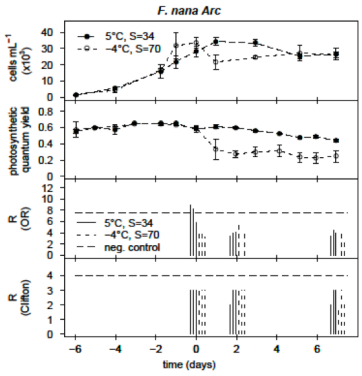


**d) KFV B4**

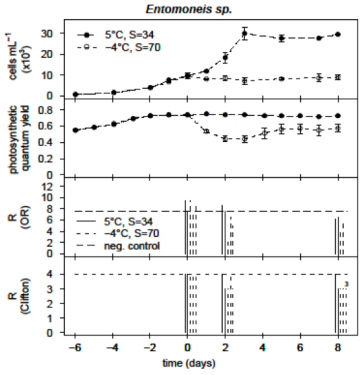

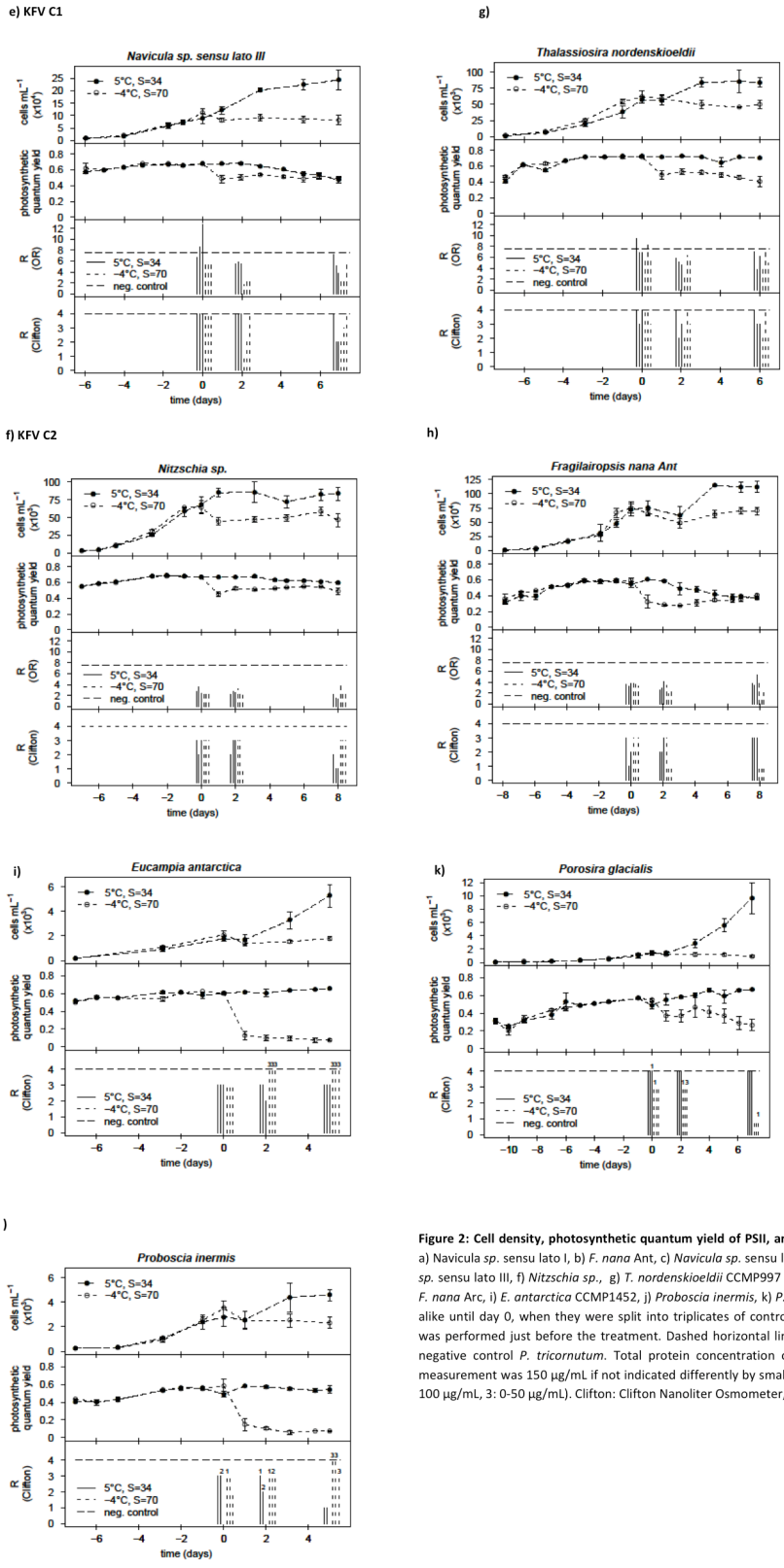


**Figure 2: Cell density, photosynthetic quantum yield of PSII, and recrystallization (R)** for 7 Arctic - a) Navicula *sp.* sensu lato I, b) *F. nana* Ant, c) *Navicula sp.* sensu lato II, d) *Entomoneis sp.*, e) *Navicula sp.* sensu lato III, f) *Nitzschia sp.*, g) *T. nordenskioeldii* CCMP997 - and 4 Antarctic diatom species - h) *F. nana* Arc, i) *E. antarctica* CCMP1452, j) *Proboscia inermis*, k) *P. glacialis*. The cultures were treated alike until day 0, when they were split into triplicates of control and treated cultures. T0 sampling was performed just before the treatment. Dashed horizontal lines indicate values obtained for the negative control *P. tricornutum*. Total protein concentration of the cell extracts used for the R measurement was 150 µg/mL if not indicated differently by small numbers (1: 100-150 µg/mL, 2: 50-100 µg/mL, 3: 0-50 µg/mL). Clifton: Clifton Nanoliter Osmometer, OR: Optical recrystallometer.

**Figure 3**

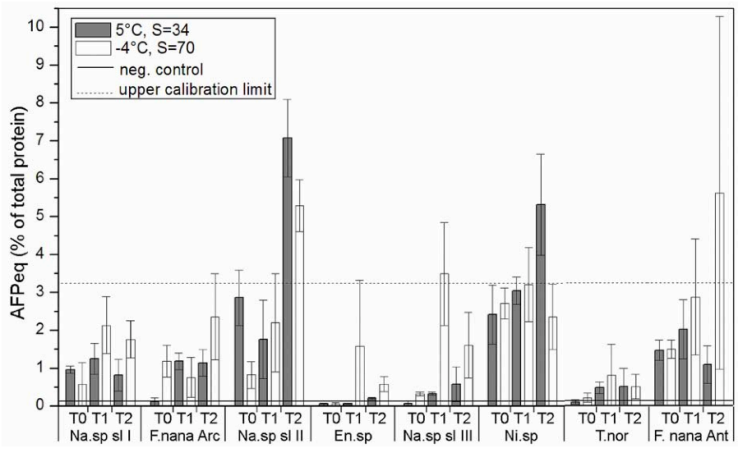


**Figure 3: AFP equivalents (AFPeq)** in % of total protein before treatment (T0), 2 days after treatment (T1), and 6 to 8 days after treatment (T2). Species abbreviations as follows: Na.sp sl I: *Navicula sp.* sensu lato I, *F.nana* Arc: *Fragilaiopsis nana* Arctic isolate, Na.sp sl II: *Navicula sp.* sensu lato I, En.sp: *Entomoneis sp.*, Na.sl III: Navicula sp. sensu lato III, Ni.sp: *Nitschia sp.*, T.nor: *Thalassiosira nordenskioeldii*, F.nana Ant: *Fragilariopsis nana* Antarctic isolate. The horizontal solid line at 0.1% indicates value calculated for the negative control *P. tricornutum*. The horizontal dashed line at 3.3% indicates the upper calibration limit.

**Figure 4**

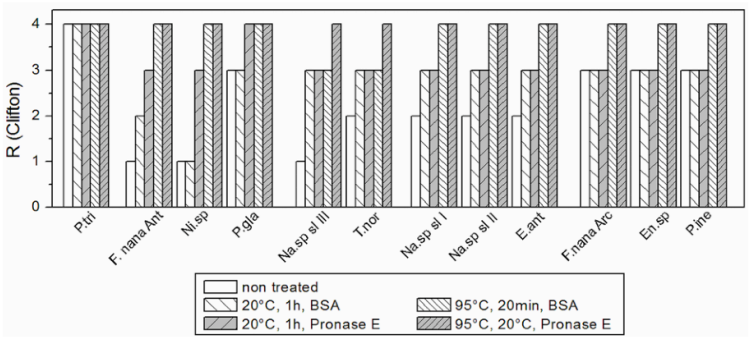


**Figure 4: Stability of AFP activity** with respect to protease and temperature treatment. Extracts were first incubated with Pronase E or BSA for 1 h at 20°C and subsequently with respective additives for 20 min at 95°C. Low R (recrystallization) value indicates high recrystallization inhibition.

# A.2. PUBLICATION 1

# SUPPLEMENTARY INFORMATION

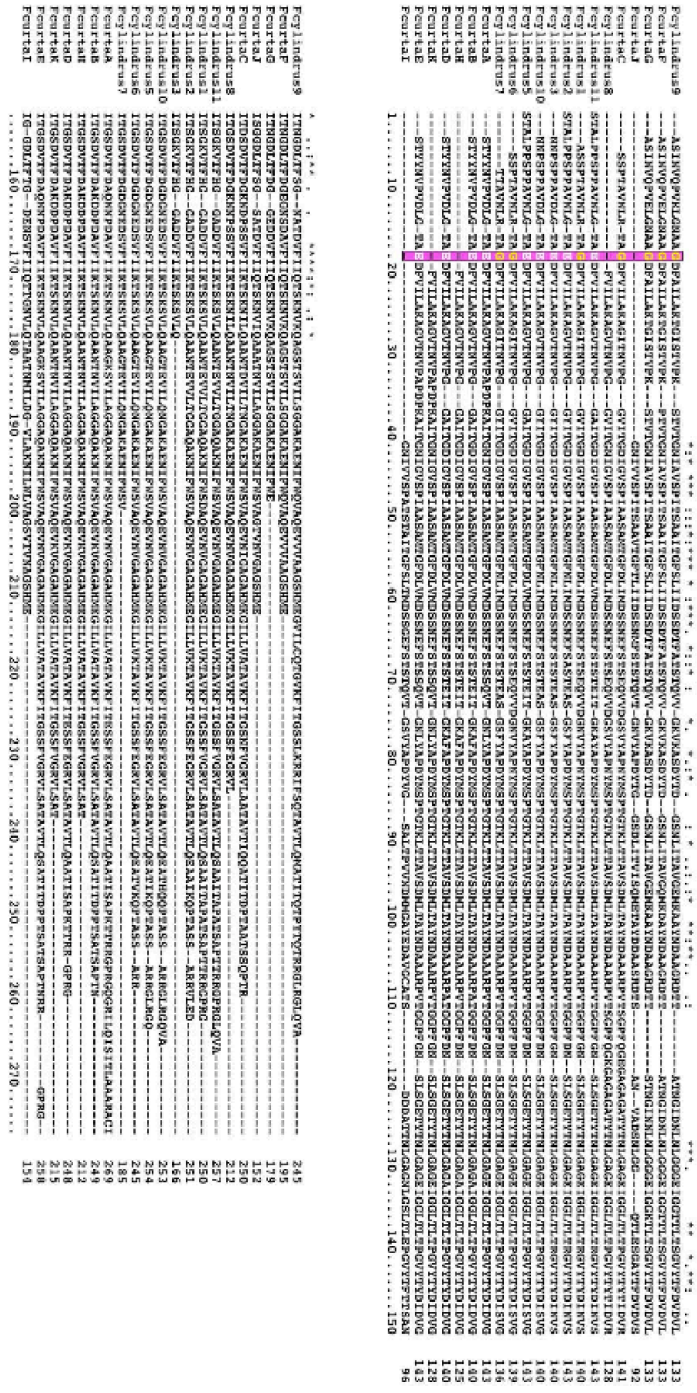

Figure A 1: Alignment of *F. cylindrus* and *F. curta* mature IAFP isoforms. The E/G point mutation at position 18 is highlighted in colour. Only mature protein sequences are shown. Signal peptides were predicted with SignalP 3.0 (Bendtsen *et al.*, 2004).

| *F. cylindrus* | | | | *F. curta* | | | |
|---|---|---|---|---|---|---|---|
| **Isoform** | **Acc. Nr.** | **Primer F** | **Primer R** | **Isoform** | **Acc. Nr.** | **Primer F** | **Primer R** |
| 1 | GQ232744 | 1fcyl_f | 1fcyl_r | A | GQ265833 | 1fcyl_f | 1fcyl_r |
| 2 | GQ232745 | 1fcyl_f | 1fcyl_r | | | 1_f | 5b_r |
| 3 | GQ232746 | 11_f | 5b_r | B | GQ265834 | 1fcyl_f | 1fcyl_r |
| 5 | GQ232747 | 1_f | 5b_r | C | GQ265835 | 1fcyl_f | 1fcyl_r |
| | | 11_f | 12_r | D | GQ265836 | 1fcyl_f | 1fcyl_r |
| | | 1fcyl_f | 1fcyl_r | E | GQ265837 | 1fcyl_f | 1fcyl_r |
| 6 | GQ232748 | 1fcyl_f | 1fcyl_r | F | GQ265838 | 1a_f | 1a_r |
| 7 | GQ232749 | 1fcyl_f | 1fcyl_r | | | 1a_f | 2a_r |
| 8 | GQ232750 | 1_f | 5b_r | | | 1a_f | 3a_r |
| 9 | EL737280 | 1a_f | 2a_r | | | 4a_f | 1a_r |
| | | fcyl08_2f | 1a_r | | | 4a_f | 2a_r |
| | | fcyl08_2f | 2a_r | | | 4a_f | 3a_r |
| | | fcyl08_2f | 3a_r | G | GQ265839 | 1a_f | 2a_r |
| 10 | EL737258 | 1fcyl_f | 1fcyl_r | | | 1a_f | 3a_r |
| | | 1_f | 5b_r | | | 4a_f | 1a_r |
| | | 11_f | 5b_r | | | 4a_f | 2a_r |
| | | 11_f | 12_r | | | 4a_f | 3a_r |
| 11 | DR026070 | 1fcyl_f | 1fcyl_r | H | GQ265840 | 1_f | 5b_r |
| | | 1_f | 5b_r | I | GQ265841 | 4a_f | 1a_r |
| | | 11_f | 5b_r | J | GQ265842 | 4a_f | 1a_r |
| | | 11_f | 12_r | K | GQ265843 | 1_f | 5b_r |
| | | 13_f | 5b_r | | | | |

Table A 1: GenBank accession numbers of *iafp* isoforms of *F. cylindrus* TM99 and *F. curta TM99*, and primer combinations used for PCR amplification of each gene.

| Name | Primer sequence |
|---|---|
| 1_f | TTC GTT ATC CTC GCM AAG GC |
| 1a_f | ATC TCT TTT TAC TAT CTG TGG C |
| 1fcyl_f | CCG GCA TGC TCA GTG TTG CC |
| 4a_f | GGC AAC ATA GTC GTC TCG C |
| fcyl08_2f | CTT GGA AAT GCC GCC GGC |
| 11_f | AYC ACA ATC CAA ATC CAA ATC C |
| 13_f | CCA GTA CTG CTC TGC CTC C |
| 1fcyl_r | GTC CTC GAG GTC CCC GG |
| 1a_r | CCT CCA TAT GCG AAC CTG C |
| 2a_r | CTC CCA GAA GAT ATT TTC AGC |
| 3a_r | TGG CTT GCT TAA CAT TCT TCG |
| 5b_r | CCG TCG CTG ATA AGA CAC G |
| 12_r | TTA CCT AGA GAT TTA TGC TAC C |

Table A 2: Primer sequences used for PCR.

| ORGANISM | TARGET GENES | FORWARD PRIMER | REVERSE PRIMER |
|---|---|---|---|
| *F. cylindrus* | ma-1 | CAT TCA TAT CGG TTG ACA GAT ACC TTA | TCA AAG GTG ACG TTC GAG TTC AT |
| | afp-1+ 6 | AGA CTT CGT TAT CCT CGC AAA GG | TCA ATT TAG TGC CAG TGG GAG AC |
| | afp-2+5+11 | CAG TGT TGC CAG TGC CAG TAC | CCA GCC TTT GCG AGG ATA ACG |
| | afp-3+10 | AGT GCC AAT AAT CCA TCT CC | CCA GTA ATA TAT CCA CCA GGT AC |
| | afp-5+11 | GTC TCA CCT ATT GCT GCT AG | ATT TAG TGC CAG TGG GAG AC |
| | afp-7 | TGC CAC TAC TGC TGT CAA CC | ACC GAT GTC GCC AGT AAT ATA TCC |
| | afp-8 | CGG CTG TCA GTG ATA TGT TG | ACC CGG TGT CAA TGT TAA AC |
| | afp-9 | CTA TCA AAG GCG CAT CCA TCA AC | CGG TGG AGA TAC CAG TCT TTG C |
| *F. curta* | ma | TCG GTT GAC AGA TAC CTT AAA GGA A | TCA AAG GTG ACG TTC GAG TTC AT |
| | afp-B+D+H | CCA ATG TAC CTG GTG GAG CTA TTAC | CTC GGT AGA CGT CGA AAA CTCA |
| | afp-J | TAT TCA AGC TGC GGC TAC CA | GGC GAC TGA CCA GAA GAT GTT C |

| ORGANISM | TARGET GENES | PROBE | EFFICIENCY | $R^2$ |
|---|---|---|---|---|
| *F. cylindrus* | ma-1 | AGG ACA TCT TCG TTG CTT | 2.00 | 0.99 |
| | afp-1+ 6 | AC**T** GT**C** CA**T** **AA**T C**A**A GT**C** A**A**A ACC | 1.95 | 1.00 |
| | afp-2+5+11 | CTT G**G**A ACT G**CA** **G**AA G**AC** T | 2.02 | 1.00 |
| | afp-3+10 | CC**T** G**C**T GTC **G**AC **C**TT GG | 2.02 | 1.00 |
| | afp-5+11 | AC**T** C**A**T T**G**G A**G**C T**G**T CC | 2.01 | 0.99 |
| | afp-7 | CGG AGA CTT CGT TAT CCT CGC AAA GGC TG | 1.99 | 1.00 |
| | afp-8 | CCC TTC **CAA** GG**C** AAA G | 2.00 | 1.00 |
| | afp-9 | ACC CGT CAA ACT TGG AAA TGC CGC CG | 2.03 | 1.00 |
| *F. curta* | ma | | 1.90 | 1.00 |
| | afp-B+D+H | | 1.80 | 1.00 |
| | afp-J | | 1.98 | 1.00 |

Table A 3: Primer and probe sequences used for qPCR. Some oligos bind multiple isoforms as shown here. Probes were labelled with 5′ FAM/3′ TAMRA. Bold letters denote LNA nucleotides.

# A.3. EXPRESSION OF RECOMBINANT fcAFP IN *E. COLI* - PROTOCOL

For heterologue expression of fcAFP a bacterial host system, *E. coli*, was chosen, due to the usually high expression rates shown compared to other systems like yeast and human cells.

Over the different fcAFP isoform expression of isoform 11 was chosen (GenBank Acc Nr. DR026070), since this isoform had been found in a salt-stress induced cDNA library [Krell et al., 2008], suggesting that it plays a relevant role in adaptation to sea ice brine conditions. Host cells and the pQE-32 vector, with a 6xHis-tag positioned upstream (in 5' direction, see Figure A 2) were chosen between the options offered by the QIAexpressionist system (Qiagen, USA). The gene was modified introducing a SphI restriction site at position 101 of the gene (changing CCATGG to GCATGC), situated at the beginning of the predicted signal peptide. The gene was digested with SphI and XhoI, the vector with ShpI and SalI, the products gel purified. The insert was ligated in frame into the vector with T4 DNA ligase under standard conditions following the Qiagen protocol, the ligated vector gel purified and chemically transformed into M15[pREP4] *E. coli* cells. These cells contain an additional plasmid (pREP4) coding a repressor for the promotor of the recombinant gene, in order to eliminate any "leakage" in the system and permit transcription only after the induction of expression of the recombinant protein by the addition of isopropyl-β-D-thiogalactoside (IPTG) at final concentration of 1 mM, added at $OD_{600}$ of 0.5 of the *E. coli* culture. Cells were harvested by centrifugation, resuspended in lysis buffer and sonicated. Purification of the recombinant protein was performed following the Qiagene protocol. The lysate was centrifuged to remove cell debris and the supernatant removed for further processing. The recombinant protein was purified through affinity chromatography with Ni-NTA silica columns (Qiagen, USA), which tightly bind to the His-tag. The loaded columns were centrifuged, repeatedly washed with washing buffer and the recombinant protein was obtained by treatment with elution buffer. Different experimental conditions were applied, concerning conditions for protein purification (native and denaturing) and varying growth temperatures for *E. coli* (37°C; 30°C) after induction.

# A.4. BIOLISTIC BOMBARDMENT PROTOCOL

**The preparation of the material**

*P. tricornutum* Bohlin (strain 646, kindly provided by Ansgar Gruber, Universität Konstanz, Germany) was cultivated in f/2 medium in 50% seawater until late exponential growth phase. Cells were centrifuged and concentration adjusted to 1 x $10^9$ cells $ml^{-1}$. Per each bombardment, 1 x $10^8$ cells were plated on a Petri dish with f/2 solid medium prepared in 50% seawater and 2% Bacto-Agar.

FcAFP isoform 11, also used for other molecular studies and protein activity analyses described here, was chosen for transformation. A SacI restriction site was introduced 3' of the gene, situated in the pQE32 plasmid with a 5' 6 x His-tag. The plasmids pQE32 and pPha-T1 were digested with EcoRI and SacI and the products gel-purified. The insert, containing the gene and the His-tag, was ligated into the pPha-T1 plasmid, which contains also the sh ble gene that confers resistance to the antibiotic Zeocin (Figure A 4). Successful insertion was checked with PCR with PTV primers (PTVseqUp: 5'-GCTTCAATTT GCTGGATGT-3'; PTVseqLo: 5'-TTAAGGAAGGATAGAGACT-3'). A GFP sequence was not included since the transformation of the gene alone, without possibly disturbing tags, had to be tested first. Moreover, a study on protein localization, which relies on fusion to GFP, was not the main purpose of this experiment. For comparison, both types of particles (microcarriers), tungsten (0.7 µm median diameter) and gold (0.6 µm diameter) (both 50 µl), were coated with DNA (5 µg) mixed to 2.5 M $CaCl_2$ (50 µl) and 0.1 M spermidine (20 µl) as described by the manufacturer Bio-Rad (USA). The mixture was repatedly washed with EtOH (100%) and finally resuspended in 50 µl EtOH (100%).

**The biolistic bombardment**

The transformation was performed in a biolistic PDS-1000 He particle delivery system (Biorad, USA). The system was set-up and bombardment performed with 10 µl of the DNA/microcarriers suspension. Cells were positioned at 7 cm from the stopping screen (position 2 in the bombardment chamber), following suggestions of Apt et al. [1996]. Vacuum was applied to 25 psi and helium pressure to 1350 psi.

**Selection of transformants**

The cells were held overnight on solid medium to allow recovery from the damages of bombardment. They were then transferred to fresh solid medium containing also the antibiotic Zeocin (75 µg/ml) and incubated for 3-4 weeks (22°C, 50 µE $m^2$ $sec^{-1}$).

Brownish colonies appeared, with cells expressing the protein for resistance to Zeocin. The presence of the target gene was tested with PCR. Primers used were PTVseqUp, PTVseqLo and, as positive control, primers designed to detect the Zeocin resistance gene (ZeoF: 5'-GACTTCGTGGAGGACGACTT-3'; ZeoR: 5'-GACACGA CCTCCGACCACT-3').

# A.5. VECTOR MAPS

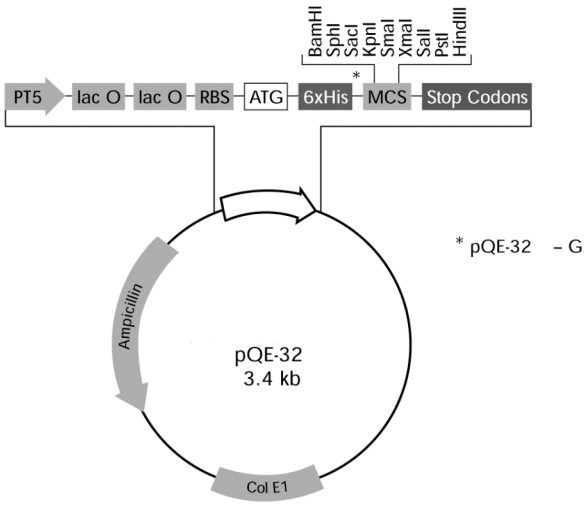


Figure A 2: Vector map of pQE-32 (Qiagen, USA). Image from http://www.qiagen.com/literature/pqesequences/pqe3x.pdf

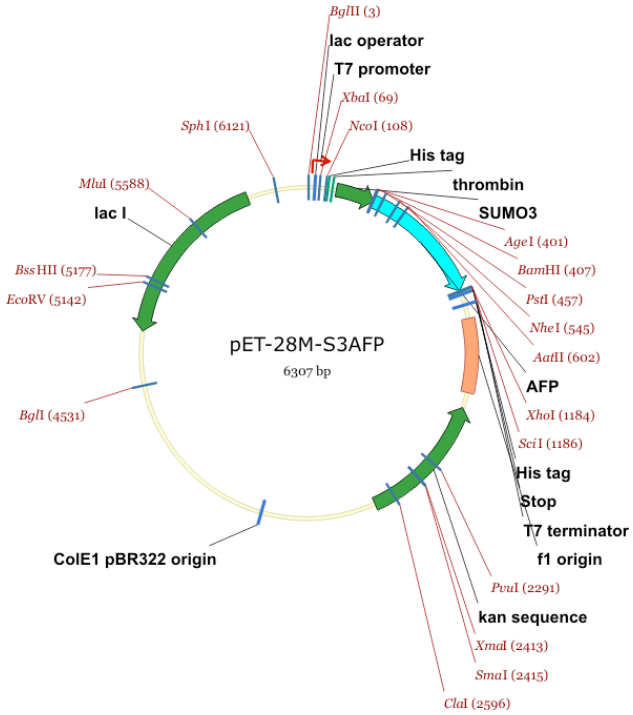


Figure A 3: Vector map of pET-28M-S3AFP (EMBL, Germany).

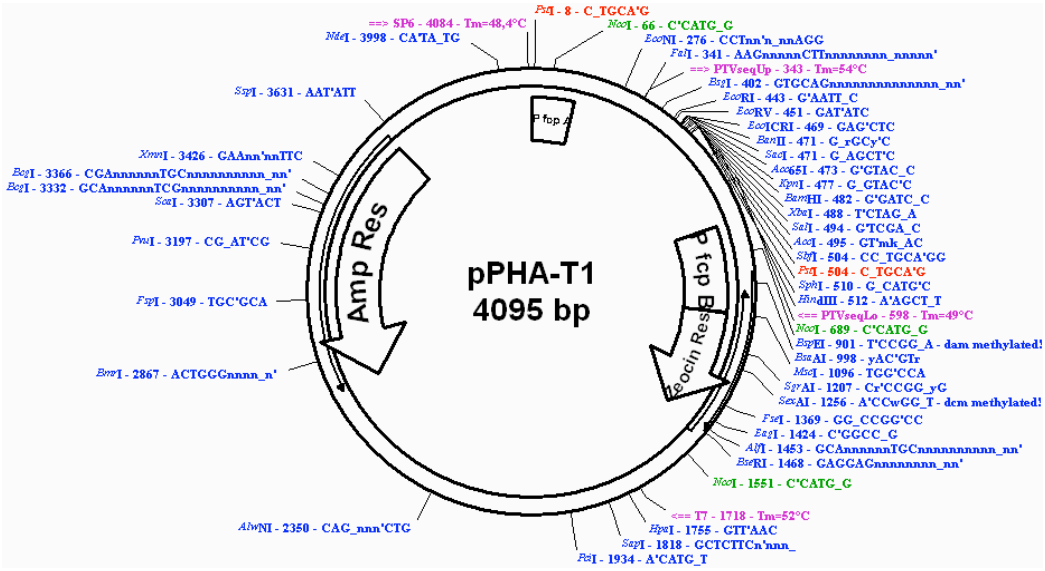


Figure A 4: Vector map of pPHA-T1 used for biolistic bombardment. The plasmid contains the *sh ble* gene, conferring resistance to the antibiotic Zeocin. The *fcafp* was inserted between promoter and terminator sequences from the gene coding the fucoxanthin chlorophyll binding protein (*fcp*).

# A.6. CONFOCAL RAMAN MICROSCOPY

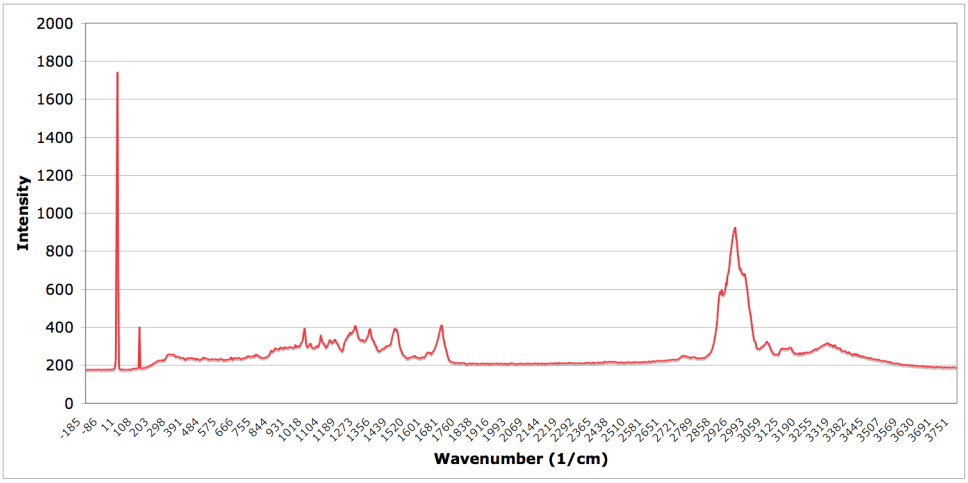


Figure A 5: Raman spectrum of dry recombinant fcAFP. A confocal Raman microscope (WITec, Germany), equipped with a diode laser (532 nm) and a Zeiss 100x (NA 0.95) objective was used to determine the spectrum of the sample. An integration time of 10 s per spectrum was used.

# AKNOWLEDGEMENTS

I would like to thank Prof. Ulrich Bathmann for giving me the possibility to work at the AWI, for his support in difficult situations and for the review of this manuscript. I also thank Prof. Allan Cembella for accepting to review this thesis.
I thank Gerhard Dieckmann for the opportunity to work in the sea ice group, for his constant moral support, his trust and last but not least for sharing with us his excellent cooking skills. I am deeply grateful to Klaus Valentin for his patient support and his interest in antifreeze proteins.
Thank you to Uwe John and Magnus Lucassen, who opened to me their labs and assisted me in answering several questions.
I thank Ilka Weikusat and Sepp Kipfstuhl for their interest, assistance and discussions on antifreeze proteins, for their openness to an interdisciplinary research, allowing me to gain a new approach to the topic.
For the good times inside and outside the lab, for their cooperation and support I thank the sea ice group: Erika Allhusen (and her precious armchair), Michal Fischer, Niko Hoch, Jessica Kegel and Christiane Uhlig, together with Thomas Mock and all former group members.
I thank Ansgar Gruber, Doris Ballert and Prof. Peter Kroth from the University of Konstanz for providing me with the pPHA-T1 vector, *Phaeodactylum tricornutum* cells and for their assistance with the biolistic transformation.
I thank my friendly and open colleagues from different groups, especially Sára and Bank Beszteri, Nina Jaeckisch, Ines Yang, the Abele-group for good intra-corridor neighbourhood and Elisabeth Helmke for her enthusiasm for my work. I am grateful to my friends Bernd Krock and Shinya Sato for useful comments on this manuscript.
This time wouldn't have been the same without the actual and former train commuting group, as well as the mensa and the Dome-D-coffee communities, whom I thank for the relaxing and inspiring moments in my daily work life.
I thank my dearest friends and my family for keeping my mind open and my heart warm.

This work was carried out at the Alfred Wegener Institute for Polar and Marine Research and was partially supported by the Friedrich Ebert Foundation.

# ERKLÄRUNG

Hiermit erkläre ich, dass ich:

- die Arbeit ohne unerlaubte fremde Hilfe angefertigt habe;
- keine anderen als die hier angegebenen Quellen und Hilfsmittel benutzt habe;
- die den benutzten Werken wörtlich oder inhaltlich entnommenen Stellen als solche kenntlich gemacht habe.

Bremen, September 2011